FINAL REPORT

Mechanical and Environmental Performance of Eco-Friendly Chip Seal with Recycled Crumb Rubber

Prepared for

Missouri Department of Natural Resources

By

Ahmed Gheni
Omar I. Abdelkarim, Ph.D.
Xuesong Liu
Mohannad Abdulazeez
Mike Lusher
Kun Liu
Mohamed ElGawady, Ph.D.
Honglan Shi, Ph.D.
Jianmin Wang, Ph.D.

Missouri University of Science and Technology, Rolla, Missouri

February 2017

TECHNICAL REPORT DOCUMENTATION PAGE.

<table>
<tr><td colspan="2">1. Report No.:</td><td>2. Government Accession No.:</td><td>3. Recipient's Catalog No.:</td></tr>
<tr><td colspan="3">4. Title and Subtitle: Mechanical and Environmental Performance of Eco-Friendly Chip Seal with Recycled Crumb Rubber</td><td>5. Report Date:</td></tr>
<tr><td colspan="3"></td><td>6. Performing Organization Code:</td></tr>
<tr><td colspan="3">7. Author(s):
Ahmed Gheni, Omar I. Abdelkarim, Ph.D., Xuesong Liu, Mohannad Abdulazeez, Mike Lusher, Mohamed ElGawady, Ph.D.,Honglan Shi, Ph.D., Jianmin Wang, Ph.D.</td><td>8. Performing Organization Report No.:</td></tr>
<tr><td colspan="3">9. Performing Organization Name and Address:
Missouri University of Science and Technology</td><td>10. Work Unit No.:</td></tr>
<tr><td colspan="3"></td><td>11. Contract or Grant No.:</td></tr>
<tr><td colspan="3">12. Sponsoring Agency Name and Address:

Missouri Department of Natural Resources</td><td>13. Type of Report and Period Covered:
Final Report.</td></tr>
<tr><td colspan="3"></td><td>14. Sponsoring Agency Code:</td></tr>
<tr><td colspan="4">15. Supplementary Notes:</td></tr>
<tr><td colspan="4">16. Abstract: A new eco-friendly chip seal, where the mineral aggregate was replaced by crumb rubber obtained from scrap tires, was investigated in this study. A total of 222 chip seal specimens were prepared and tested to investigate five different aspects namely aggregate retention, the microtexture, macrotexture, skid resistance, and skid resistance under high temperature. Furthermore, an extensive leaching study was carried out on chip seal having scrape rubber aggregate. Ambient processed crumb rubber was found to have about 20% higher surface area compared to cryogenic crumb rubber. The aggregate retention was measured using five tests which included the standard sweep test, modified sweep test, Vialit test, modified Vialit test, and Pennsylvania test. The performance of the new chip seal was also compared with that of conventional chip seal manufactured using two different types of mineral aggregate. The examined tests specimens were manufactured using two types of emulsions and two types of asphalt cement binders. This study concluded that the crumb rubber can be used in the chip seal as partial or full replacement of mineral aggregates. The crumb rubber showed a remarkable performance in aggregate retention. This performance was mainly because of the low weight of the crumb rubber and its rough surface, which increased the adhesion of the crumb rubber with the asphalt emulsion or cement asphalt. Furthermore, using the Vialit and Pennsylvania tests showed that the crumb rubber chip seal overcame the performance of mineral aggregate chip seal in terms of aggregate retention. Finally, the leaching study showed that using scrap tires as an aggregate in construction does not have significant environmental impact.</td></tr>
<tr><td colspan="2">17. Key Words:
Chip seal – rubber – scrape tires - recycling</td><td colspan="2">18. Distribution Statement:</td></tr>
<tr><td>19. Security Classification (of this report):
Unclassified.</td><td>20. Security Classification (of this page):
Unclassified.</td><td>21.</td><td>22. Price:</td></tr>
</table>

EXECUTIVE SUMMARY

Chip seal is a widespread type of pavement that is used either for maintenance or as the main pavement. This study presents an investigation on eco-friendly chip seal, where crumb rubber obtained from scrap tires replaced the mineral aggregate. This will help in diverting millions of tons of tires from landfills. Replacing mineral aggregates with crumb rubber aggregate can address several issues linked to using mineral aggregates in chip seal. Mineral aggregate when dislodge represents a serious safety issue to vehicles and human beings. Mineral aggregate chip seal features noisy driving. In addition, it is a common practice in the U.S. to apply a fog seal to finished chip seal to hide its rocky color and display a dark color. The applied fog increases the pavement cost and reduces the pavement friction. Crumb rubber aggregate potentially can address all these issues.

A total of 222 chip seal specimens were prepared to investigate five different aspects namely aggregate retention, the microtexture, macrotexture, skid resistance, and skid resistance under high temperature. The aggregate retention was measured using five tests included the standard sweep test, modified sweep test, Vialit test, modified Vialit test, and Pennsylvania test. The performance of the new chip seal was also compared with that of conventional chip seal manufactured using two different types of mineral aggregate. The examined tests specimens were manufactured using two types of emulsions and two types of asphalt cement binders. This study concluded that the crumb rubber can be used in the chip seal as partial or full replacement of mineral aggregates. The crumb rubber showed a remarkable performance in aggregate retention. This performance was mainly because of the low weight of the crumb rubber and its rough surface, which increased the adhesion of the crumb rubber with the asphalt emulsion or cement asphalt. Furthermore, using the Vialit and Pennsylvania tests showed that the crumb rubber chip seal overcame the performance of mineral aggregate chip seal in terms of aggregate retention. High-resolution 3D microscope, image processing, and a volumetric method showed that using crumb rubber to replace mineral aggregate has a significant impact on improving both macrotexture and microtexture of chip seal. In addition, the low thermal conductivity of crumb rubber helped the chip seal to resist high temperature without significant loss in friction resistance. A 3D geometrical model then was proposed to simulate the aggregate embedment so it can be used to predict the required binder application rate.

An extensive leaching study was carried out as well. Using scrap tires as an aggregate in construction does not have significant environmental impact. The toxic heavy metals leached from the tire or tire used with asphalt samples were below EPA drinking water standard. The major leached heavy metal from the tire is Zn which is consistent with the tire component. However, Zn is not regulated in the primary drinking water regulations.

ACKNOWLEDGEMENTS

The authors would like to acknowledge the many individuals and organizations that made this research project possible. The authors wish to extend a very sincere thank you to the Missouri Department of Natural Resources (MoDNR). In addition to their financial support, the authors appreciate MoDNR's vision and commitment to innovative concepts and pushing the boundaries of current practice. In particular, the success of this project would not have been possible without the support, encouragement, and patience of Messrs. Chris Nagel, Dan Fester, and Jeff Heisler as well as Ms. Brenda Ardrey. Appreciation is extended to The Pettis County Commissioners Brent Hampy and Jim Marcum. Sincere thank you is also extended to Mr. Randy White of the Pioneer Trails Regional Planning Commission.

The authors would also like to thank Mr. Mike Mitchell from Vance Brothers for coordinating the donation of the different asphalt binders used during this study. Finally, the authors would like to thank the many undergraduate and graduate students that contributed to this project including Nicholas B. Colbert, Andrew Chapko, Ashley Crannick, Yasser Darwish, Eslam Gomaa, Monika Nain, and Janine Williams of Missouri S&T as well as Mr. Florian Lang of Karlsruhe Institute of Technology, Germany.

The authors also appreciate the tireless staff of the Department of Civil, Architectural, and Environmental Engineering. Their assistance both inside and out of the various laboratories was invaluable to the successful completion of this project.

Contents

LIST OF ILLUSTRATIONS

LIST OF TABLES

PART 1

Mechanical assessment of using scrap tires as an aggregate in chip seal

1. Literature review

1.1. Introduction to chip seal

Chip seal is a type of pavement coating treatment that consists of a single application of asphalt directly on the existing pavement or substrate, followed by the application of aggregate chips that are rolled with a pneumatic roller. In this process, the aggregate chip layer is one-stone thick (Fig.1a). Chip seal types include single (conventional), double (Fig.1b), triple, racked-in (choke stone), cape, inverted, and sandwich seals. Double and triple chip seals are constructed similar to the single seal but with two or three consecutive applications of both the asphalt binder and the aggregate, respectively. Hence, the thickness of the chip seal depends on the aggregate size and type of chip seal. However, single seal is the most common type of chip seal and it is the focus of this report.

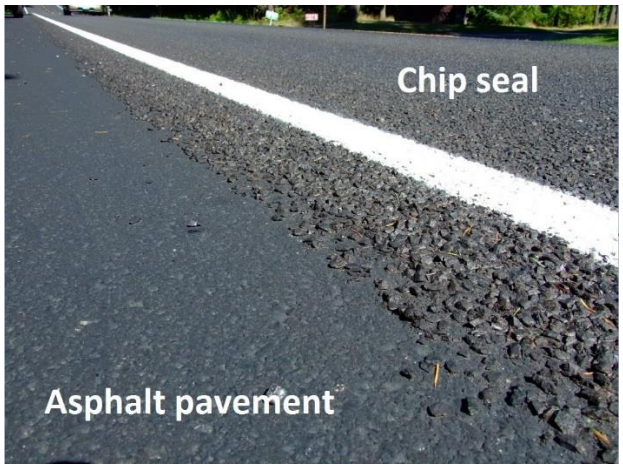

(a)

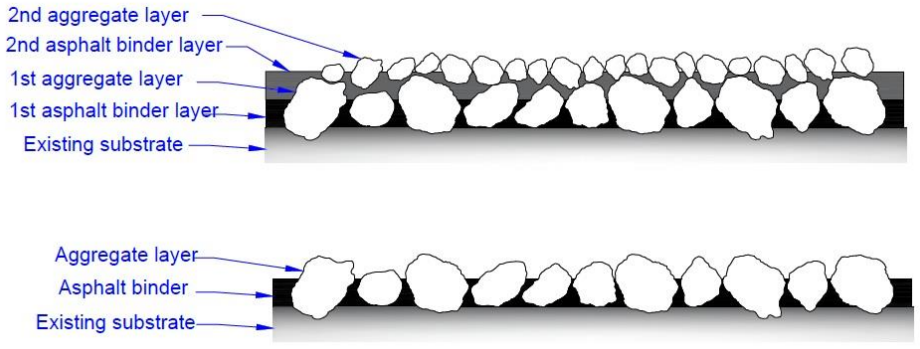

(b)

Figure 1: Chip seal pavement, (a) chip seal vs asphalt pavement and, (b) types of chip seal

Binders used in chip seal can be either asphalt cements or emulsified asphalts. Many factors such as local weather during construction and aggregate's characteristics play an important role in determining the binder type and rate (McLeod et al. 1969, Gransberg et al. 1998). Most chip seal in the U.S. is carried out using emulsions due to weather challenges as the asphalt cement is sensitive to aggregate moisture content; however, few states use both emulsions and asphalt cement (Gransberg and James 2005). The main difference between an asphalt cement and an emulsion is the water content and other admixtures that keep the emulsions flowable and workable at relatively lower temperatures of about 35 ^{o}C compared to 165 ^{o}C for asphalt cement. Hence, the main advantage of using asphalt cement is the ability to quickly open the road for traffic after chip seal application versus the required breaking long time in the case of emulsified asphalt.

1.2. Aggregates in chip seal

The type, size, and grading of aggregate is an important factor in determining the required amount of binder as well as construction procedure. It is more common to use normal weight aggregate in chip seals. Recently, a few DOTs have started to use natural and synthetic lightweight aggregate as cover stone for chip seals. The lightweight aggregate displays superior skid-resistance (Islam 2010, Islam and Hossain 2011, Alvarado and Howard 2014). Moreover, lightweight aggregate has a specific gravity much lighter than natural stone aggregate and hence would reduce the windshield breakage due to aggregate dislodging.

The size of the selected aggregate has a significant effect on the performance of the pavement. Larger aggregate size requires higher asphalt volume to retain the chips in place. Larger aggregate size results in higher rougher texture, more traffic noise, and great potential to damage cars. Furthermore, larger aggregate particle sizes result in chip seal that is more durable and less sensitive to variations in binder application rate (Gransberg et al. 1998).

Aggregates used in chip seal are preferred to be uniformly graded to provide high surface friction and better waterproofing (Wood et al. 2006). Using well-graded aggregates results in each aggregate having a different embedment depth. Hence, some aggregates will not have enough embedment depth (Fig. 2), leading to dislodging of the aggregate, which might cause vehicle damage and human injury.

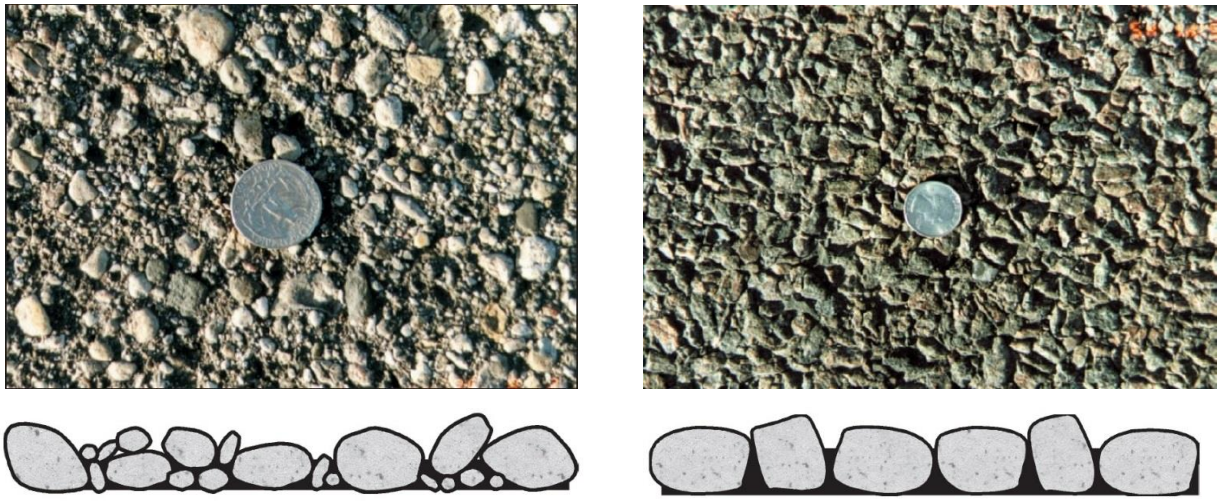

(a) (b)

Figure 2: Example of chip seal (a) well graded, and uniformly graded aggregate (b)

(Wood et al. 2006)

After compaction, aggregates are typically embedded approximately 50% to 80% of its median size into the binder. Using the lower limit of embedment, i.e. 50%, allows traffic on the newly sealed road to finish the embedment process. However, leaving 50% of the aggregate size rising into the air will make the aggregate susceptible to dislodging by moving vehicles. Using the upper limit, i.e. 70%, of embedment will reduce the potential of the aggregate dislodging; however, it may lead to bleeding. Hence, embedment is a crucial issue that needs careful consideration (Gransberg et al. 2004).

The aggregate's angularity is an important factor in determining the performance of chip seal. Cubical aggregates are more stable and tend to lock together which reduces the potential for dislodging and/or reorientation of the aggregate under heavy traffic. Elongated and flat particles are susceptible to bleeding (Janisch and Gaillard 1998, Wood and Olson 2007).

Polishing and abrasion resistances are important factors for long-term durability of a given aggregate. Degradation to polishing resistance leads to reduced friction and skid resistance. Abrasion resistance is important during construction to ensure that there will be no change in the required particles degradation due to the handling or construction process. Moreover, during service, it is also important to have high abrasion resistance to ensure that travelling vehicles will not cause local crushing to the aggregate particles (Gransberg and James 2005, Asi 2007, Shuler 2011).

1.3. Performance of chip seal

The effects of construction procedure and requirements, binder types, and aggregate types on the performance of chip seal pavement have been widely investigated (Temple et al. 2002, Gransberg 2006, Howard and Baumgardner 2009, Liu et al. 2010, Islam and Hossain 2011, Kim and Adams 2011, Banerjee et al. 2012, Karasahin et al. 2014). The performance of chip seal is usually identified by measuring the aggregate retention, which is a key parameter of the design. Many factors affect the relationship between the aggregate and the binder, such as properties compatibility, porosity, texture, mineralogy, surface chemical, and binder polymer content. In general, the asphalt cement or polymer-modified emulsion has better performance in terms of aggregate retention compared to that of the conventional emulsion due to the elastic membrane effect that holds the asphalt particles (Rahman et al. 2012).

There are a number of standard tests that measure aggregate retention, such as the sweep test, Vialit test, and Pennsylvania test. However, some of these standard tests are still under development with the recent increase of research studies on chip seal (Kandhal and Motter 1991, Jordan III and Howard 2011, Rahman et al. 2012).

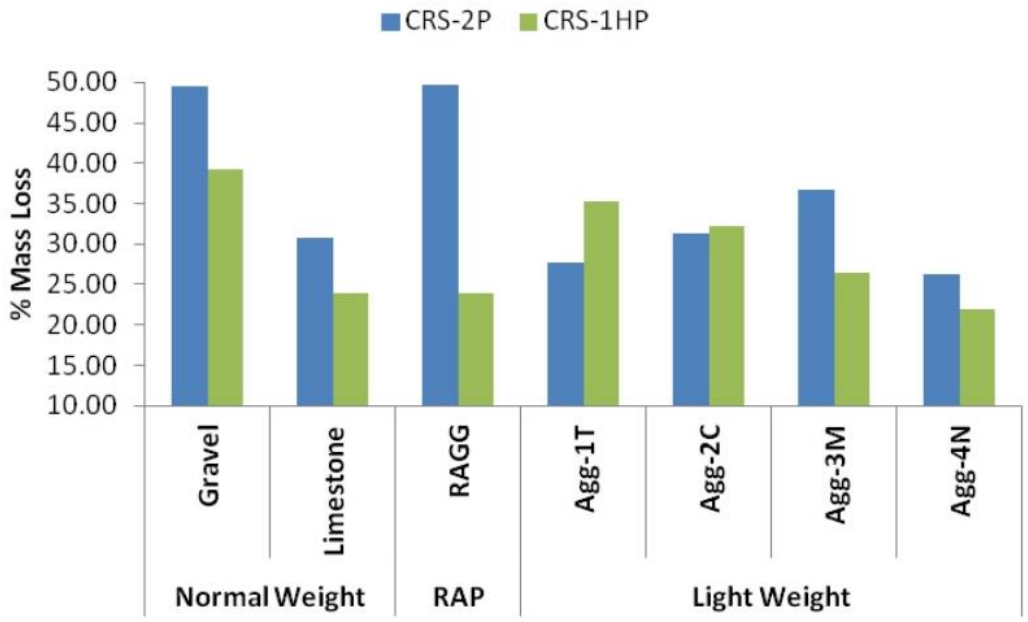

Figure 3: Effect of aggregate type on chip retention

1.4. Functions of chip seal

Chip seal was originally developed as a surface treatment for low-volume traffic roads with approximately 500-2400 vehicles/day. However, with the evolvement of preventative maintenance in the US, chip seal has further evolved into a cost effective surface-treatment and maintenance technique. Chip seal can be used as a maintenance measure to restore weathered surfaces, address bleeding, define shoulders, and prevent water intrusion into the existing pavement by sealing existing fine cracks (Brown 1988, O'Brien 1989). Fig. 5 summarizes the results of a survey representing 42 states, 12 cities, and numerous international partners about using chip seal for maintenance. Such maintenance can be used with traffic volumes higher than 7,500 vehicles per day per lane should the aggregate embedment depth is increased, the traffic is controlled at early age using pilot vehicle, and a push or vacuum sweeper is used instead of the traditional sweep methods (Shuler 1998).

Figure 4: Using chip seal as cracks sealant

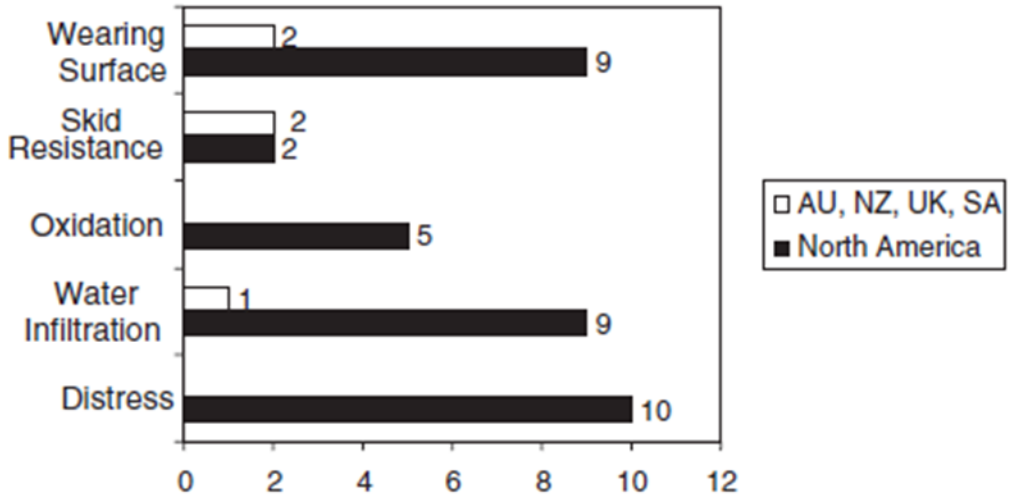

Figure 5: Maintenance reasons for using chip seal (Gransberg and James 2005)

Chip seal plays an excellent role in resisting tire-damage actions and creates a macrotexture that provides a good skid-resistant surface to ensure a safe driving atmosphere (Gransberg and James 2005). Chip seal has been widely used for road preventive maintenance (Fig.6) to avoid further surface deterioration. The affordability and easiness of application of chip seal makes it a competitive maintenance techniques (Gransberg and James 2005, Karasahin et al. 2014). A chip seal layer would cost approximately \$1.5 per yd^2 with 4 to 7 years of service. Therefore, three to four chip seal layers, may be required as pavement maintenance before a pavement can reach its design life (Asi 2007; Gransberg and James 2005; Testa et al. 2014).

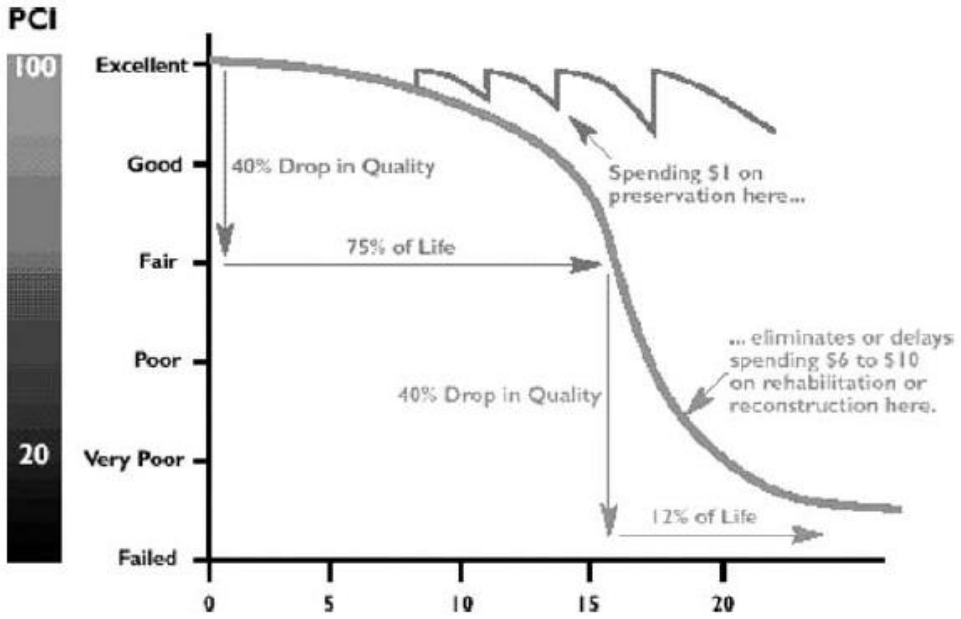

Figure 6:The concept of preventive maintenance that can be applied using chip seal (Gransberg and James 2005)

1.5. Friction resistance of chip seal

The surface texture of chip seal is an important feature linked to traffic safety, ride quality, and noise control (Yandell 1971, Forster 1981, Yandell and Sawyer 1994, Do et al. 2000). The surface texture can be categorized, based on the wavelength of the surface indentations, into unevenness, megatexture, macrotexture, and microtexture for wavelengths of 500-50000 mm, 50-500 mm, 0.5-50 mm, and 0.001-0.5 mm respectively (Fig.7).

The friction and skid resistance of pavement are strongly connected with both the macrotexture and microtexture of the pavement surface which are function of the age of pavement (Yandell 1971, Forster 1981, Yandell and Sawyer 1994, Do et al. 2000). Furthermore, the skid resistance is affected by vehicle speed, load factors, road geometry, humidity, and temperature, as well as prior accumulation of rainfall, and rainfall intensity and duration (Moore 1972, Wallman and Åström 2001, Choubane et al. 2004, Wilson and Dunn 2005, Persson 2013)

Microtexture, a fine-scale texture that describes the roughness through small prominences on grains of the stone particles' surface. Microtexture is affected by the type, component, and the manufacturing process. As shown in Fig.5, microtexture has a direct impact on adhesion

component of friction because it influences the tire-chip seal contact area. Microtexture has a major impact on skid resistance when for vehicles having speed up to 40 km/h.

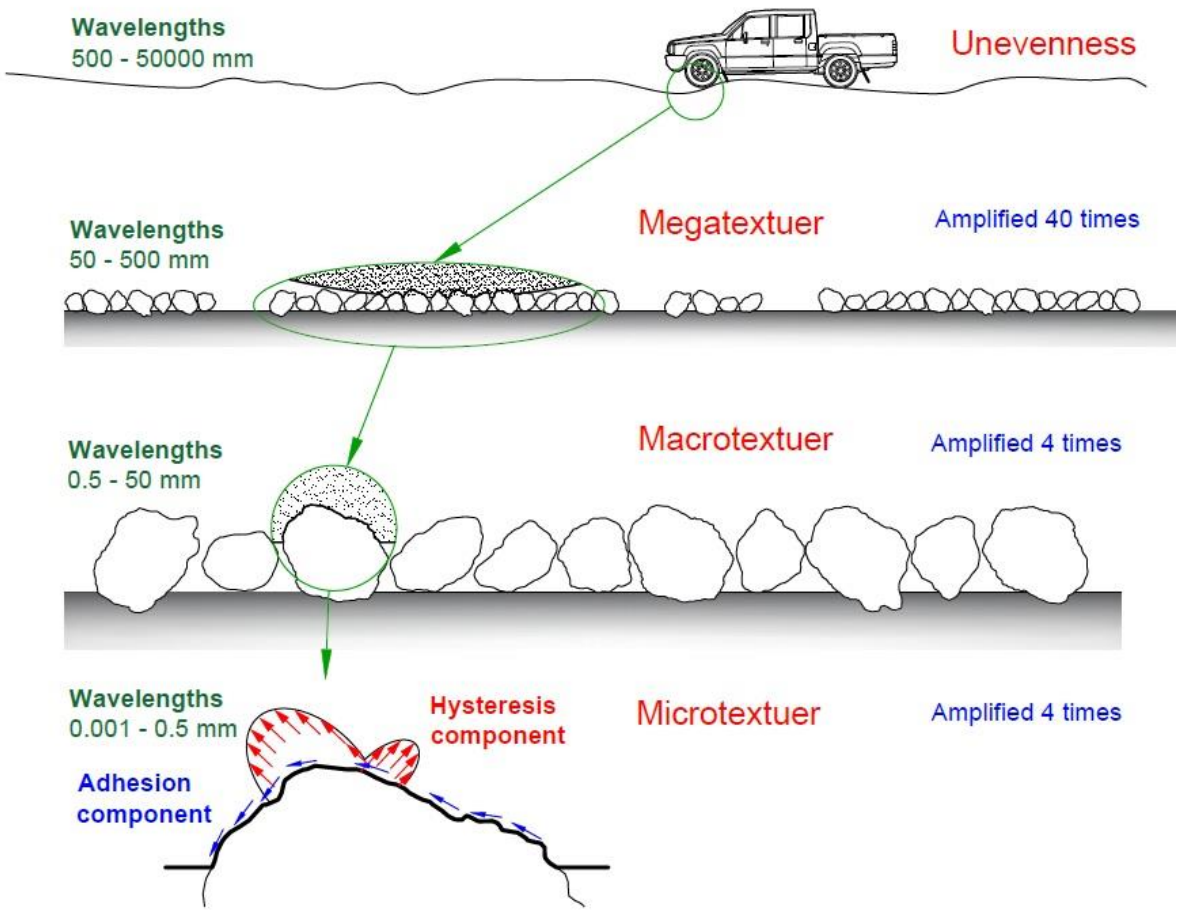

Figure 7: Simple explanation of four different surface textures

Several methods can be used to measure the microtexture of aggregates such as laser-based analysis system, aggregate imaging system (AIMS), University of Illinois aggregate image analyzer (UIAIA), and the standard test method for index of aggregate particle shape and texture (ASTM D3398).

Macrotexture, a coarse-scale texture, that caused by the organization of the aggregate particles on the chip seal surface and it can be defined as the roughness of the road surface instead of the aggregate particle itself. Macrotexture is affected by aggregate gradation, size, and shape among other parameters. Macrotexture affects the hysteretic component of the skid

resistance of vehicles which is related to the stored and dissipated energy due to the compression and decompression in vehicles' tires. As macrotexture affects the drainage of chip seal surface, it indirectly affects the adhesion components by improving the contact between the tires and chip seal particles (Henry 2000, Flintsch et al. 2003, Choubane et al. 2004). Macrotexture will control the skid resistance for vehicles having speed exceeding 40 km/h (Kotek and Kováč 2015). Megatexture and unevenness, however, do not significantly affect the skid resistance.

Macrotexture is quantified by measuring the mean texture depth (MTD). The MTD can be measured using volumetric methods such as sand patch method (ASTM E965), the Outflow Meter Test (OFT), or advanced laser technology methods including the mini texture meter, the Selcom laser system, and circular texture meter (CT Meter).

1.6. Design of chip seal

Several DOTs in the U.S. perceive chip seal as an art rather than an engineering design task. This empirical design approach typically involves experience-based in-house prescriptive requirements that have been evolved over the history of applying chip seals in a given district or region. Fewer DOTs are using the Kearby (1953), Modified Kearby (Stockton and Epps 1975), or McLeod (McLeod et al. 1969) design approaches. Chip seal design for given traffic characteristics (volume, speeds, and weight), conditions of exiting pavement, and seasonal climate conditions involves determining the appropriate chip seal type, the aggregate characteristics (size and type), and the corresponding binder type, and rate of application (Shuler 2011).

The volume of traffic plays an important role in design of chip seal. Roads having heavy traffic volumes require reduced binder rates as vehicles continue to embed the new aggregate into the existing underlying surface after the road is open for traffic. Roads and intersections that suffer from significant change in speed (traffic lights, turning movements, etc.) may impose significant demands on the aggregate leading to potential bleeding. Hence, these roads will require careful design.

1.7. Sustainability of chip seal construction

Depletion of natural resources forces the construction industry to explore using recycled material as replacements of or additives to virgin construction materials. Furthermore, transportation infrastructure is a major contributor to global greenhouse gas emissions with 23% of global carbon dioxide (CO2) emissions (Fig. 8), which makes it the second largest contributor, only behind electricity generation (Ang and Marchal 2013). Hence, there is an urgent need to partially replace virgin material with recycled material. Researches have shown that crumb rubber obtained from scrap tires can be used to replace mineral aggregate leading to more environment-friendly construction industry (Papagiannakis and Lougheed 1995, Hanson et al. 1996, Amirkhanian 2001, Shuler 2011, Rangaraju and Gadkar 2012, Moustafa and ElGawady 2015, Youssf et al. 2016).

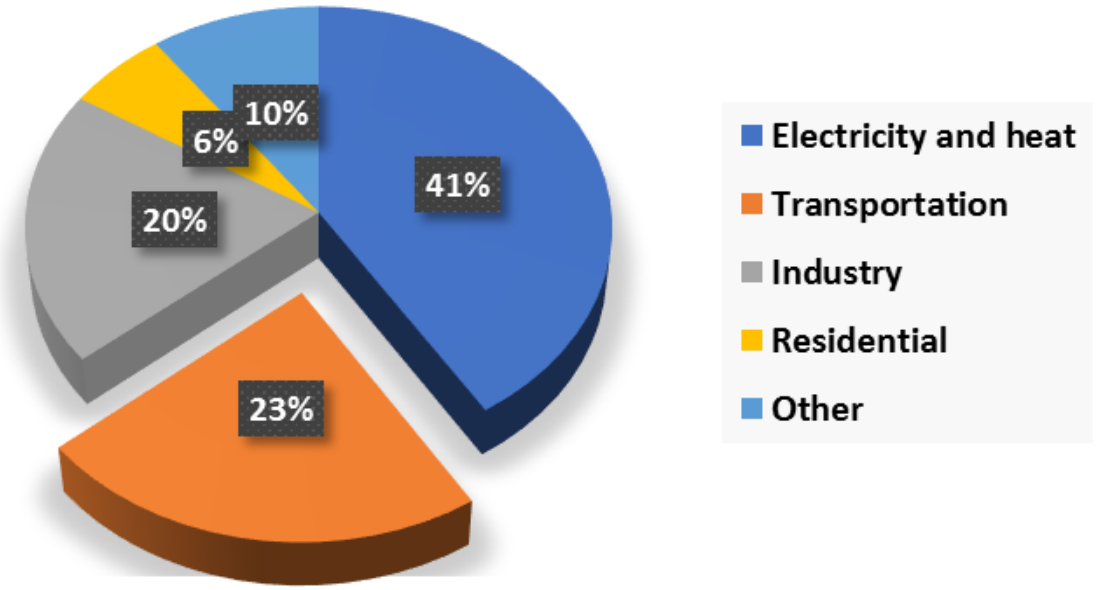

Figure 8: World CO2 emissions by sector (Ang and Marchal 2013)

The world is facing a serious problem dealing with scrap tires; as shown in Fig. 9, approximately more than four million tons of scrap tires were dumped in the U.S. during 2015 alone taking up valuable space in landfill and wasting valuable resources in the form of the rubber material, textile and metal cord (RMA 2016).

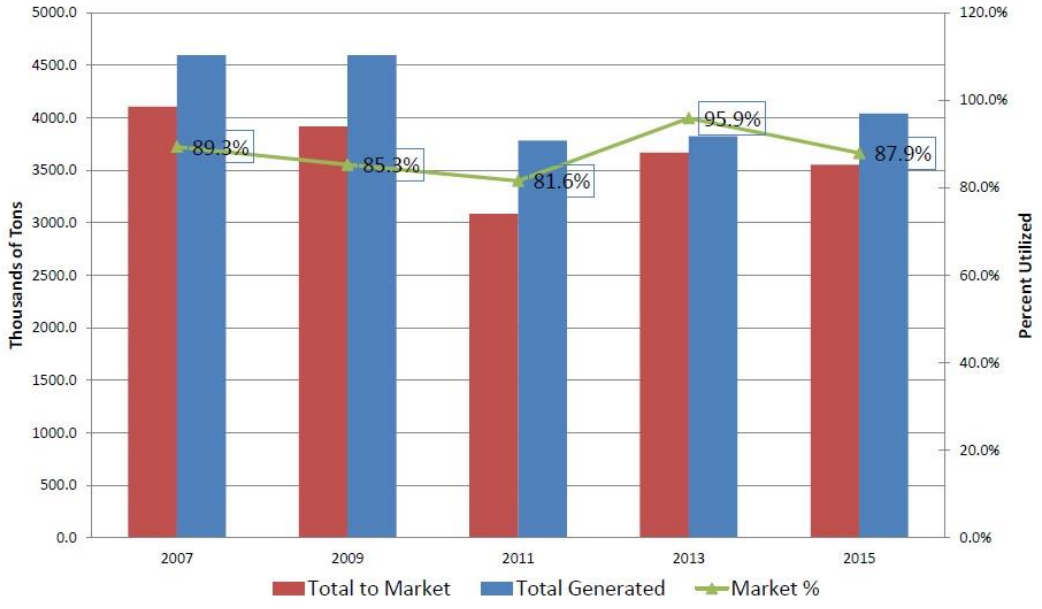

Figure 9: U.S. Scrap Tire Trends 2007 – 2015 (RMA 2016)

Fires from scrap tires release hazardous substances into the air. When the oil melts from the tires, it can seep into groundwater sources creating environmental problems and intense fires leave tremendous scarring on the land. Fig. 10 shows scrap tire dumpsite before and after burning.

(a)

(b)

Figure 10: Photo of scrap tires, Red's Tires, (a) on Nov. 2000, and (b) on March 2001

Significant portion of scrape tires used to be used fuel in cement kilns. However, there has been a marked decrease in the use of tire-derived fuel (TDF) in Missouri and across the county during the past eight years due to changes in the federal air pollution regulations. Hence, there is an opportunity to recycle scrap tires in different civil engineering applications (Fig.11).

However, this opportunity is bounded by the cost competitiveness of recycled tires and development of technical standards for using recycled tires.

One application where scrap tire material may prove to be used successfully is in the roadway construction. Previous studies used crumb rubber as asphalt binder modifier, which improves the general performance of the binders in terms of temperature susceptibility, viscosity, and stiffness (Lee et al. 2008, Presti 2013). However, there has been no research on using crumb rubber as an aggregate in chip seal which, if successful, will significantly increase the sustainability of chip seal.

Figure 11: Photo of a mountain of shredded scrap tires, April 2011

1.8. Project scope

This project investigates using crumb rubber as a partial and full replacement of mineral aggregates in chip seal construction. The resulting chip seal is more environment-friendly than the conventional one. Furthermore, replacing mineral aggregates in chip seal with crumb rubber aggregate will potentially address several issues linked to using mineral aggregates in chip seal. Mineral aggregate when dislodged represents a serious safety issue to vehicles and human beings. Mineral aggregate chip seal features noisy driving. In addition, it is a common practice in the U.S. to apply a fog seal to finished chip seal to hide its rocky color and display a dark color for better perception by the local community at the chip seal site. The applied fog increases the pavement cost and reduces the pavement friction. Hence, the crumb rubber aggregate will potentially address all three issues.

Chip seal with two different types of mineral aggregates, two types of emulsions, and two types of cement asphalt was investigated during this study. In addition, this study proposes

improvements to two of the aggregate retention tests (i.e., sweep and Vialit tests) in order to be more representative of the in-service conditions of chip seal. Both macrotexture and microtexture of chip seal were investigated and their link to skid resistance of chip seal is discussed. In addition, this report presents an extensive study on the design of chip seal and finding the optimum aggregate embedment depth. Finally, leaching of crumb rubber aggregate used in chip sealed was investigated.

This report includes two parts: part 1 includes the mechanical and physical characterization of rubberized chip seal, part 2 includes leaching studies of rubberized chip seal. The first part including five chapters and appendix. Chapter 1 presents an introduction to chip seal, scrape tire issue, and scope of work. Chapter 2 presents the experimental work including material characterization and different tests carried out on chip seal specimens. Chapter 3 presents the results of experimental investigation of the chip seal specimens. Chapter 4 presents field implementation of the rubberized chip seal to two sections. Chapter 5 presents the conclusions and recommendations for the mechanical characterization of chip seal having scrap rubber as an aggregate. Appendix A presents extra data and pictures for the different tests and characterization. The second part includes five chapters. Chapter 1 is an introduction to the leaching study. Chapter 2 presents the objectives of the leaching study. Chapter 3 introduces the experimental work. Chapter 4 presents the experimental work. Chapter 5 introduces the conclusions for the leaching study.

2. Experimental program

2.1 Material characterization and properties

Two types of asphalt cement, namely PG 64-28 and PG 70-28, and two types of emulsions, namely CRS-2P and CHFRS-2P, were used during this study. Hereinafter, these two asphalt cement and two emulsions will be referred as binder 1, binder 2, emulsion 1, and emulsion 2, respectively. Tables 1 and 2 summarize the properties of these emulsions and asphalt cement. Both emulsion 1 and emulsion 2 are Cationic, which is defined as the migration of asphalt particles under an electric field towards the cathode (negative electrode). Emulsion 1 is a rapid-setting and high-viscous type, while emulsion 2 is a high-float, rapid-setting, high-viscous type.

The main difference between the two asphalt cement types is the softening temperature. The main difference between asphalt cement and emulsion is the water content and other admixtures such as emulsifiers that keep the emulsions flowable and workable at a low temperature of 35 ^{o}C compared to 165 ^{o}C for asphalt cement. Table 1 and 2 summarizes the properties of the used and emulsions asphalt cement.

The water breakout of the emulsions was examined for weight loss during exposure time at room temperature of 35 ^{o}C, as shown in Fig. 12. The figure shows that approximately 81% of the water breakout occurred after 6 hours for the both types of emulsions, while there was almost no evaporation after 24 hours of exposure.

Table 1: Emulsions properties

Properties	**Test Method**	CRS-2P		CHFRS-2P	
		Min	**Max**	**Min**	**Max**
Viscosity, SFS @ 122°F	ASTM D-7496	100	300	100	400
Sieve Test, %	ASTM D-6933		0.3		0.1
Demulsibility, % 35 mls 0.8% sodium dioctyl sulfosuccinate	ASTM D-6936	40		60	
Storage Stability, 1 day, %	ASTM D-6930		1		1
Particle Charge	ASTM D-7402	Positive		Positive	
Distillation Test:					
Residue by distillation, % by weight	ASTM D-244	65		65	
Oil Distillate, % by volume of emulsion	ASTM D-6997		3		0.5
Tests on Residue from Distillation:					
Polymer content, wt. % (solids basis)		3		3	
Penetration, 77°F, 100g., 5 secs.	ASTM D-5	100	150	80	130
Viscosity, 140°F, poise	ASTM D-2171	NA	NA	1300	
Solubility in TCE, %	ASTM D-2042	NA	NA	95	
Elastic Recovery, 50°F., %	ASTM D-6084	60		65	
Softening Point, °C,	ASTM D-36			54	
Float Test, 60°C, secs.	ASTM D-139			1800	
Ductility, 39.2°F., 5 cm/min, cms	ASTM D-113	30			

Table 2: Asphalt cement properties

Properties		**Test Method**	**Spec.**	**Results**	
				PG 64-28	PG 70-28
Flash Point, °C		AASHTO T 48	230 min.	307	311
Rotational Viscosity, Pa·s	@ 135°C	AASHTO T 316	3.0 max.	0.718	0.829
	@ 165°C		Report	0.217	0.245
Specific Gravity	@ 15.6°C	AASHTO T 228	Report	1.027	1.034
Density, lbs/gal				8.55	8.61
Dynamic Shear kPa	@ 64°C	AASHTO T 315	1.0 min.	1.40	1.26
Separation Test, 163°C, 48 hrs,		ASTM D 5976	---	---	---
Top Softening Point, °C			Report	52.2	62.2
Bottom Softening Point, °C			Report	52.2	62.2
Difference, °C			2 max	0.0	0.0
After RTFOT					
Mass Loss, %		AASHTO T 240	1.0 max.	0.476	0.572
Dynamic Shear kPa	@ 64°C	AASHTO T 315	2.2 min.	3.12	3.15
Elastic Recovery, 10 cm, cut immed. %	@ 25°C	ASTM D 6084	45 min.	81.0	81
Pressure Aging Residue (100°C, 300 psi, 20 hr.)		AASHTO R 28			
Dynamic Shear kPa	@ 22°C	AASHTO T 315	5,000 max.	2,510	2163
Creep Stiffness, Stiffness, MPa (60 sec.)	@ -18°C	AASHTO T 313	300 max.	166	243
m Value			0.300 min.	0.345	0.308

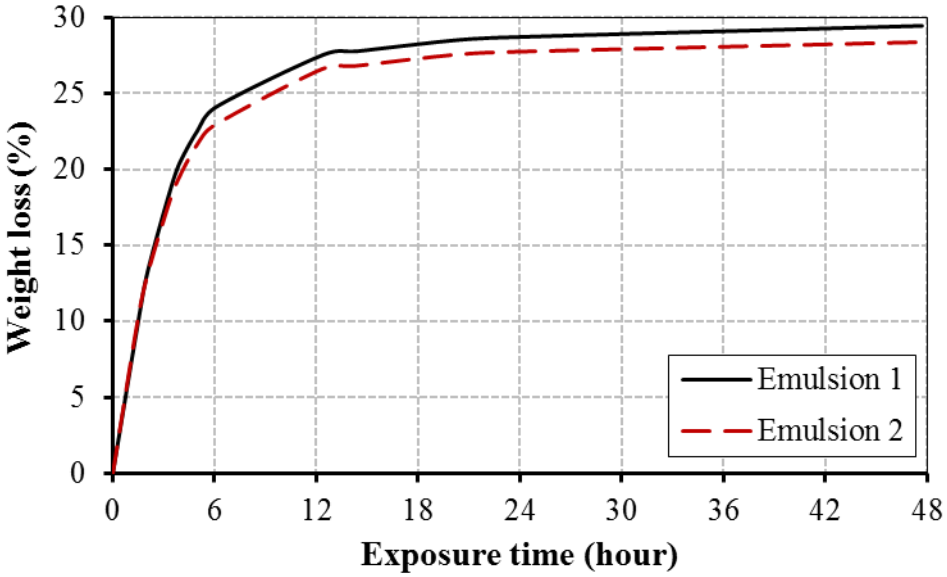

Figure 12: Emulsion weight loss due to water breakout

Two types of mineral aggregates, namely creek gravel, and trap rock were used during this study (Fig.13a&b). Hereinafter these two types will be referred as aggregate 1, and aggregate 2, respectively. A third synthetic aggregate, crumb rubber, obtained from recycled tires was used during this study (Fig. 13c). Two grades for each aggregate type were used during this study with a contribution of 50% of each grade. The first grade was aggregate passing the 9.5 mm (0.37 in.) sieve and retained on the 6.3 mm (0.25 in.) sieve. The second grade was aggregate passing the 6.3 mm (0.25 in.) sieve and retained on the 4.75 mm (0.19 in.) sieve. Fig. 14 and Table 3 present the sieve analysis and properties of the three types of aggregates, respectively. As shown in Table 3, the rubber had much higher Micro-Deval and Los Angeles abrasion resistance compared to the other two types of mineral aggregates.

(a) (b) (c)

Figure 13: Aggregates used throughout this study (a) creek gravel, (b) trap rock, and (c) crumb rubber

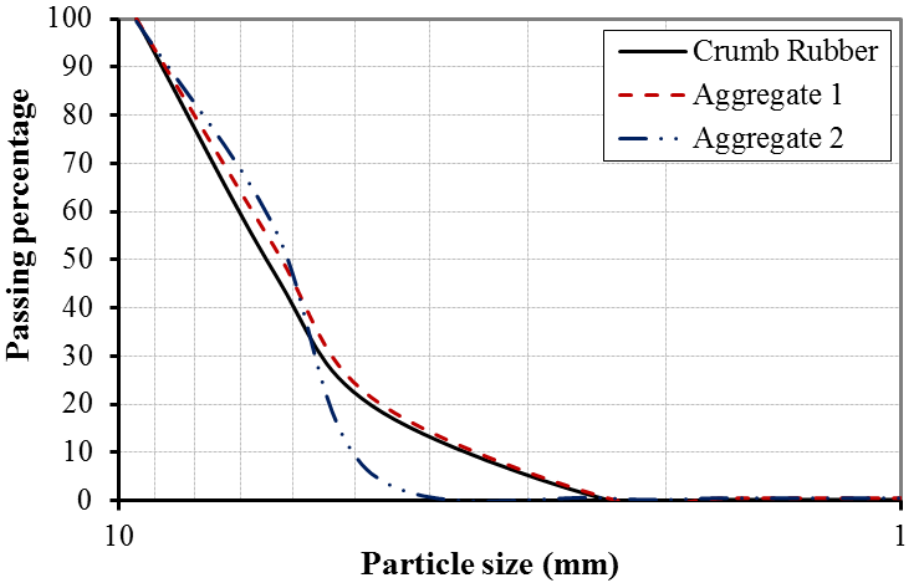

Figure 14: Sieve analysis of the aggregates

Table 3: Aggregates properties

Type of Aggregate		Rubber	Aggregate 1 (creek aggregate)	Aggregate 2 (crushed trap rock)
Bulk specific gravity		0.87	2.35	2.62
Absorption, %		0.1%	4.7%	0.8%
Coefficient of Uniformity		1.9	1.9	1.3
Fractured faces	Percent of non-fractured faces	0.0%	4.6%	0.0%
	Percent of faces with one or more faces	100.0%	95.4%	100.0%
	Percent of faces with two or more faces	88.7%	93.1%	100.0%
Loose dry unit weight, kg/m^3		423	1,180	1,249
Voids in loose aggregates, %		15.4	49.8	52.8
Los Angeles loss by abrasion and impact, %		0.3%	18.7%	8.2%
Micro-Deval weight loss, %		0.0%	6.0%	2.1%
Materials passing No. 200 sieve, %		0.20%	0.50%	0.52%
Median particle size, mm		6.5	6.2	6.1
Flakiness index, %		31.3%	37.6%	42.0%

All the used aggregate types had approximately the same median size of approximately 6.3 mm with max. aggregate size of 9.5 mm (3/8”). The crumb rubber had a low bulk specific gravity of 0.87, which was approximately 37% and 33% of that of aggregates 1 and 2, respectively. Furthermore, the crumb rubber had a dry unit weight of 423 kg/m^3 that was approximately 36% and 34% of that of aggregates 1 and 2, respectively. Aggregate 1 had a water absorption of 4.7% which is 488% higher than that of aggregate 2. The water absorption of the crumb rubber was negligible. The dust, materials passing No. 200 sieve, in the three aggregate types ranged from 0.20% to 0.52% with the crumb rubber having the lowest percentage of dust followed by aggregate 1, aggregate 2, respectively. The crumb rubber and aggregate 2 had higher fractured faces than aggregate 1 because they went through the cutting process during the production while aggregate 1 had the smoothest face due to the continuous flow of water during its formation in the creek.

The flakiness index, defined as the percentage by weight of the used aggregates whose least dimension is less than three-fifths of its mean dimension, is another important factor in the design of chip seal. The lower the flakiness index is the better aggregate. The flakiness indices of the aggregates ranged from 31.3% to 42% with aggregate 2 had the highest index followed by aggregate 1 and crumb rubber, respectively.

2.2 Design of chip seal specimens

There is no consensus in the U.S. on how to design a chip seal. A recent survey includes 54 U.S. states and cities showed that only 18% of respondents use McLeod, Kearby, and modified Kearby methods to design chip seal while 26% of the respondents do not use a formal design method. The remaining 56% of the respondents use their local, empirical, or past experience design approach (Gransberg and James 2005). The goal of all these design approaches is to determine the aggregate application rate to form a blanket of one stone in depth and determine the corresponding asphalt binder application rate to satisfy a given aggregate embedment depth ranging from 50% to 80% of the median aggregate size.

The test specimens during the course of this study were first designed using different approaches. McLeod method resulted in aggregate application rates of 7.4 kg/m^2 (13.7 lb/yd^2), 7.8 kg/m^2 (14.4 lb/yd^2), 3.0 kg/m^2 (5.5 lb/yd^2) for for aggregate 1, aggregate 2, and crumb rubber, respectively. Kearby and modified Kearby methods resulted in aggregate application rates of 7.05 kg/m^2 (13 lb/yd^2), 7.65 kg/m^2 (14.1 lb/yd^2), 2.71 kg/m^2 (5.0 lb/yd^2) for aggregate 1, aggregate 2, and crumb rubber, respectively. Furthermore, the ASTM D7000-11 (ASTM 2011) provides equation 1 for determining the aggregate application rate for sweep test.

$$Aggregate\ weight\ \left(\frac{kg}{m^2}\right) = \left(\frac{A\ (202.1\ X - 15.8)}{100} + \frac{B\ (146.4\ X - 4.7)}{100}\right) * \frac{1}{61.6} \qquad (1)$$

where A is the percentage of the aggregate with grade 1 from 9.5 to 6.3 mm, B is the percentage of the aggregate grade 2 from 6.3 to 4.75 mm, and X is bulk specific gravity. Equation 1 resulted in application rates of 7.4 kg/m^2 (13.6 lb/yd^2), 8.2 kg/m^2 (15.1 lb/yd^2), 2.7 kg/m^2 (5.0 lb/yd^2) for aggregate 1, aggregate 2, and crumb rubber, respectively. Since the results of equation 1 were more conservative than the other two approaches, except for the rubber case compared to the

McLeod method, it was decided to use the aggregate application rate resulting from equation 1 throughout this research.

Determining the binder rate of application is more challenging as there are more discrepancies between the different approaches. The main reason behind this discrepancy is the time to achieve the design aggregate embedment depth. For example, McLeod assumed that the design aggregate embedment depth will be satisfied after two years of service. This, generally, will result in a smaller binder application rate compared to Kearby and Modified Kearby approaches. McLeod, Kearby, and modified Kearby design approaches resulted in emulsion application rates of 1.0 liter/m^2 (0.22 gal/yd^2), 2.22 liter/m^2 (0.49 gal/yd^2), and 2.22 liter/m^2 (0.49 gal/yd^2), respectively.

To validate the application rate results, a trial and error approach was adopted during the experimental work. A rectangular mold having a height equal to the average least dimension (ADL) was used around the chip seal sample to find experimentally the required binder application rate that exactly fills the mold after spreading and compacting the aggregate. After several trials, a binder application rate of 2.13 liter/m^2 (0.47 gal/yd^2) was found to fill the mold with emulsion after placing and compacting the aggregate. Assuming the emulsion had 30 to 35% water content (McLeod et al. (1969) and Wood et al. (2006)), the selected emulsion application rate will result in 70% to 65% aggregate embedment ratio after emulsion's water brock out. The experimentally calculated emulsion rate was in a good agreement with that calculated using Kearby's approach. Hence, the empirical value of the emulsion application rate was used throughout this experimental work. For specimens where asphalt cement binders were used, the binder application rate was adjusted to address he water content of the emulsion, which equal to 30%, and then was used.

Once the binder and aggregate application rates were determined, the required specimens were prepared using aggregate having median sizes of 6.2 mm (0.244 inch), 6.1 mm (0.24 inch), 6.5 mm (0.256 inch) for aggregate 1, aggregate 2, and crumb rubber, respectively.

2.3 Standard and modified sweep tests

During the construction of a chip seal roadway, the pavement surface should be swept after compacting the aggregates to remove any loose aggregates or dust before opening the road for transportation. During this research, a standard sweep test was conducted according to ASTM D7000-11 on chip seal specimens with ten different combinations to investigate the sweeping effect on them after the standard time of curing for 1 hour. However, since the 1 hour curing time might not be enough time during field implementation to justify opening the road, this study carried out a sweep test at curing times of 3, 6, 24, and 72 curing hours. Other 40 chip seal specimens were tested under the modified sweep test. Hence, 50 specimens were investigated during the standard and modified sweep test. Three types of aggregate and two types of emulsions were examined in this task as listed in Table 4. The two types of asphalt cement were not examined during the sweep tests because of the difficulty of dealing with them at the ambient temperature as they harden very quickly.

Each emulsion was covered with crumb rubber only, aggregate 1 only, aggregate 2 only, or a combination of 50% crumb rubber and 50% of either aggregate 1 or 2. Table 5 presents the weight of each aggregate type in each mix calculated using Equation 1 (ASTM D7000-11). As it is presented in table 5, the volume of each mix of aggregate was constant regard less the rubber replacement ratio. This volume was calculated to provide one layer of aggregate on the asphalt felt with least amount of voids.

Table 4: Specimens variables of the standard and modified sweep tests

Groups	Specimen label	Type of test	Curing time (hours)	Emulsion type	Percentage of the Aggregate type (by volume)			Weight loss (%)
					Rubber	Aggregate 1	Aggregate 2	
Group A	CS-1	Standard sweep test	1	Emulsion 1	100%	0%	0%	58.9%
	CS-2				50%	50%	0%	50.0%
	CS-3				50%	0%	50%	49.9%
	CS-4				0%	100%	0%	39.9%
	CS-5				0%	0%	100%	43.7%
	CS-6			Emulsion 2	100%	0%	0%	54.9%
	CS-7				50%	50%	0%	44.5%
	CS-8				50%	0%	50%	43.5%
	CS-9				0%	100%	0%	34.4%
	CS-10				0%	0%	100%	35.8%
Group B	CS-11	Modified sweep test	3	Emulsion 1	100%	0%	0%	32.4%
	CS-12				50%	50%	0%	22.5%
	CS-13				50%	0%	50%	28.2%
	CS-14				0%	100%	0%	10.2%
	CS-15				0%	0%	100%	23.1%
	CS-16		6		100%	0%	0%	20.6%
	CS-17				50%	50%	0%	11.1%
	CS-18				50%	0%	50%	10.7%
	CS-19				0%	100%	0%	6.6%
	CS-20				0%	0%	100%	8.1%
	CS-21		24		100%	0%	0%	13.4%
	CS-22				50%	50%	0%	9.6%
	CS-23				50%	0%	50%	7.7%
	CS-24				0%	100%	0%	5.0%
	CS-25				0%	0%	100%	4.9%
	CS-26		72		100%	0%	0%	10.7%
	CS-27				50%	50%	0%	7.3%
	CS-28				50%	0%	50%	6.9%
	CS-29				0%	100%	0%	3.4%
	CS-30				0%	0%	100%	3.3%
	CS-31		3	Emulsion 2	100%	0%	0%	35.4%
	CS-32				50%	50%	0%	20.7%
	CS-33				50%	0%	50%	28.8%
	CS-34				0%	100%	0%	13.3%
	CS-35				0%	0%	100%	19.3%
	CS-36		6		100%	0%	0%	22.3%
	CS-37				50%	50%	0%	9.9%
	CS-38				50%	0%	50%	12.2%
	CS-39				0%	100%	0%	4.6%
	CS-40				0%	0%	100%	6.4%
	CS-41		24		100%	0%	0%	11.3%
	CS-42				50%	50%	0%	6.3%
	CS-43				50%	0%	50%	6.9%
	CS-44				0%	100%	0%	3.3%
	CS-45				0%	0%	100%	3.3%
	CS-46		72		100%	0%	0%	8.6%
	CS-47				50%	50%	0%	5.2%
	CS-48				50%	0%	50%	5.5%
	CS-49				0%	100%	0%	3.2%
	CS-50				0%	0%	100%	3.2%

Table 5: Specimens variables of the standard and modified sweep tests

Sweep test mixes	Rubber (gm)	Aggregate 1 (gm)	Aggregate 2 (gm)	Total volume (cm^3)
0% Rubber & 100% Aggregate 1	0	400	0	336
50% Rubber & 50% Aggregate 1	70.5	200	0	336
100% Rubber & 0% Aggregate 1	141	0	0	336
0% Rubber & 100% Aggregate 2	0	0	446	336
50% Rubber & 50% Aggregate 2	70.5	0	223	336
100% Rubber & 0% Aggregate 2	141	0	0	336

The procedure of the sweep test started by applying and leveling 83 ± 5 gm (0.183 ± 0.011 lb) of asphalt emulsion on a standard asphalt felt disk (Fig. 15a). This was followed by spreading uniformly the required amount of aggregates (Fig. 15a). The aggregates were embedded into the emulsion using standard compactor with a minimum curved surface radius of 550 ± 30 mm (21.6 ± 1.2 inches) (Fig. 15b). The specimens were cured at 35 ^{o}C (95 ^{o}F) for the required curing times. After curing, the asphalt felt was rotated 90^{o} and the loose aggregates were removed (Fig. 15c). Then, each specimen was weighed (W_{S1}) right before the test followed by setting for 3 minutes in the sweep test mixer. Thereafter, the test mixer ran for one minute of abrasion (Fig. 15d). Any loose aggregates were removed and the specimen was weighed (W_{S2}). The percentage of the weight loss was calculated using Equation 2. Fig. 16 illustrate a sample of the investigated specimens just before placing them into the sweep test mixer.

$$Sweeping\ weight\ loss = \frac{W_{S1} - W_{S2}}{W_{S1}} \times 100 \quad (2)$$

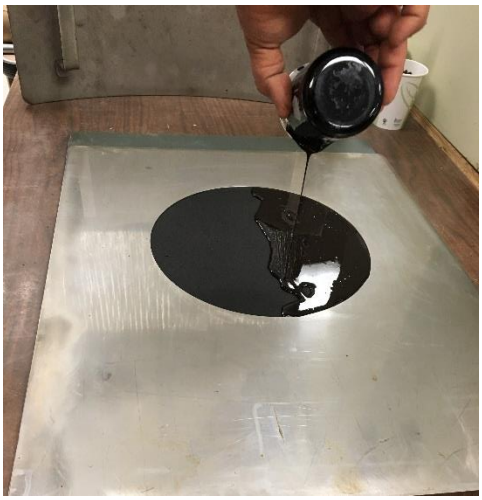

(a)

(b)

(c)

(d)

(e)

(f)

Figure 15: Sweep test (a) applying emulsion, (b) leveling emulsion, (c) applying aggregate, (d) compacting the aggregates, (e) removing excess aggregates, and (f) running the test

CS-1 CS-2 CS-3

CS-4 CS-5

Figure 16: Samples of sweep test specimens

2.4 Standard and modified Vialit tests

The Vialit test is an important test that investigates the aggregate retention in the asphalt binder of the chip seal pavements. A standard Vialit test was conducted on 12 chip seal specimens according to the British Standard 12272–3 (EN 2003) to investigate the aggregate retention, as listed in Table 6.

Table 6: Specimens variables of the standard and modified Vialit tests

Groups	Specimen label	Type of test	No. of drops	Emulsion/ Asphalt cement type	Aggregate type	Percentage of retained aggregates
Group C	CS-51	Standard Vialit Test	3	Emulsion 1	Rubber	100.0%
	CS-52				Aggregate 1	100.0%
	CS-53				Aggregate 2	100.0%
	CS-54			Emulsion 2	Rubber	100.0%
	CS-55				Aggregate 1	100.0%
	CS-56				Aggregate 2	100.0%
	CS-57			Asphalt cement 1	Rubber	100.0%
	CS-58				Aggregate 1	60.0%
	CS-59				Aggregate 2	41.0%
	CS-60			Asphalt cement 2	Rubber	100.0%
	CS-61				Aggregate 1	71.0%
	CS-62				Aggregate 2	52.0%
Group D	CS-63	Modified Vialit Test	30	Emulsion 1	Rubber	100.0%
	CS-64				Aggregate 1	88.0%
	CS-65				Aggregate 2	75.0%
	CS-66			Emulsion 2	Rubber	100.0%
	CS-67				Aggregate 1	96.0%
	CS-68				Aggregate 2	89.0%
Group E	CS-69		40	Emulsion 1	Rubber	100.0%
	CS-70				Aggregate 1	80.0%
	CS-71				Aggregate 2	68.0%
	CS-72			Emulsion 2	Rubber	100.0%
	CS-73				Aggregate 1	92.0%
	CS-74				Aggregate 2	75.0%

The procedure of the Vialit test started by applying the emulsion at 60 °C (140 °F) or asphalt cement at 165 °C (329 °F) to standard square steel pan with dimensions of 200 mm (7.8 inches) × 200 mm (7.8 inches). Thereafter, 100 aggregates with a uniform size of approximately 9.5 mm (0.375 inches) were applied in a uniform grid of 10 × 10. Then, the specimens were cured in the oven at 60 ^{o}C (140 °F) for 48 hours (Fig. 17).

(a) (b) (c)

Figure 17: Vialit test specimens with different aggregate types (a) rubber (Specimen CS-49), (b) aggregate 1 (Specimen CS-50), and (c) aggregate 2 (Specimen CS-51)

The pan was then removed from the oven and allowed to cool for 30 minutes at 25 ± 5 °C (77 ± 41 °F). Each specimen was placed after that in a freezer with a temperature below 0 ^{o}C for 30 minutes and was tested within 10 seconds after being removed from the freezer. Each steel pan was turned upside down and fixed in the test setup at four points as shown in Fig. 18. Then, a standard stainless steel ball was dropped three times from a height of 500 mm on the steel pan as shown in Fig. 18a. The fallen aggregates were counted and recorded after each impact of the ball on the steel pan. The retention percentage after each impact was then calculated.

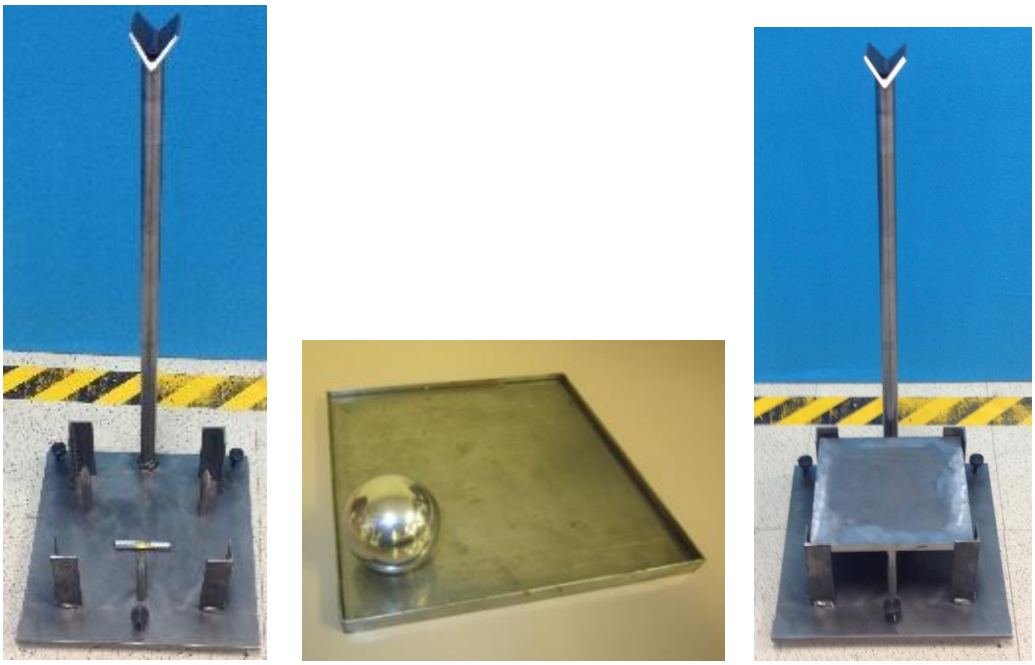

(a) (b) (c)

Figure 18: Vialit test (a) test setup, (b) testing pan and ball, and (c) specimen installed in the test setup

(a) (b) (c)

Figure 19: Specimens (a) cured at 60 °C, (b) conditioning at 25 °C, and (c) freezing at -22 °C

The standard Vialit test, which requires three drops of the stainless-steel ball on a test specimen, was adequate to distinguish the performance of the specimens made out of asphalt cement. However, it was not enough to distinguish the performance of the different specimens made out of emulsions. Therefore, a modified Vialit test was conducted by increasing the number of ball drops to 30 and 40. A total of 24 specimens were investigated for the standard and modified Vialit tests, as listed in Table 6. The three aggregates and the two emulsions were

examined under both standard and modified Vialit tests. Figs. 18b to 18e illustrate samples of the specimens and the conditions of the detached aggregates after conducting the Vialit test.

2.5 Pennsylvania test

This test was developed by Kandhal and Motter (1991) in order to evaluate the aggregate retention in asphalt emulsion. Specimens having 100% crumb rubber, 100% aggregate 1, and 100% aggregate 2 in combination with either emulsion 1 or emulsion 2 were examined under the Pennsylvania test, as listed in Table 7. However, the asphalt cement was not examined due to the difficulty of dealing with them at the ambient temperature, as they harden very quickly.

Table 7: Specimens variables of the standard Pennsylvania tests

Groups	Specimen label	Type of test	Emulsion type	Aggregate type	Knock-off Weight loss (%)
Group F	CS-75	Pennsylvania Test	Emulsion 1	Rubber	1.3%
	CS-76			Aggregate 1	8.8%
	CS-77			Aggregate 2	6.8%
	CS-78		Emulsion 2	Rubber	2.8%
	CS-79			Aggregate 1	12.0%
	CS-80			Aggregate 2	8.5%

The test primarily uses six sieves and two pans with a diameter of 200 mm (8.0 in.) and depth of 50 mm (2.0 in.), a sieve shaker, and rubber pads to prepare the specimens. The test procedure started by pouring an asphalt emulsion into a clean pan with a standard application rate of 1.13 liter/m^2 (0.25 gallon/yd^2) at 60 ^oC (140 ^oF) as shown in Fig. 20. The aggregates used during the experiment weigh (W_{P1}) 300 gm (0.66 lb).

A column of sieves was set above the pan of the emulsion and the whole assembly was inserted into the sieve shaker. The sieve shaker was inclined at 60^o and run for 5 minutes. During running the sieve shaker, the aggregates were added from the top of the sieve column passing through the different sieves until they dropped into the bottom pan that had the emulsion (Fig. 20a). This sequence ensured uniform distribution of the aggregates on top of the emulsion. Within 15 minutes, the pan was covered with a neoprene bearing pad with a diameter of 190 mm

(7.5 in.) (Fig. 20d) and placed under a constant compressive load of 8.9 kN (2,000 lbs.) using a compression machine for about 5 seconds (Fig. 20e). After compacting the aggregates, the bearing pad was removed and the pan was cured at 35 ^{o}C (95 ^{o}F) for 24 hours. After that, the pan was inverted to drop the excess aggregates. The collected aggregates were weighed (W_{P2}). The pan then was placed upside down atop of the same system of sieves that was used for filling the pan before (Fig. 20f.). Another clean pan was placed at the bottom of the sieves' column. The whole column was inserted into the sieve shaker and it was turned on for 5 minutes (Fig. 20f). The weight of the knocked-off aggregates (W_{P3}) in the bottom pan was measured. The knock-off weight loss was determined using Equation 3 and used as a representative of aggregate retention:

$$Percentage\ of\ Knock-off\ loss = \frac{W_{P3}}{W_{P1} - W_{P2}} \times 100 \quad (3)$$

(a)

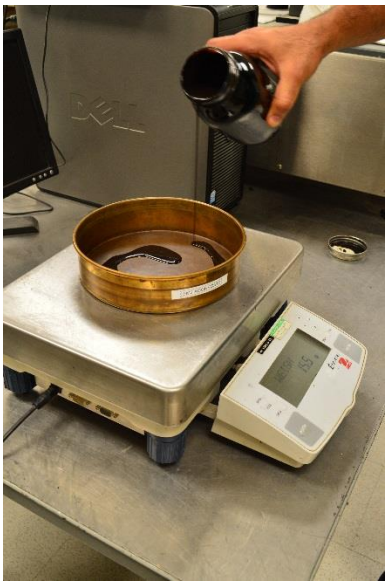

(b)

(c)

(d)

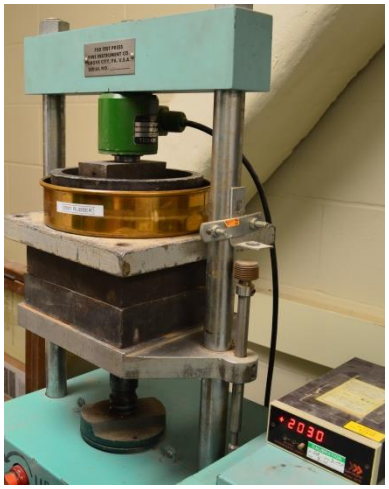

(e)

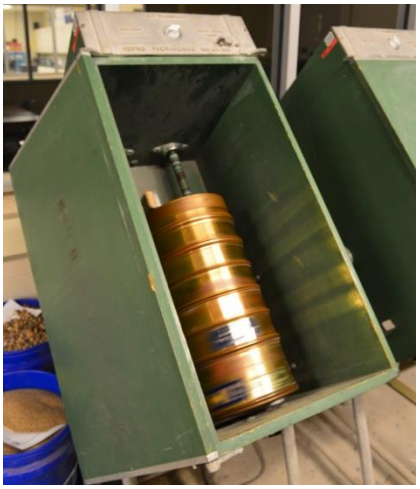

(f)

Figure 20: Pennsylvania test preparation (a) weigh the pan, (b) add the emulsion, (c) adding the aggregates, (d) using neoprene pad to cover the aggregate, (e) compacting the specimen, and (f) running the sieve shaker of the upside-down specimen

(a) (b) (c)

Figure 21: Sample of Pennsylvania test specimens with different aggregates: (a) crumb rubber, (b) aggregate 1, and (c) aggregate 2

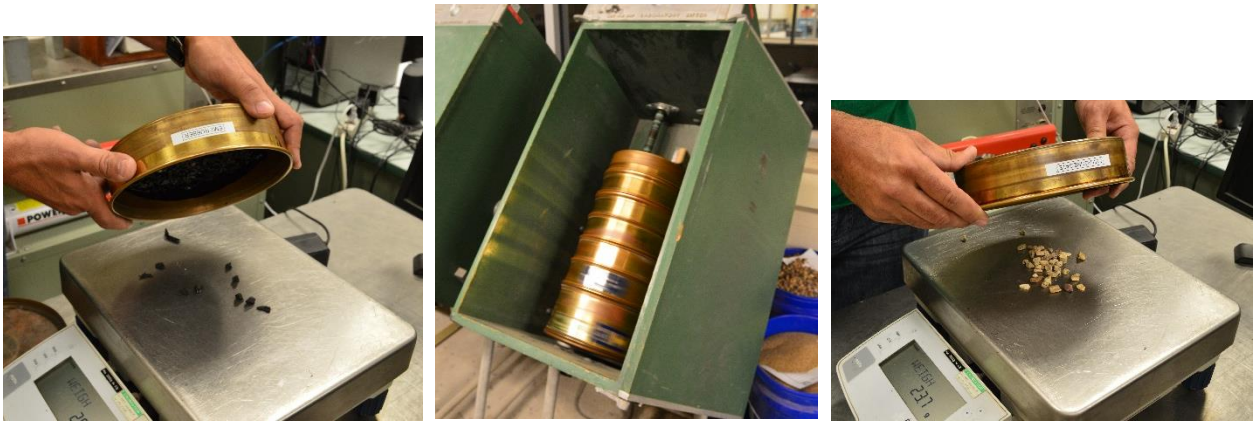

(a) (b) (c)

Figure 22: Pennsylvania test (a) initial retention loss, (b) running the sieve shaker of the upside down specimen, and (c) knock-off loss

2.6 Measuring the microtexture of chip seal

Measurement of the surface's microtexture deals with very small dimensions and it demands a high-resolution reading resulting in either expensive to do or inaccurate measurements (Masad 2007). This study used a 3D digital microscope KH-8700 to study the aggregates' microtexture. The technique can provide a quantitative data for aggregate's microtexture such as aggregate's profile lines and surface area measurements. Such measurements can be linked to the adhesion, friction, and skid resistance as discussed in the next chapter.

Crumb rubber is manufactured by either ambient or cryogenic grinding. The former is processed by tearing and shredding the recycled tires in cutting mills at ambient temperature. The cryogenic crumb rubber is processed by freezing the recycled tires followed by cracking them to the required sizes. Hence, cryogenic crumb rubber uses an excessive amount of energy

and is less economically and environmentally competitive compared to ambient crumb rubber. During this task, the microtexture surfaces of both types of rubber as well as mineral aggregates were investigated using the 3D digital microscope. Fig. 23 shows examining aggregate 1 using the KH-8700 digital microscope.

(a) (b)

Figure 23: Imaging the aggregates surfaces (a) 3D digital microscope, and (b) aggregate 1 under the microscope

2.7 Measuring the macrotexture of chip seal

During the course of this study, two different methods were used to measure the macrotexture depth (MTD). The first method is a new approach where image processing and analysis software, ImageJ™, was used to process different sections of different chip seal specimens with different types of aggregates and binder applications rate. A second approach was to use the sand patch test which is simple, economical, easy to apply, and reliable approach. High correlations were found between sand patch and circular texture (CT) Meter methods (Flintsch et al. 2003, Hanson and Prowell 2004) as well as between sand patch and Laser Profiler methods (Abe et al. 2001).

2.7.1 Image processing analysis method

Specimens of chip seal with two types of aggregate namely creek gravel and crumb rubber were prepared using different binder application rates. However, to have a better image processing, a transparent epoxy having a specific weight of 1.106 gm/cm^3 (69 lb/ft^3) was used to

prepare these specimens instead of the emulsions was used (Fig. 24). The specimens were then sectioned using a highly precise high-pressure waterjet cutting machine (Fig. 25). The sections were scanned using high-resolution scanner and then examined using ImageJ™ image processing program to determine the MTD and aggregate embedment depth per binder application rate. To determine the aggregate embedment depth, the area of the binder that was enclosed by the upper level of the binder and the base of the specimen was measured using the software (Fig. 26a). The calculated area was then divided by the length of the specimen to find the average depth of the binder and then the embedment depth. Once the aggregate embedment depth was determined, the MTD was calculated by subtracting the aggregate embedment depth from the total chip seal depth.

Figure 24: Chip seal specimens for image processing test

Figure 25: Sectioning the chip seal specimens using water jet cutter

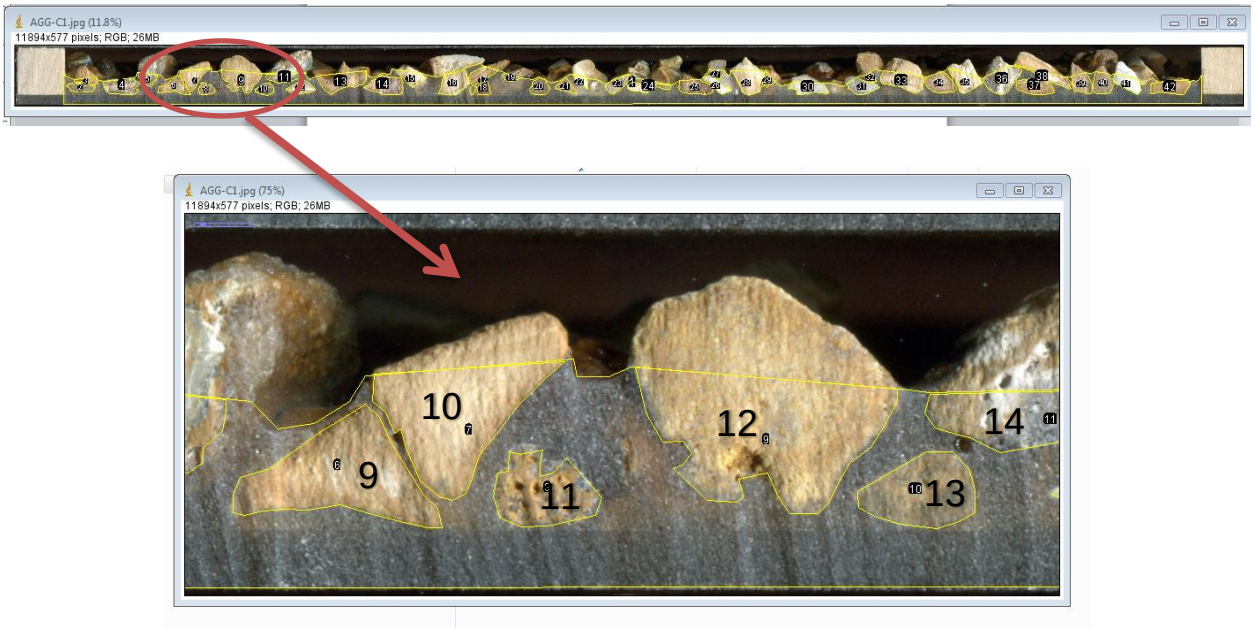

(a)

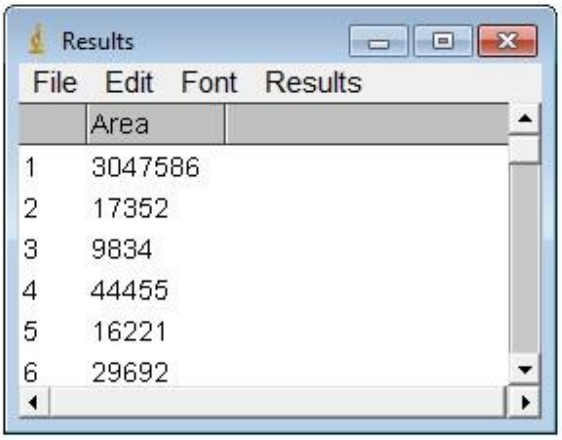

(b)

Figure 26: An example of using image processing ImageJ™ program to find the mean depth of binder (a) chip seal cross-section, and (b) surface areas of binder and embedded particles

2.7.2 Sand patch method

The sand patch specimens were prepared by applying asphalt emulsion of 150 gm (0.331lb) corresponding to binder application rate of 2.13 liter/m2 (0.47 gal/yd2) on asphalt felt disk having a diameter of 300 mm (11.8 in.). Then, the designed aggregate quantities being 516 gm (1.14 lb), 530 gm (1.17 lb), and 191 gm (0.42 lb) for aggregate 1, aggregate 2, and crumb rubber, respectively, were uniformly distributed on the surface of the test specimen. The weight of the used aggregates for each specimen corresponding to aggregate application rates of 7.4 kg/m2 (13.6 lb/yd2), 8.2 kg/m2 (15.1 lb/yd2), 2.7 kg/m2 (5.0 lb/yd2) for aggregate 1, aggregate 2, and crumb rubber, respectively. The aggregates were embedded into the emulsion using a standard compactor having a weight of 7500 gm (16.5 lb) and a minimum curved surface radius of 550 ± 30 mm (21.65 ± 1.18 inches). After compacting the aggregates, the asphalt felt was rotated 90^{o} so that the loose aggregates fell down. The specimens were then cured at 35^{o}C (95^{o} F) for 5 days followed by ambient curing for 2 days to break out all the water in the emulsion.

The standard sand patch method was used to determine the MTD of 14 specimens manufactured using the three types of aggregate and the two types of emulsions. Each emulsion was covered with either 100% of a single aggregate type or a combination of different aggregate types per Table 8. The two cement asphalt binders were not examined during these tests because of the difficulty of dealing with them at the ambient temperature as they harden very quickly.

The procedure to carry out the sand patch test was as follows. A 125 ml (7.63 in^3) of sand, passing a No. 60 sieve and retained on a No. 80 sieve was prepared in a container. Then, it was spreading uniformly on the surface of each of the investigated specimens using an ice hockey puck with its bottom surface be covered with a hard rubber material. The diameter of the spreading sand on each investigated specimen was measured at least four times in different orientations (Fig. 27d). The average diameter, D, was determined and implemented in equation 2 to determine the MTD which is an indication of the aggregate embedment depth.

$$MTD = \frac{4\,V}{\pi\,D^2} \tag{2}$$

where V is the sand volume which equals 125 ml (7.63 in^3).

Table 8: Sand patch test specimens' details and results

Specimen label	Emulsion type	Percentage of the Aggregate type			MTD, mm (inch)
		Rubber	Aggregate 1	Aggregate 2	
CS-57		100	0	0	5.21 (0.21)
CS-58		50	50	0	4.71 (0.19)
CS-59		25	75	0	4.17 (0.16)
CS-60	Emulsion 1	0	100	0	3.87 (0.15)
CS-61		50	0	50	4.78 (0.19)
CS-62		25	0	75	4.34 (0.17)
CS-63		0	0	100	4.19 (0.16)
CS-64		100	0	0	5.45 (0.23)
CS-65		50	50	0	4.87 (0.19)
CS-66		25	75	0	4.21(0.16)
CS-67	Emulsion 2	0	100	0	3.83 (0.15)
CS-68		50	0	50	4.43 (0.17)
CS-69		25	0	75	4.25 (0.17)
CS-70		0	0	100	4.06 (0.16)

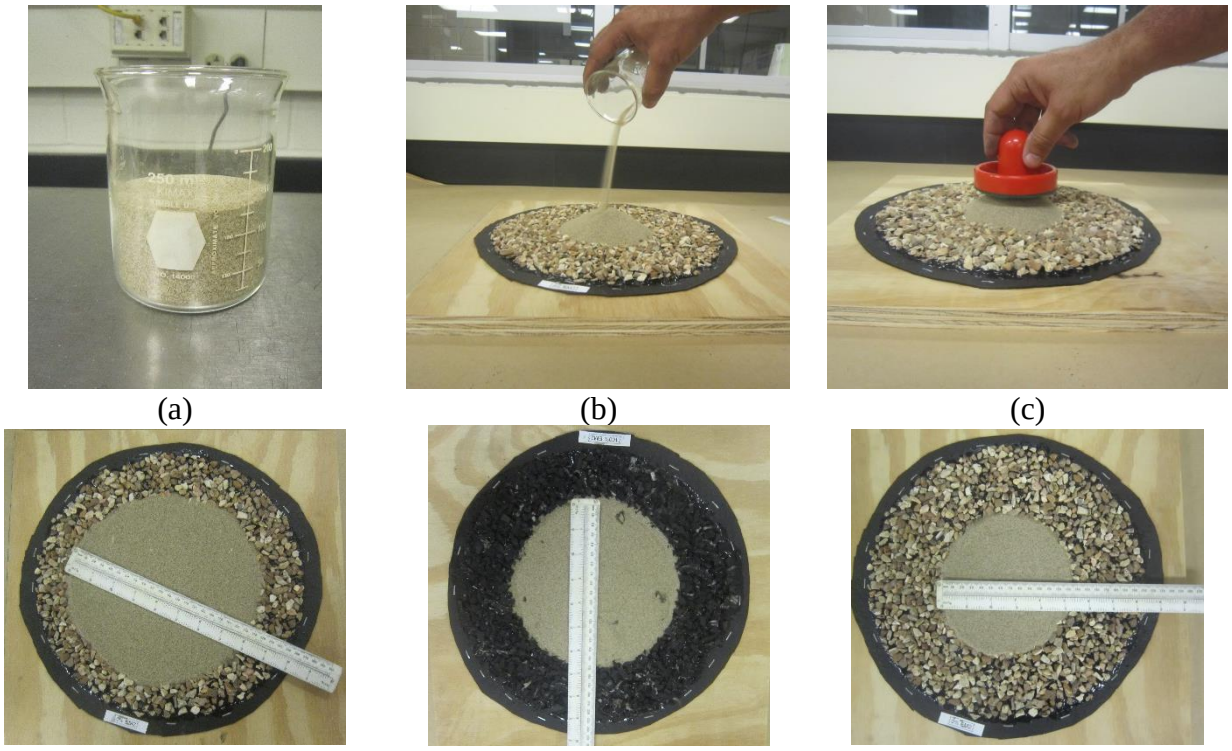

(a) (b) (c) (d)

Figure 27: Procedure of sand patch test: (a) weigh the sand, (b) applying sand, (c) distributing the sand, and (d) measuring the diameter of sand in several directions

2.8 Skid friction resistance tests

Friction resistance of chip seal is an important aspect linked to traffic safety and stopping distance as well as riding quality (Ruud 1981, Hemdorff et al. 1989). In this study, the British pendulum tester (BPT) was used to measure the friction values of different chip seal surfaces per ASTM E-303.

For the British pendulum test specimens, the required emulsion at a temperature of 60 ^{o}C (140 ^{o}F) or asphalt cement at a temperature of 160 ^{o}C (320 ^{o}F) was applied on an aluminum plate. Each aluminum plate has dimensions of 88.9 mm (3.5 in.) wide and 152.4 mm (6.0 in.) length per the requirement of ASTM E303 (Fig. 28a). Then, the appropriate aggregate quantity being 100 gm (0.22 lb), 110 gm (0.24 lb), and 37 gm (0.08 lb), representing an aggregate spread rate of 7.4 kg/m2 (13.6 lb/yd2), 8.2 kg/m2 (15.1 lb/yd2), 2.7 kg/m2 (5.0 lb/yd2) for aggregate 1, aggregate 2, and crumb rubber respectively were uniformly spread on the asphalt cement or emulsion (Fig. 28b). The aggregate was then compacted for three passes using rubber roller compactor (Fig. 28c) having a weight of 2 kg (4.4 lb), diameter of 127 mm (5 in.), and length of 152 mm (6 in.). The rubber used in the compactor have hardness type 75A. The specimens were cured at 35^{o}C (95^{o} F) for 5 days followed by ambient curing for 2 days to break out all water. Fig. 29 shows different specimens ready for testing. Twenty-eight specimens having different aggregates and asphalt combinations (Table 9) were tested.

(a)

(b)

(c)

(d)

Figure 28: Skid test specimen preparation (a) apply emulsion, (b) adding aggregates on the emulsion, (c) compacting the aggregates, and (d) cure the test specimens

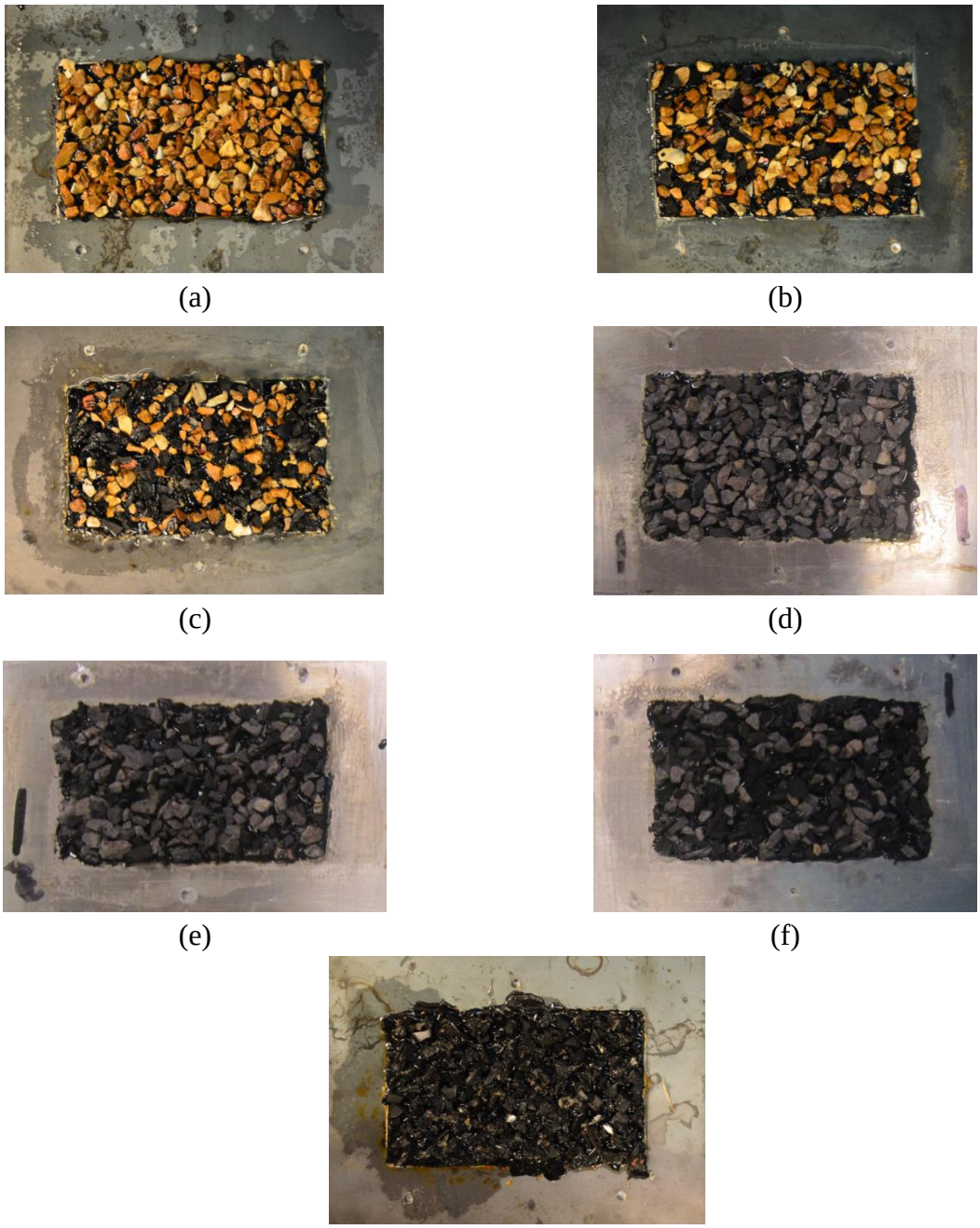

(a) (b) (c) (d) (e) (f) (g)

Figure 29: Skid test specimens ready for testing (a) 100% aggregate 1, (b) 75% aggregate 1 -25% crumb rubber, (c) 50% aggregate 1 - 50% crumb rubber, (d) 100% aggregate 2, (e) 75% aggregate 2 - 25% crumb rubber, (f) 50% aggregate 2 - 50% crumb rubber, and (g) 100

Table 9: Standard skid test specimens' details and results

Specimen label	Emulsion type	Percentage of the aggregate types			BPN
		Rubber	Aggregate 1	Aggregate 2	
CS-1	Emulsion 1	100	0	0	59.5
CS-2		50	50	0	61.0
CS-3		25	75	0	64.0
CS-4		0	100	0	69.0
CS-5		50	0	50	64.2
CS-6		25	0	75	66.4
CS-7		0	0	100	67.4
CS-8	Emulsion 2	100	0	0	51.8
CS-9		50	50	0	55.4
CS-10		25	75	0	60.0
CS-11		0	100	0	64.8
CS-12		50	0	50	61.6
CS-13		25	0	75	62.8
CS-14		0	0	100	63.2
CS-15	Asphalt cement 1	100	0	0	59.0
CS-16		50	50	0	65.2
CS-17		25	75	0	66
CS-18		0	100	0	68
CS-19		50	0	50	64
CS-20		25	0	75	70
CS-21		0	0	100	76.6
CS-22	Asphalt cement 2	100	0	0	56.5
CS-23		50	50	0	64
CS-24		25	75	0	64
CS-25		0	100	0	65
CS-26		50	0	50	62
CS-27		25	0	75	67.5
CS-28		0	0	100	75.2

Each specimen was screwed into a plywood table and the pendulum was positioned to barely contact the specimen surface (Fig. 30). The pendulum was vertically adjusted in order to achieve a slider contact path on the chip seal surface of 125 ± 1.6 mm (5 ± 1/16 inch). The distance between the center of gravity of the pendulum and the center of oscillation was 411 ± 5 mm (16.2 ± 0.2 in.). Water was sprinkled on the specimen surface before running the test per the ASTM E-303. After releasing the pendulum, the British Pendulum Number (BPN) was recorded and used to represent the friction resistance of the surface. The test was repeated four times after one trial test to get the average BPN for each specimen.

In addition to the standard procedure, two independent modifications were carried out on the standard test procedure to investigate the effects of chip seal surface moister, and temperature. A set of tests was conducted on specimens having dry surfaces to investigate the effects of moisture content on the performance of chip seal. Another set of specimens was carried out where the temperature of the aluminum plate of each specimen was increased to 65 ^{o}C (149 ^{o}F) (Fig.30c) which represents the worst-case scenario occurred in the asphalt pavements in the U.S. (Mohseni 1998). A controlled heat coil was connected to each aluminum plate underneath the chip seal specimens to increase the temperature of the plate and hence the chip seal specimens as shown in Fig 30c. Then, the BPT was used to run the skid friction resistance test. Thirty-two specimens were tested during the modified tests as listed in Tables 10 and 11.

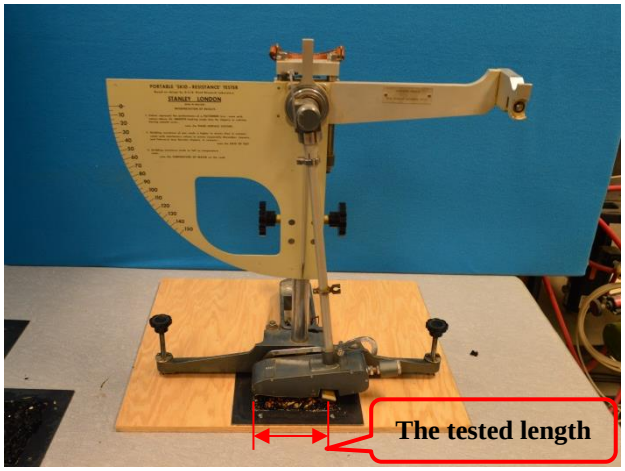

(a)

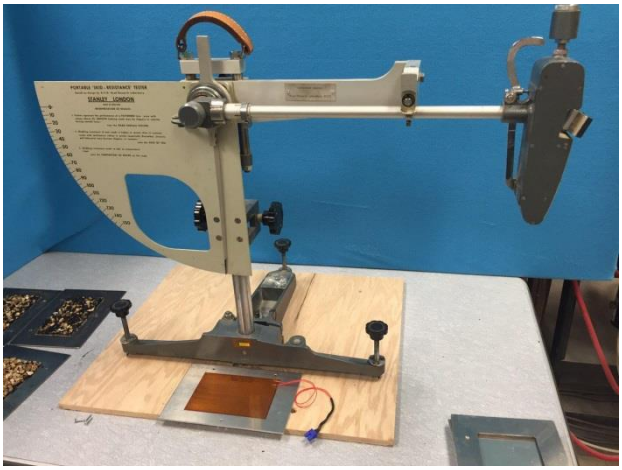

(b)

(c)

Figure 30: Skid test procedure: (a) adding aggregates on the emulsion, (b) compacting the aggregates, (c) applying the test, (d) heating chips, and (e) temperature measurement of the specimen

Table 10: Skid test reference specimens' details and results

Specimen label	Emulsion type	Percentage of the Aggregate type			BPN
		Rubber	Aggregate 1	Aggregate 2	
CS-29	Emulsion 1	100	0	0	77.8
CS-30		50	50	0	90.0
CS-31		25	75	0	91.3
CS-32		0	100	0	94.5
CS-33		50	0	50	83.2
CS-34		25	0	75	85.0
CS-35		0	0	100	87.8
CS-36	Emulsion 2	100	0	0	69.0
CS-37		50	50	0	84.0
CS-38		25	75	0	85.5
CS-39		0	100	0	90.0
CS-40		50	0	50	82.2
CS-41		25	0	75	83.4
CS-42		0	0	100	87.0
CS-43	Binder 1	100	0	0	80.0
CS-44		50	50	0	84.2
CS-45		25	75	0	85.0
CS-46		0	100	0	86.8
CS-47		50	0	50	85.0
CS-48		25	0	75	90.0
CS-49		0	0	100	99.0
CS-50	Binder 2	100	0	0	65
CS-51		50	50	0	74
CS-52		25	75	0	75
CS-53		0	100	0	75
CS-54		50	0	50	70
CS-55		25	0	75	75
CS-56		0	0	100	85

Table 11: Skid test specimens' details and results for dry surface at 65 ^{o}C

Specimen label	Surface condition	Emulsion type	Percentage of the Aggregate type			BPN	Loss in BPN
			Rubber	Aggregate 1	Aggregate 2		
CS-57	Dry and temperature of 65 ^{o}C	Emulsion 1	100	0	0	78.0	0
CS-58			50	50	0	83.0	7.8
CS-59			25	75	0	83.3	8.8
CS-60			0	100	0	85.0	10.1
CS-61			50	0	50	79.0	5.0
CS-62			25	0	75	79.5	6.5
CS-63			0	0	100	80.0	8.8
CS-64		Emulsion 2	100	0	0	69.0	0
CS-65			50	50	0	83.0	1.2
CS-66			25	75	0	83.5	1.3
CS-67			0	100	0	86.3	4.2
CS-68			50	0	50	81.5	0.9
CS-69			25	0	75	82.0	1.7
CS-70			0	0	100	85.0	2.3
CS-71		Binder 1	100	0	0	80.0	0
CS-72			50	50	0	84.2	0
CS-73			25	75	0	84.0	1.2
CS-74			0	100	0	84.8	2.3
CS-75			50	0	50	85.0	0
CS-76			25	0	75	89.0	1.1
CS-77			0	0	100	97.0	2.0
CS-78		Binder 2	100	0	0	65.0	0
CS-79			50	50	0	74.0	0
CS-80			25	75	0	74.5	0.7
CS-81			0	100	0	74.0	1.3
CS-82			50	0	50	70.0	0
CS-83			25	0	75	74.3	0.9
CS-84			0	0	100	84.0	1.2

2.9 Acoustic absorption and transmission loss test

Sound absorption test was performed according to the requirements of ASTM E1050 using a tube, two microphones and a digital frequency analysis system. Chip seal specimens with different amount of rubber replacement ratio were tested. Specimens with both aggregate 1 and aggregate 2 were examined. Two types of emulsions were used to prepare the chip seal specimens. Fourteen specimens were tested during this tests as listed in Tables 12

Table 12: Sound absorption test specimens' details

Specimen label	Emulsion type	Percentage of the Aggregate type		
		Rubber	Aggregate 1	Aggregate 2
CS-85		100	0	0
CS-86		50	50	0
CS-87		25	75	0
CS-88	Emulsion 1	0	100	0
CS-89		50	0	50
CS-90		25	0	75
CS-91		0	0	100
CS-92		100	0	0
CS-93		50	50	0
CS-94		25	75	0
CS-95	Emulsion 2	0	100	0
CS-96		50	0	50
CS-97		25	0	75
CS-98		0	0	100

2.9.1 Testing apparatus

The plane wave tube was carefully machined using stainless steel tube with a wall thickness of 3.2mm (0.126 inches) for an accurate measurement of sound pressure amplitude and phase (Fig. 31a). The phase response of the tube is less than 0.1 degrees over the operating range from 50-5650 Hz. The precision machined flanges, side ports, and microphone holders accurately maintain microphone alignment. A 16 ohms high frequency compression JBL compression driver was used to produce sound (Fig. 31b). Two ½ inches high accuracy microphones were used with microphone holders to ensure stable positing the testing apparatus (Fig. 31c). A fully integrated ACUPRO Software and DT 9837A data acquisition module was used to collect and analyze the output data form the testing apparatus (Fig. 31d)

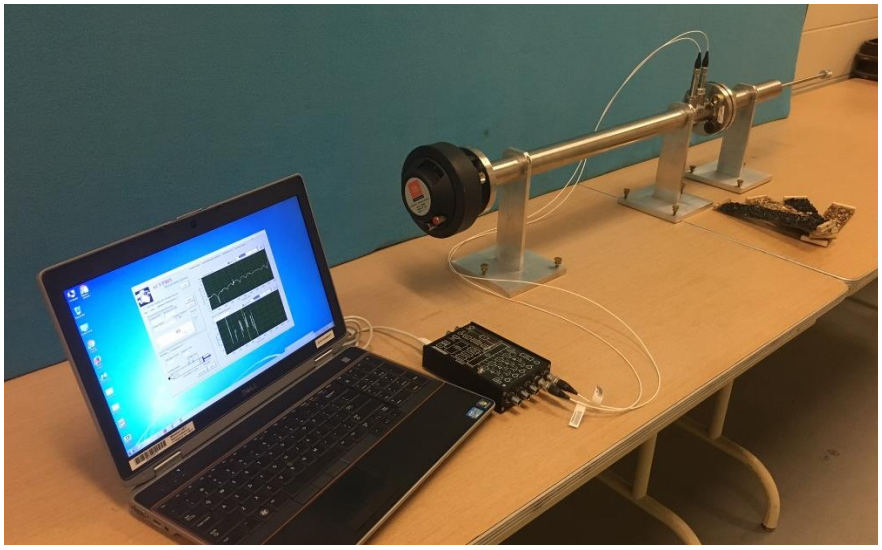

(a)

(b)

(c)

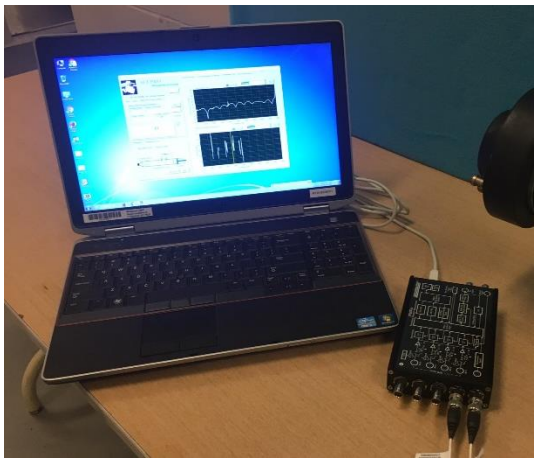

(d)

Figure 31: Acoustic absorption test: (a) testing apparatus, (b) Sound source (compression driver), (c) microphones with holders, (d) ACUPRO Software with data acquisition module

3. Results and discussions

3.1 Standard and modified sweep tests result

Fig. 32 shows a sample of the test specimens after the sweep test. The weight of the loss aggregates from the sweep tests was measured and used for the comparisons between the specimens. Table 4 summarizes the results of all the examined specimens under the standard and modified sweep tests. Figs. 33a and 33b illustrate the weight loss of the aggregates versus the percentage of the crumb rubber contribution in the specimens made of aggregates 1 and 2, respectively, for the standard sweep test.

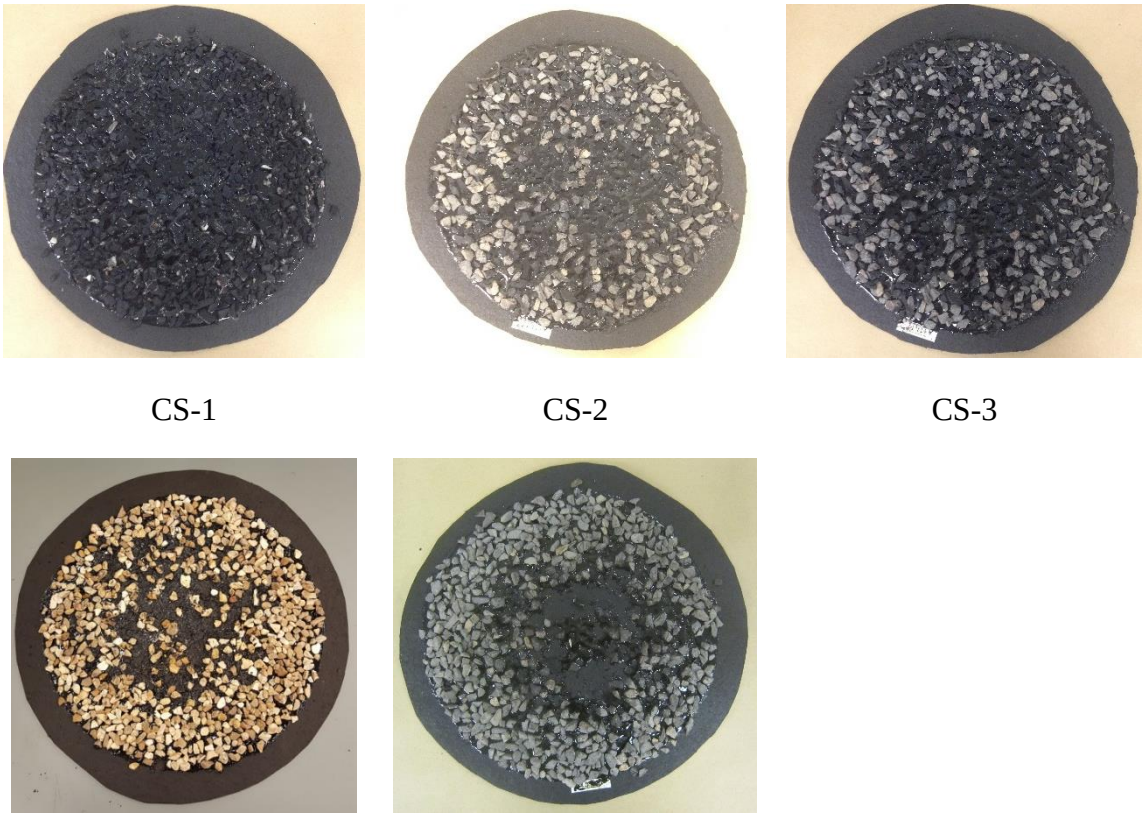

CS-1 CS-2 CS-3

CS-4 CS-5

Figure 32: Sample of specimens after standard sweep test

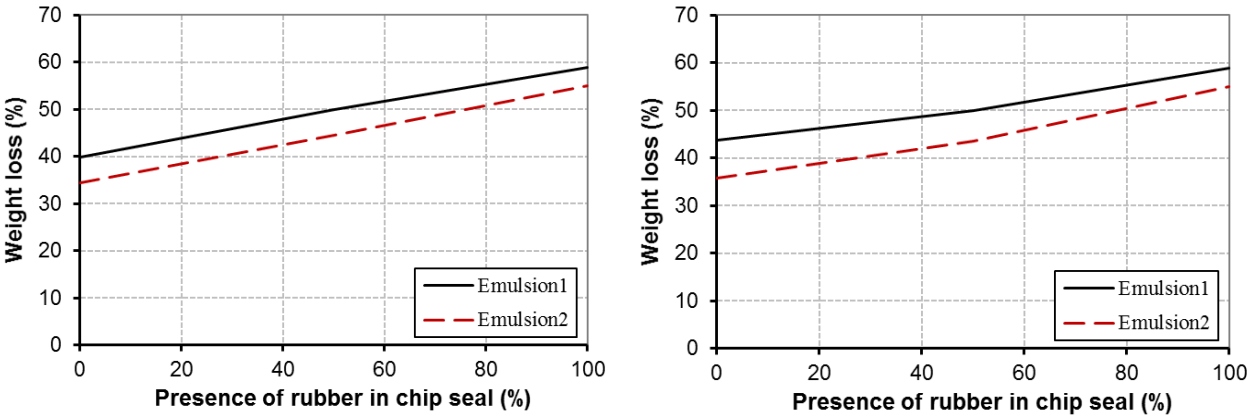

Figure 33: Weight loss versus the percentage of crumb rubber content in the chip seal: (a) with aggregate 1 and (b) with aggregate 2, for the two emulsions

As shown in the figure, the trend of the performance of the specimens is similar regardless of the aggregate type. The weight loss linearly increased with increasing the crumb rubber percentage. The aggregates weight loss increased by approximately 33% when the crumb rubber increased by 100%. Although the crumb rubber had a higher surface area in the microtexture than the other two aggregates, it did not show better performance under the sweep test. This behavior was due to the minimal water absorption of the crumb rubber compared to the other two types of aggregates, leading to slow hardening of the used asphalt emulsion. In addition, the crumb rubber had a low unit weight approximately 34 - 36% of that of the other two aggregates, causing the crumb rubber to be swept easily.

Specimens made with emulsion 2 had better performance than those made with emulsion 1 in terms of weight loss for mineral aggregates and all rubber contents. The reason for this behavior was the high flowability of emulsion 2 which helped the emulsion to capsulate the aggregate particles and be in touch with troughs and crests in all types of aggregate.

Aggregate 1 showed slightly better performance than aggregate 2 at zero-rubber replacement. After one hour curing, the weight loss of aggregate 1 was 40% compared to 44% for aggregate 2 due to the high absorption of aggregate 1 over aggregate 2 which help in breaking out the emulsion's water.

During the modified sweep test, the weight loss of the aggregates was determined at curing times of 1, 3, 6, 24, and 72 hours, as shown in Figs. 34 and 35 for emulsion 1 and 2, respectively.

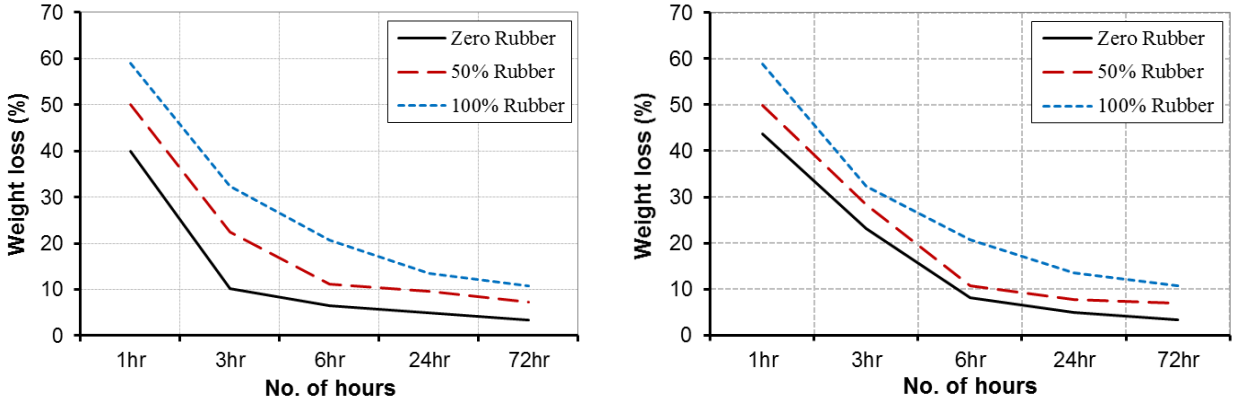

(a) (b)

Figure 34: Weight loss versus the curing time for different rubber percentages in the chip seal (a) with aggregate 1 and (b) with aggregate 2, in emulsion 1

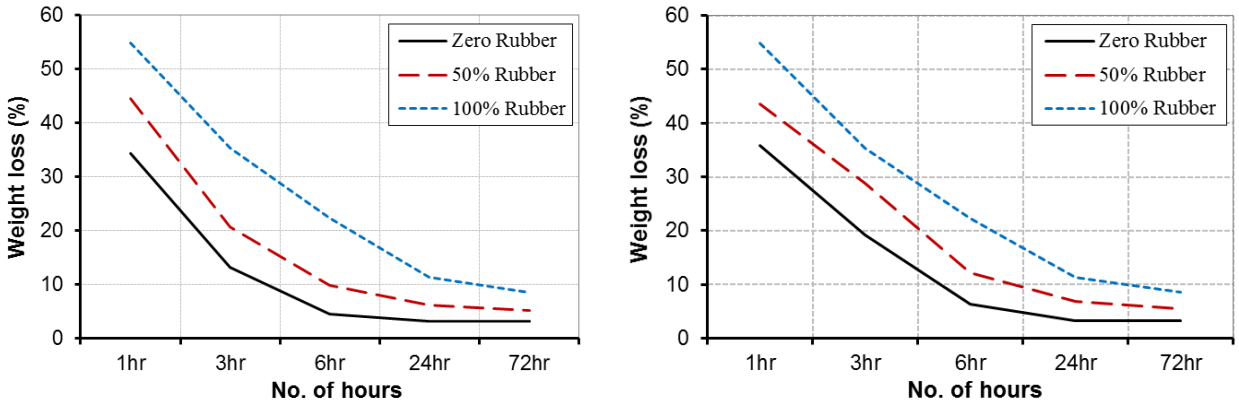

(a) (b)

Figure 35: Weight loss versus the curing time for different rubber percentages in the chip seal: (a) with aggregate 1 and (b) with aggregate 2, in emulsion 2

The weight loss of the aggregates decreased significantly after 6 hours of curing, reaching a range between 5% and 20% for all specimens, while it decreased slightly beyond 6 hours of curing. The rapid decrease in the weight losses in the first 6 hours is due to early water breakout leading to emulsion hardening. As shown in Fig. 12, 73% of the water breakout occurred for both emulsions in the first 6 hours of exposure. Beyond that, the water breakout is very slow.

Figs. 34 and 35 also show that rubberized chip seal will require a more curing time compared to mineral aggregate to achieve a given percentage of weight loss. For example, the

weight loss in chip seal with 50% rubber replacement will achieve the same weight loss as that in the chip seal with mineral aggregate, when the curing time is increased from 1 hour to 1.75 hours for both emulsion 1 and 2. For chip seal with 100% rubber, a mass loss equal to or less than that in conventional chip seal can be achieved when the curing time is increased from 1 hour to approximately 2.5 hours.

Figs. 36 and 37 show the weight losses for different crumb rubber replacements at different curing times for emulsion 1 and emulsion 2, respectively. As shown in the figures, a minimum curing time of 6 hours is required to keep the weight losses below 20% for all types of emulsions and mineral aggregates. For aggregate replacement up to 100%, a curing time of approximately 6 hours seems appropriate as well. At 100% rubber replacement, a curing time of 24 hours is required to keep the weight losses below approximately 12%. Finally, for a given curing time, specimens having aggregate 1 with crumb rubber showed better performance than those having aggregate 2 with crumb rubber due to the higher water absorption of aggregate 1 leading to faster hardening of the emulsion.

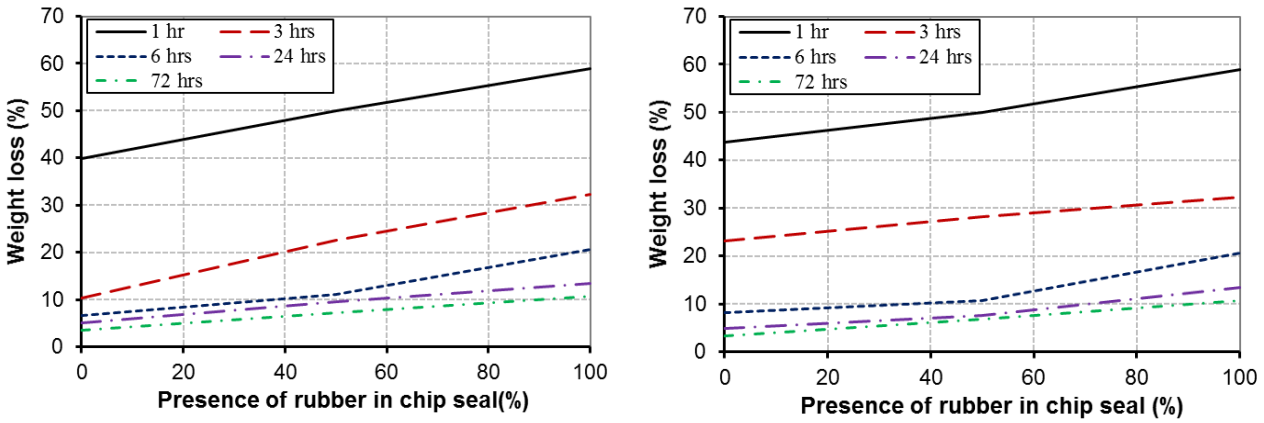

(a) (b)

Figure 36: Weight loss at different curing times versus the percentage of rubber presence in the chip seal: (a) with aggregate 1 and (b) with aggregate 2, in emulsion 1

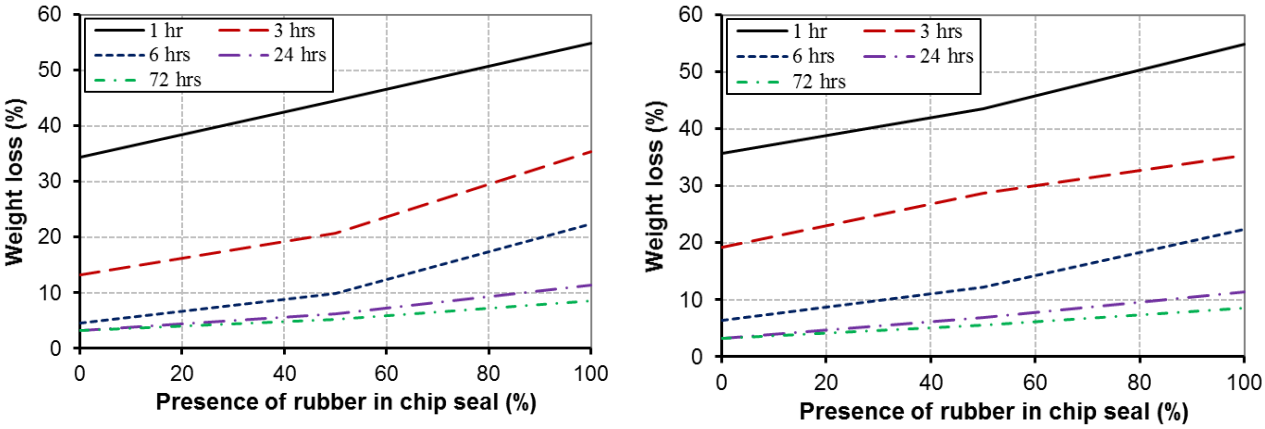

(a) (b)

Figure 37: Weight loss at different curing times versus the percentage of rubber presence in the chip seal: (a) with aggregate 1 and (b) with aggregate 2, in emulsion 2

3.2 **Standard and modified Vialit tests results**

Fig. 38 shows a sample of the test specimens after being subjected to the Vialit and modified Vialit tests.

(a) (b) (c)

Figure 38: Vialit and modified Vialit tests test specimens (a) creek gravel with emulsion 1, (b) creek gravel with asphalt cement, and (c) crumb rubber with emulsion 1

The number of retained aggregates out of 100 aggregates in the binder was recorded for each specimen. Table 6 summarizes the results of the standard Vialit test. The performance of the three types of aggregates in conjunction with each type of asphalt cement for the standard Vialit test is shown in Fig. 39.

Aggregates 1 and 2 had better performance with the two emulsions than with the two asphalt cement during the standard test (Fig. 39). The retention rate was 100% for both emulsions while it ranged from 40% to 60% and 50% to 70% for binder 1 and binder 2, respectively. This behavior occurred because the asphalt cement shrank after the curing time

more than the emulsions, causing some tension on the bond with the aggregate, and the asphalt cement became glassy and fragile after freezing the specimens at -25 ^{o}C per the test requirements.

The crumb rubber showed a superior performance of 100% retained aggregates for the two asphalt cement and two emulsions due to the compatibility between the rubber and the asphalt cement/emulsion as both the rubber and asphalt cement/emulsions are made with hydrocarbon organic base. This compatibility gave high cohesion strength between the crumb rubber's outer surface and the asphalt cement.

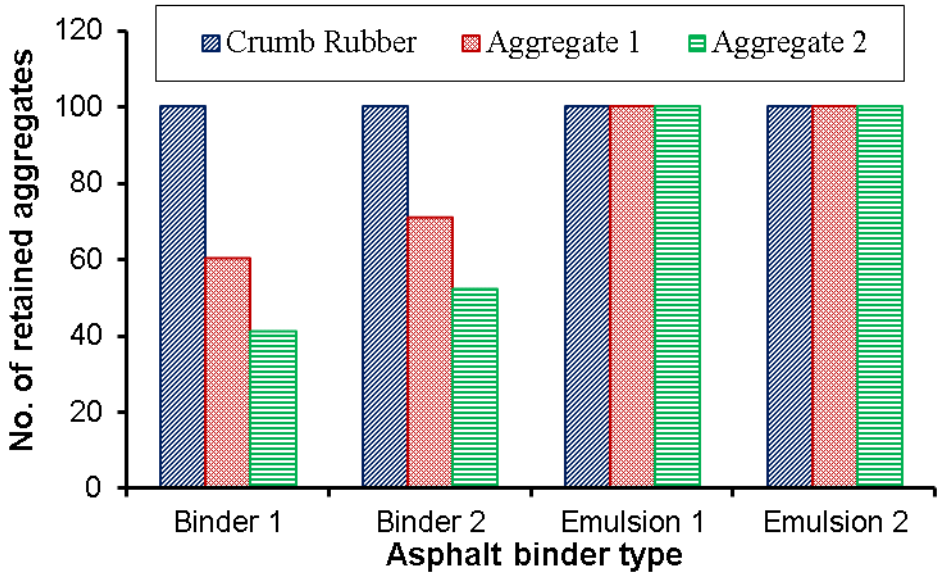

Figure 39: Number of retained aggregates in Vialit test

To better understand the performance of rubberized chip seal with asphalt cement, the melting point of crumb rubber was first determined using the differential scanning calorimeter (DSC) test per ASTM D1519 – 95. As shown in Fig. 40, the melting point for scrap tire rubber Tp was 97 °C. This temperature is significantly higher than the asphalt cement temperature of 165 °C during the aggregate application. Hence, partial melting of the surface of the crumb rubber particle occurred especially in the embedment depth inside the asphalt cement, which creates a stronger bond with the surrounding cement. However, this effect did not appear with the other two aggregates. Also, the crumb rubber did not easily fall down during the test because of its low unit weight.

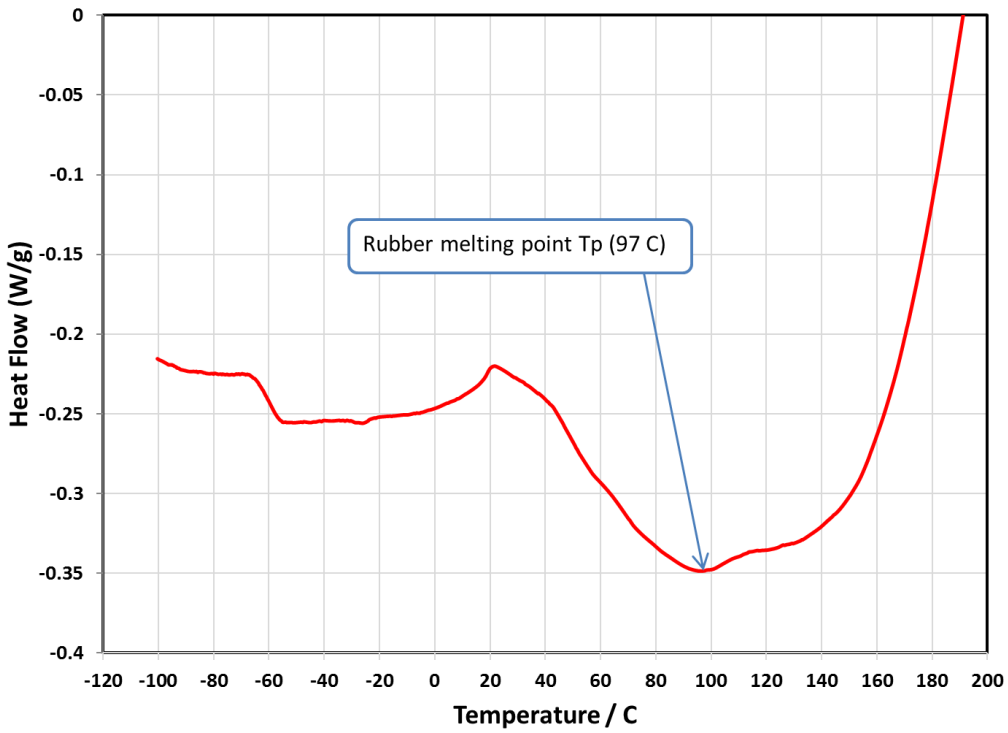

Figure 40: Differential scanning calorimetry (DSC) for scrap tire rubber

For the modified Vialit test where 30 or 40 drops of the ball were conducted, Fig. 41 shows the number of drops versus the number of the retained aggregates during the modified Vialit test for the two emulsions. The crumb rubber showed an excellent performance with 100% retained aggregates. Aggregate 1 had slightly better performance than aggregate 2 because of its lower unit weight. The aggregates' surface area did not affect their performance during this test because dislodging of the aggregates was due to rupture in the binder and not at the interfaces between the binder and aggregates, as shown in Fig. 38a. Also, the aggregate's absorption and the emulsion water breakout did not significantly affect the chip seal performance because the Vialit test was conducted after 24 hours of curing.

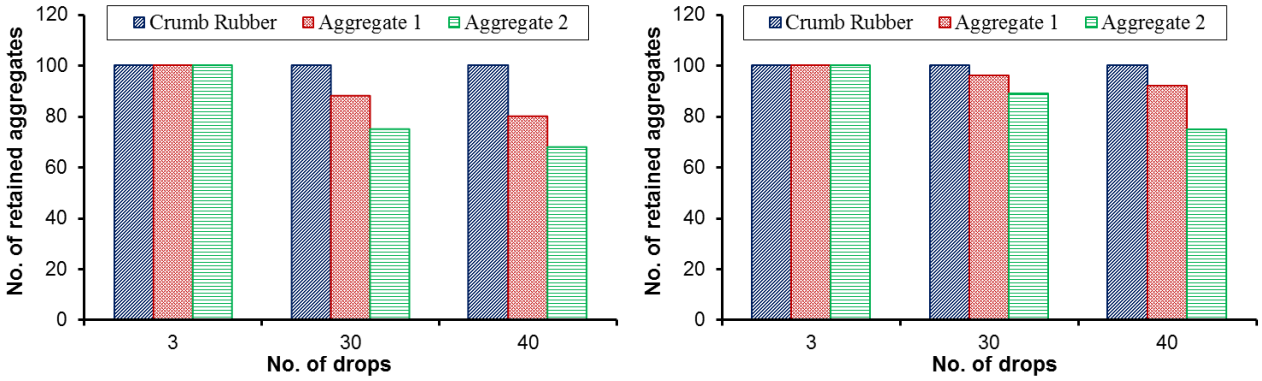

Figure 41: Number of retained aggregates versus no. of drops for specimens constructed out of (a) emulsion 1, and (b) emulsion 2

3.3 Pennsylvania test results

Fig. 21show example of the tested specimens. The knock-off weight losses of the aggregates were determined for all of the specimens of the Pennsylvania test. Table 7 summarizes the results of the Pennsylvania test. Figs. 42 and 43 illustrate the knock-off weight loss of the aggregates for the different emulsions and aggregates, respectively.

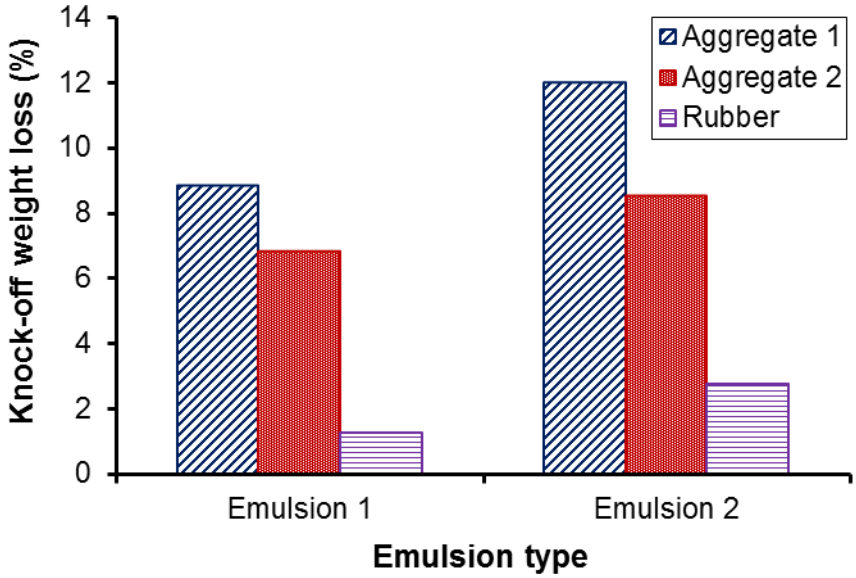

Figure 42: Knock-off weight loss for chip seal specimens with different aggregates

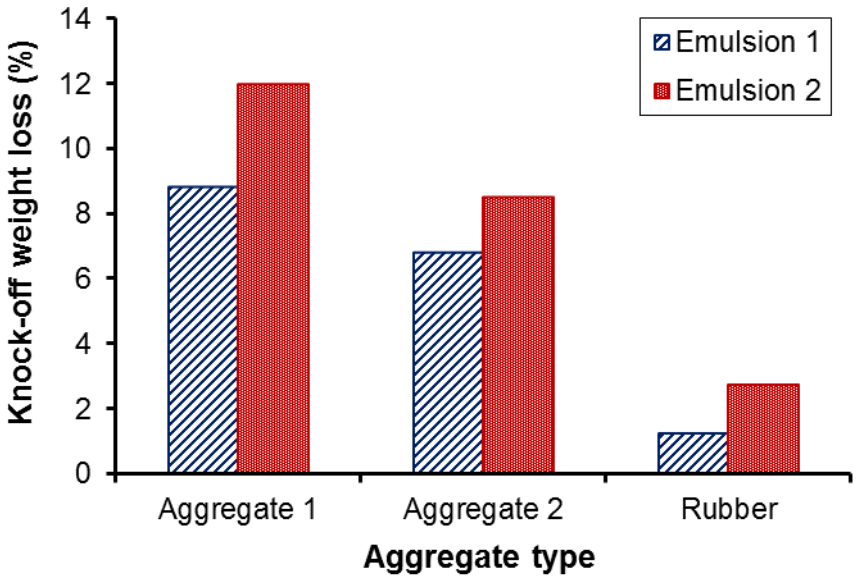

Figure 43: Knock-off weight loss for different chip seal specimens with emulsions 1 and 2

The Pennsylvania test examined the aggregate retention based mainly on the aggregate self-weight and surface area because each specimen was subjected to high compression forces to achieve good embedment depth. Therefore, the crumb rubber showed distinguished performance with knock-off loss of about 1% and 2% for emulsion 1 and emulsion 2, respectively. This behavior was due to the low unit weight and the high, rough surface of the crumb rubber.

Aggregate 2 had better performance than aggregate 1 during Pennsylvania test because of its rougher surface. The aggregate's absorption and the emulsion water breakout did not affect the performance of the chip seal specimens because the Pennsylvania test was conducted after 24 hours of curing.

As shown in Fig. 43, emulsion 1 had better performance than emulsion 2 during the Pennsylvania test, which contradicted the results from the other tests (sweep and Vialit). This behavior was because of the compaction load that was applied to each specimen. Emulsion 1 was more viscous than emulsion 2. Therefore, the applied load achieved higher embedment depth in the case of emulsion 1 than in the case of emulsion 2, which was considerably flowable. However, this effect did not appear in the other tests because there was no applied compaction force.

3.4 The microtexture of chip seal

This study used a 3D digital microscope to investigate the surfaces microtexture conditions of two types of mineral aggregates in addition to two types of crumb rubber aggregates. Fig. 44 illustrates the surface images and elevation profiles in a range of 250 µm of the aggregates. The ambient processed crumb rubber had a rough surface with numerous troughs and crests that would improve its retention with the binders as shown in Fig. 44a, while the cryogenically processed crumb rubber had a smooth surface as shown in Fig. 44b. For example, the surface area of a projection of 1-inch width x 1-inch length of the aggregates shown in Fig. 44 were 1.028, 1.222, 1.032 and 1.042 $inch^2/inch^2$ for the cryogenically processed rubber, ambient processed rubber, aggregate 1, and aggregate 2 respectively. The surfaces were rougher in the case of ambient crumb rubber due to the cutting process. Hence, the ambient crumb rubber had a surface area 19%, 18%, and 17% higher than that of cryogenic, aggregate 1, and aggregate 2 respectively. Aggregate 2 had a rougher surface than aggregate 1 but smoother than the ambient crumb rubber. The surface of aggregate 1 was smoother than aggregate 2 because it was subjected to continuous water flow and rolling of the aggregate particles during its formation in creeks. This test was carried out early during this project and hence the ambient processed crumb rubber was used during this study and the cryogenically processed crumb rubber was discarded. The larger surface area of ambient processed crumb rubber will provide about 20% extra contact area with tires which increase the adhesion component by about 20% as well.

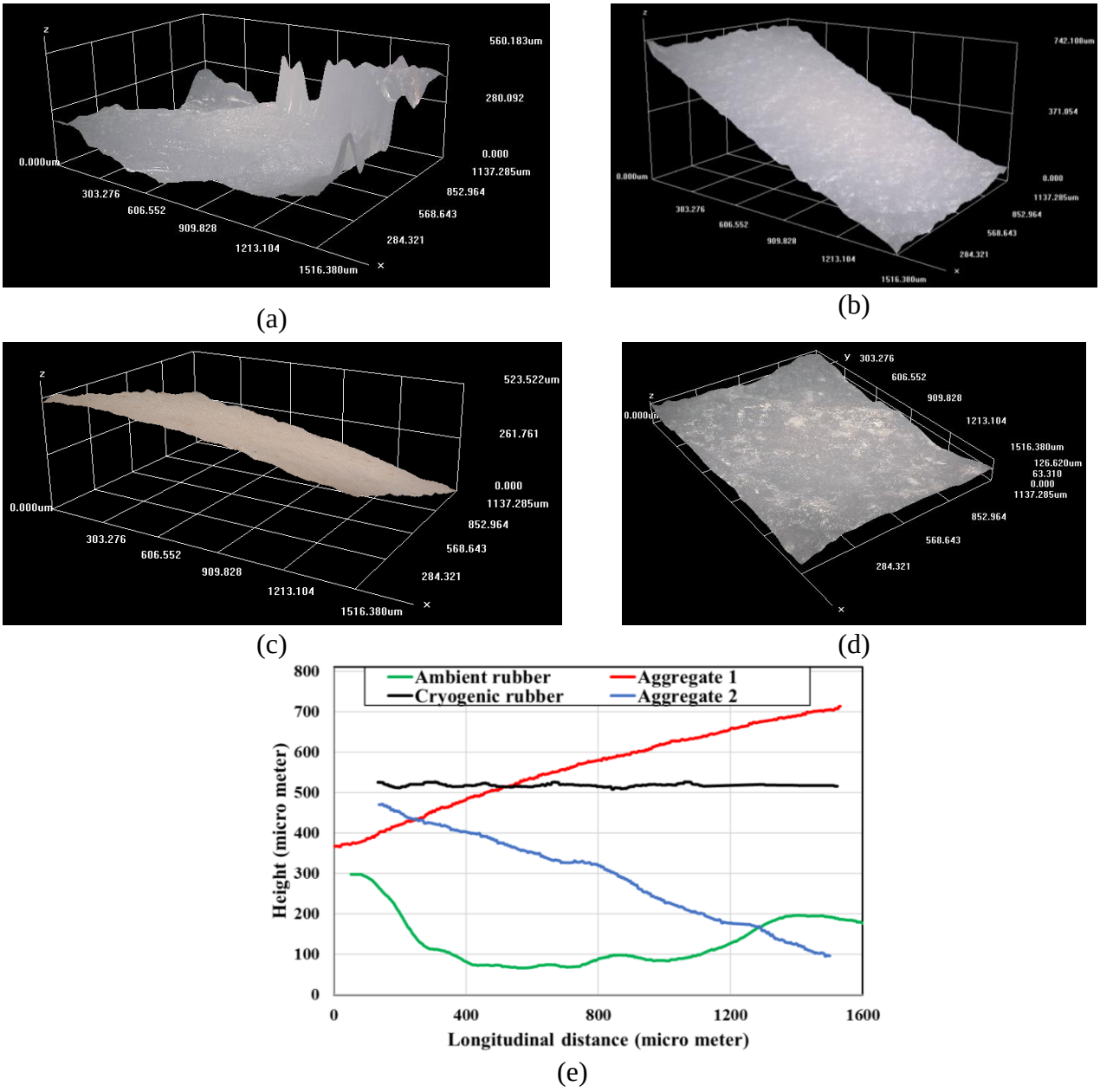

Figure 44: Microscope results of the aggregates' surface in range of 250 µm: (a) image of ambient crumb rubber, (b) image of cryogenic crumb rubber, (c) image of aggregate 1, (d) image of aggregate 2, and (e) surfaces' profiles of the different aggregates

3.5 The macrotexture of chip seal

3.5.1 Image processing method

As shown in Fig. 45, 72 specimens with nine different binder application rates were examined for both creek gravel and crumb rubber. As mentioned in chapter 2, the binder used in these specimens were clear color epoxy to facilitate the image processing.

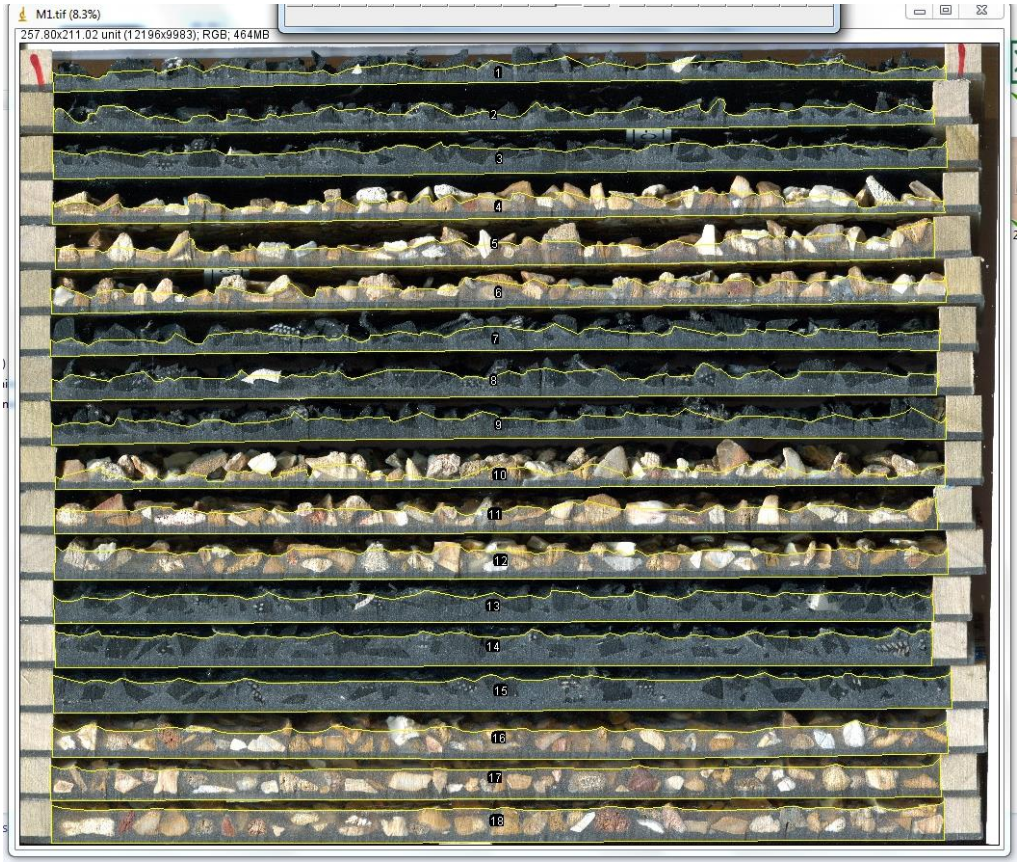

Figure 45: Different chip seal sections for image processing

The binder application rate versus the mean texture depth (MTD) curve was then obtained (Fig. 46). For the same binder application rate, the crumb rubber specimens had larger MTD than the creek gravel specimens. The increase in MTD was between 1.2 to 1.0 mm which is equivalent to an increase from 16% to 100% based on the binder application rate. This increase is equal to 16% to 19% of the median aggregate size. Taking into account that the crumb rubber had 0.3 mm larger median aggregate size than that of the creek gravel, the increase in the MTD values of the crumb rubber specimens was not only due to this small difference in

particle size but mainly due to the rough surface of crumb rubber particle as shown by the microtexture measurements.

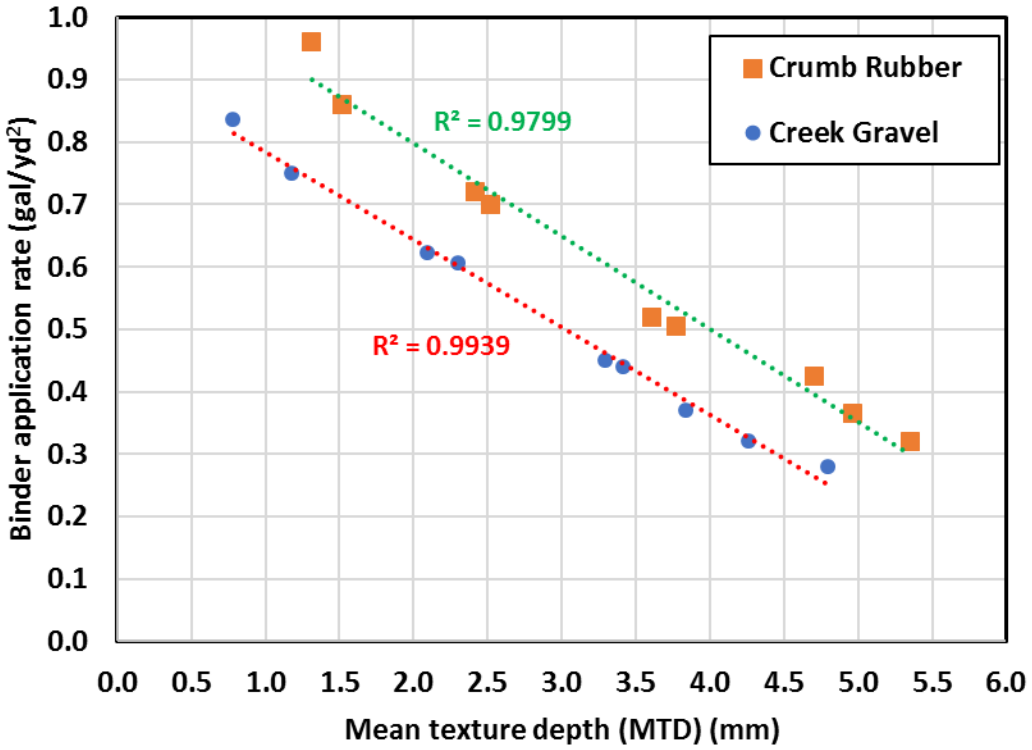

Figure 46: Binder application rate versus mean texture depth (MTD)

3.5.2 Sand patch method

Chip seal specimens with different aggregates and emulsions were prepared and tested as illustrated in Table 8 and Fig. 47. Fig. 48 shows the MTD vs. the percentage of rubber for emulsion 1 and 2 for both types of aggregate. As the rubber percentage increased, the MTD value increased. An increase of 25% in MTD was observed when 100% of the trap rock was replaced with crumb rubber. Similarly, an increase of 33% was measured in the MTD when 100% of the creek gravel was replaced with crumb rubber. The difference in the increase percentage between the creek gravel and trap rock was because of the smoother surface of the creek gravel. As the test was conducted after extensive samples curing that caused full water broke out, there was not a significant difference in the values of MTD when using emulsion 2 or emulsion 1.

(a)

(b)

Figure 47: Sand patch test specimens with different aggregate combinations for specimens with: (a) creek gravel, and (b) trap rock in combination with crumb rubber.

A strong correlation between the image processing method and the sand patch method was noticed. The MTD was 5.2 mm and 5.0 mm for the sand patch and image processing method respectively with 100% rubberized chip seal. In the case of 100% creek gravel chip seal, MTD values of 4.00 mm and 4.15 mm were calculated for the sand patch and image processing method respectively.

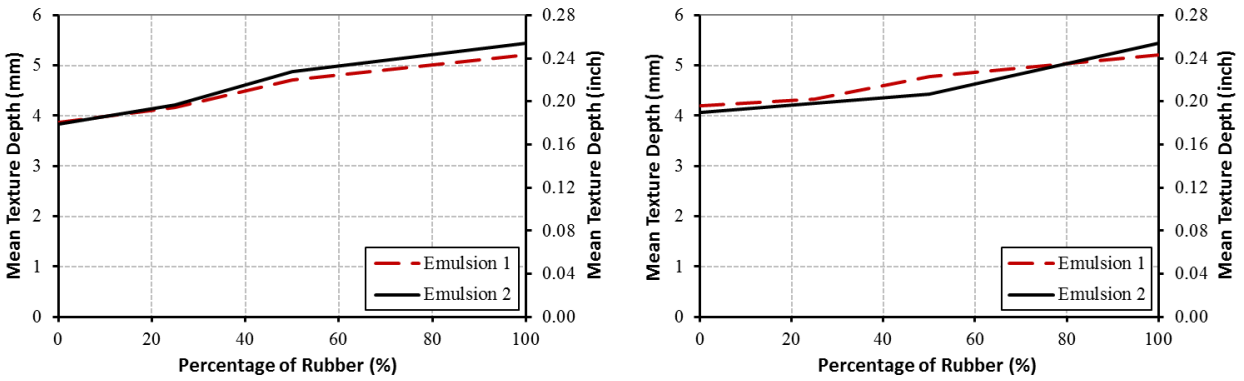

Figure 48: Percentage of crumb rubber versus the macrotexture depth from sand patch test for (a) specimens with aggregate 1, and (b) specimens with aggregate 2

3.6 Skid friction resistance tests

Fig. 49 shows the measured BPN vs rubber content the different binders and aggregates. While the sand patch and image processing indicated that the micro and macro texture of the crumb rubber were better than those of the mineral aggregates, the skid friction tests showed that the BPNs decreased with increasing the rubber replacement ratio regardless of the binder or mineral aggregate types (Fig. 49). A decrease in the BPNs ranging from 7% to 20% and 0% to 13% were measured for specimens with aggregate 1 having rubber content ratios ranging from 25% to 100% with emulsion-based and asphalt cement-based chip seals, respectively. Similarly, a decrease in the BPNs ranging from 4% to 20% and 8% to 23% were measured for specimens with aggregate 1 having rubber content ratios ranging from 25% to 100% with emulsion-based and asphalt cement-based chip seals, respectively.

The contradiction between the skid resistance test and the texture characterization results are attributed to three main reasons. First, the adhesion component which is part of the skid friction resistance cannot be fully captured by the British pendulum tester (BPT) as the contact area between the BPT slider and specimen is infinitesimal. Mataei et al. (2016) reported that BPT displayed unreliable behavior when used on coarse textured pavement, which is the case for chip seal, due to the infinitesimal contact area. Second, the BPT measures the friction at low speed where microstructure of the pavement is controlling the behavior. Third, the hysteresis part of the friction is related to the energy loss that occurs as rubber layers in tires are alternately compressed and decompressed; since crumb rubber aggregate is less rigid than mineral

aggregate, the hysteretic component should be less in the case of rubberized chip seal. The hysteresis effect can't be captured during the surface characterization process.

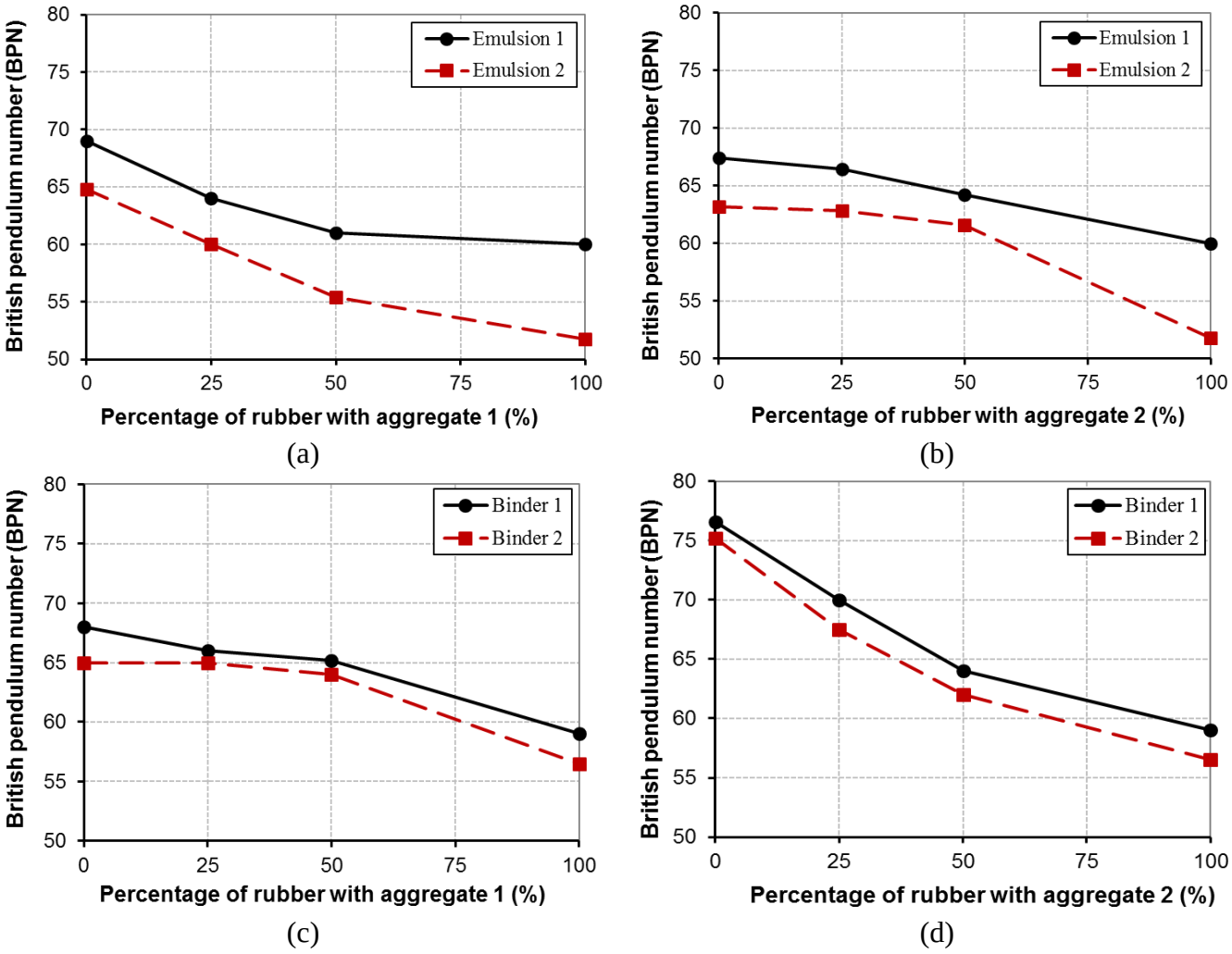

Figure 49: Standard skid test BPN versus percentage of rubber with: (a) aggregate 1, (b) aggregate 2, (c) aggregate 1, and (d) aggregate 2.

For the modified skid resistance tests at high temperature of 65 °C, Fig. 50 shows that all specimens made with 100% crumb rubber did not display any loss in BPN compared to those measured at ambient temperature (~20 °C). Conventional chip seal having 100% mineral aggregates showed an average loss of 10% in BPNs for samples made with emulsion and 2% in BPNs for samples made with asphalt cement indicating degradation in the friction skid resistance. This occurred as the crumb rubber has low thermal conductivity. At the ambient temperature, the average thermal conductivity of mineral aggregate is between 1.83 - 2.90 (w/m.k) while the average thermal conductivity of rubber is 0.12 (w/m.k). The very low thermal

conductivity of rubber compared to that of mineral aggregates significantly reduced the heat propagation into the binder; hot binders display stiffness degradation compared to binders at ambient temperature. However, such reduction was not severe for the asphalt cement as the 65 °C was not enough to trigger severe stiffness reduction.

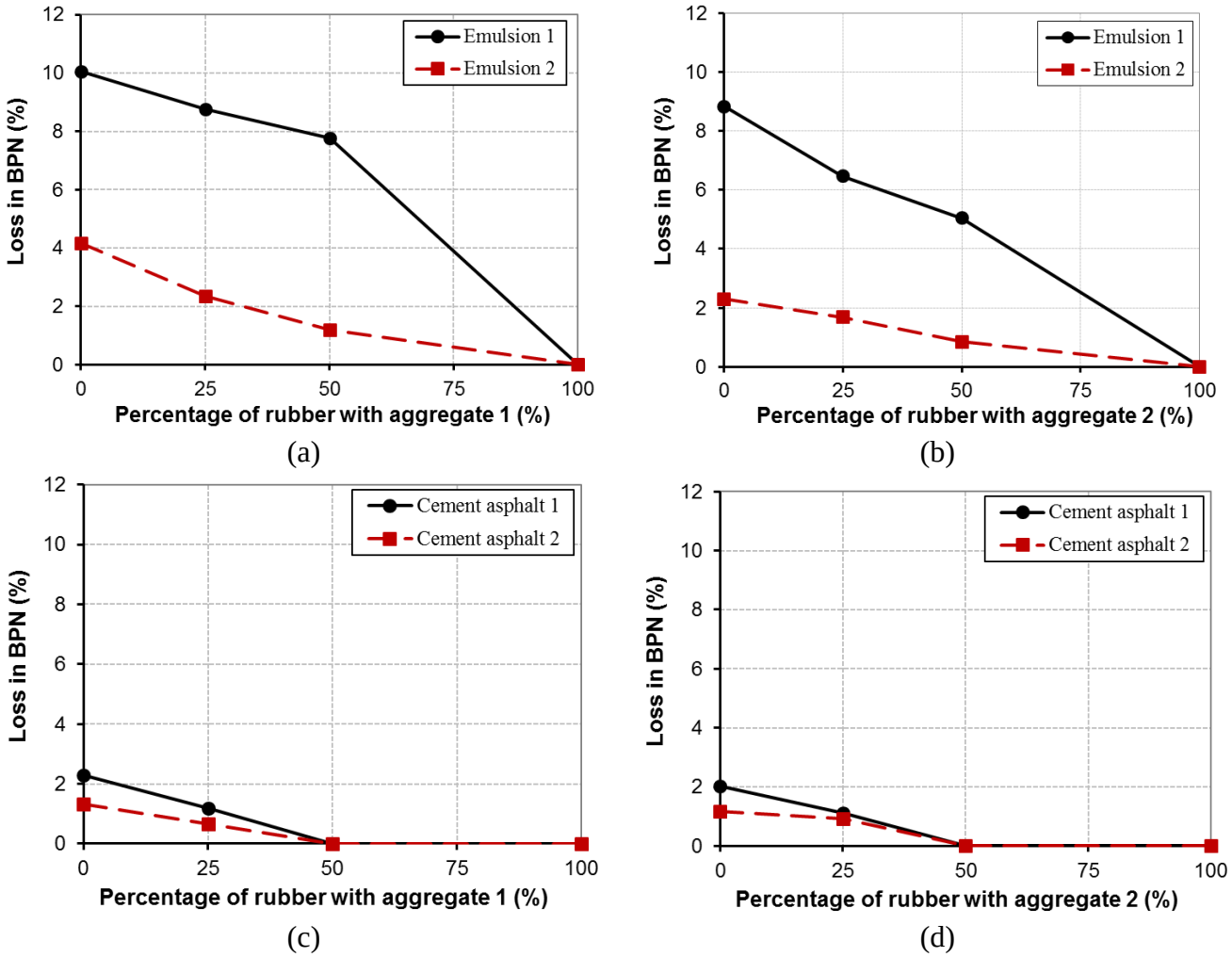

Figure 50: Modified skid test loss in BPN versus percentage of rubber with: (a) aggregate 1 in emulsions, (b) aggregate 2 in emulsions, (c) aggregate 1 in cement asphalt, and (d) aggregate 2 in cement asphalt

3.7 Binder application rate

Chip seal design in most U.S. states is considered as an art based on experience and empirical design rather than a rigorous engineering sound design. Many factors contributed to this lack of consensus on a design approach. The irregular shape of aggregate particles significantly contributed to this challenge.

To examine the ability of the existing design approaches to determine the correct binder application rate for a given aggregate embedment depth, chip seal specimens with ten different binder application rates varied from 0 to 0.96 gal/yd^2 were prepared for aggregate 1 and crumb rubber aggregate. The embedment depth of each specimen was determined using the image processing procedure explained earlier in this report. Fig. 51 shows the binder application rate versus the aggregate embedment depth as a percentage of aggregate least dimensions.

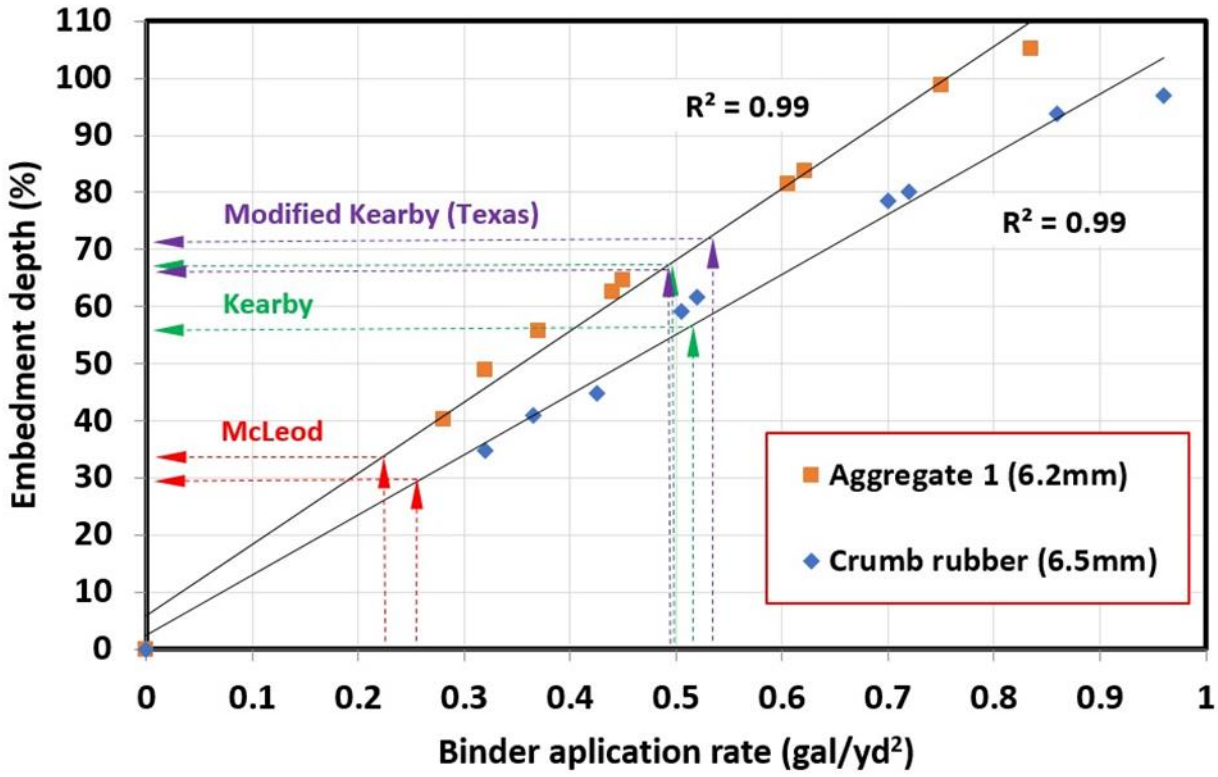

Figure 51: Binder application rate versus embedment depth for aggregate 1 and crumb rubber

As shown in Fig. 51, using McLeod application rate resulted in embedment ratio of 32% and 28.5% of the least aggregate dimension for aggregate 1 and crumb rubber aggregate, respectively. McLeod design approach assumes that the embedment ratio would reach 70% after

two years in service. However, it is not anticipated that particles rearrangement and consolidation that take place, during service life of a chip seal, due to traffic will double the aggregate embedment depth ratio. Furthermore, for low-volume traffic roads, the compaction due to passing traffic would be quite low for such dramatic increase in embedment. For high-volume roads, these roads typically have high speeds and initial higher embedment ratio would be required to avoid dislodge of aggregates at high speeds.

Kearby method produced chip seal with embedment ratios of 67% and 55% for aggregate 1 and crumb rubber, respectively. However, Kearby design approach was developed based on 50% embedment. The modified Kearby method produced chip seal with embedment ratios of 72% and 66% for aggregate 1 and crumb rubber, respectively, while it was developed assuming 40% embedment depth. Hence, neither of the existing methods were able to provide the required application rate for the design embedment ratio. Hence, there is a need for a simple method to determine the required application rate for a given embedment ratio.

This study proposed a simplified method to determine the binder application rate given an embedment ratio of the median aggregate size. In this approach, aggregate was simulated considering three different regular geometrical shapes namely, sphere having diameter equal to the median aggregate size (Fig. 52), square pyramid with a base leg and height equal to the median aggregate size (Fig. 53), and an inverted square pyramid with the same dimensions for the regular pyramids (Fig. 54).

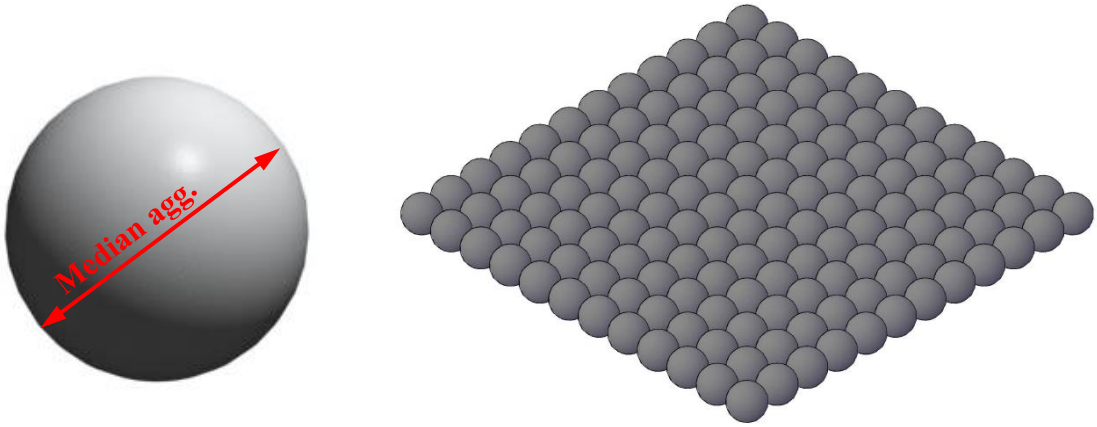

(a) (b)

Figure 52: Modeling aggregate particle (a) particle shape, and (b) chip seal aggregate model

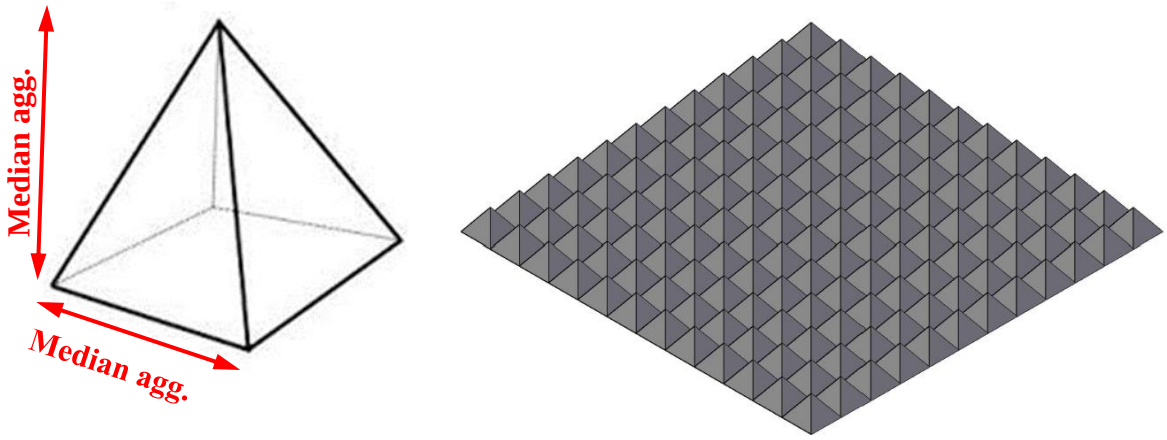

(a) (b)

Figure 53: Modeling aggregate particle (a) particle shape, and (b) chip seal aggregate model

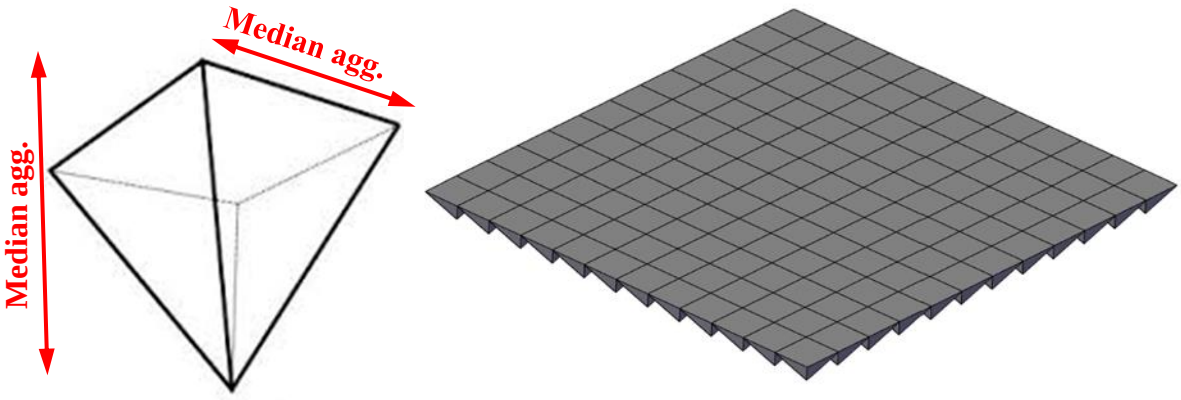

(a) (b)

Figure 54: Modeling aggregate particle (a) particle shape, and (b) chip seal aggregate model

Using each of these shapes, the volume of voids and hence the required binder application rate for a given embedment ratio was determined and plotted in Fig. 45. Furthermore, the results obtained from the experimental work corresponding to embedment ratios of 50%, 66%, and 80% for aggregate 1 and crumb rubber aggregate were plotted on the same figure. As shown in the figure, the assumption of the regular pyramid was able to predict the required application rate for the considered embedment ratios with an error ranging from 2% to 19% for aggregate 1 and 0% to 30% for crumb rubber. As shown in Fig. 55 and Table.13, for 66% embedment ratio, the model was able to predict the application rate with an accuracy of 93.52% and 98.04% for crumb rubber and creek gravel respectively. For the other models the errors in predicting the application rates ranged from 2% to 22% and 18 to 32% for the case of aggregate 1 and crumb rubber assuming sphere aggregates while it ranged from 31% to 63% and 21% to 57% for the case of aggregate 1 and crumb rubber assuming inverted pyramid aggregates

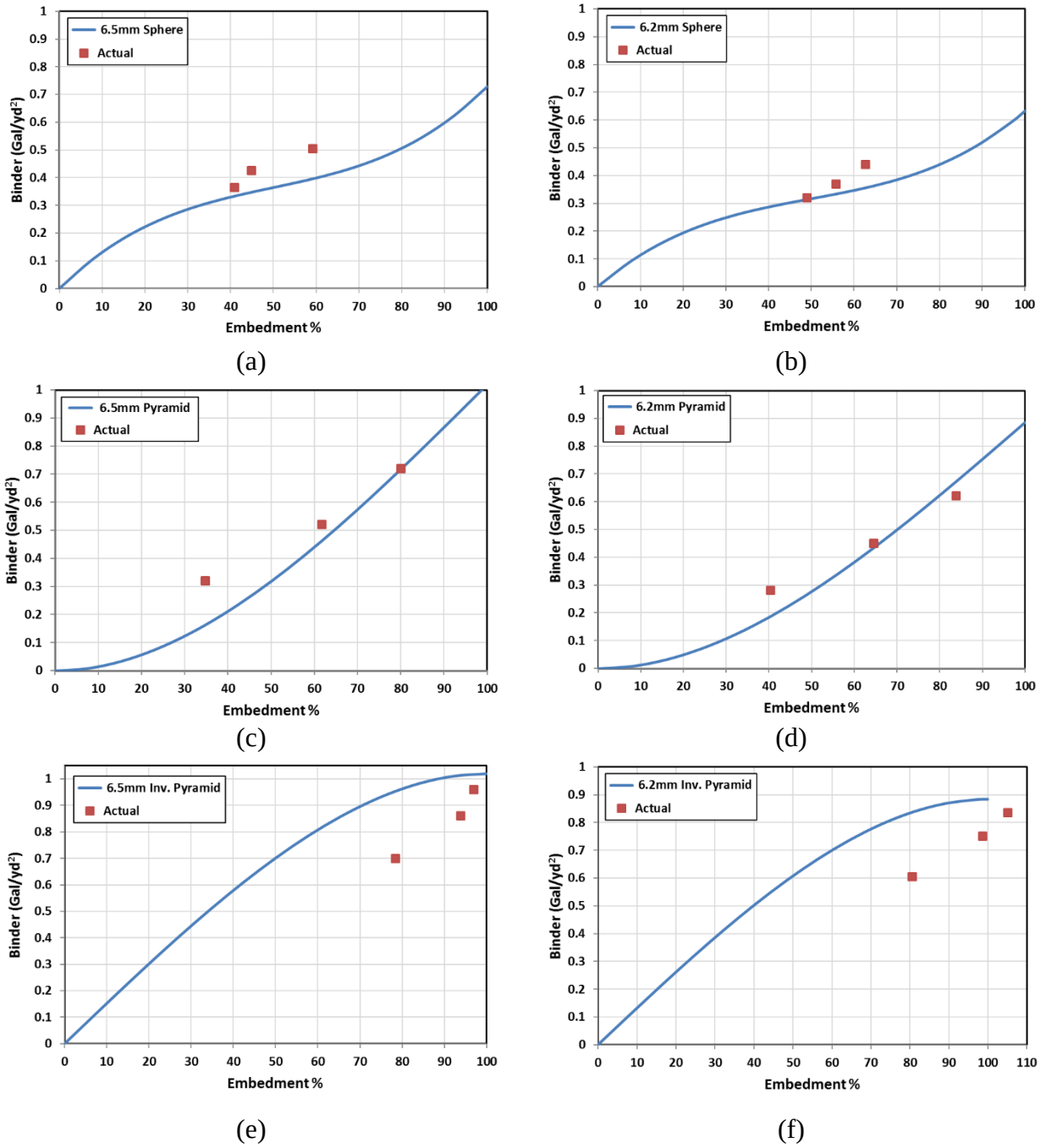

Figure 55: Analytical and experimental binder application rate versus aggregate embedment ratio (a) 6.5mm sphere model, (b) 6.2mm sphere model, (c) 6.5mm pyramid model, (d) 6.2mm pyramid model, (e) 6.5mm inverted pyramid model, and (d) 6.2mm inverted pyramid mode

Table 13: Accuracy of evaluating binder application rate using different aggregate models

Model's shape and agg. type	Median particle size (mm)	Embedment ratio for models	Binder application rate from models (gal/yd^2)	Targeted embedment depth from models (mm)	Actual embedment depth (mm)	Accuracy of the models (%)
Sphere Rubber	6.5	50%	0.365	3.25	2.66	81.85
		66%	0.425	4.29	2.92	67.97
		80%	0.505	5.2	3.85	74.00
Sphere Creek gravel	6.2	50%	0.32	3.1	3.04	97.92
		66%	0.37	4.09	3.46	84.59
		80%	0.44	4.96	3.89	78.33
Pyramid Rubber	6.5	50%	0.32	3.25	2.26	69.68
		66%	0.52	4.29	4.01	93.52
		80%	0.72	5.2	5.22	100.29
Pyramid Creek gravel	6.2	50%	0.28	3.1	2.50	80.72
		66%	0.45	4.09	4.01	98.04
		80%	0.622	4.96	5.20	104.84
Inv. Pyramid Rubber	6.5	50%	0.7	3.25	5.11	157.23
		66%	0.86	4.29	6.10	142.18
		80%	0.96	5.2	6.31	121.28
Inv. Pyramid Creek gravel	6.2	50%	0.605	3.1	5.05	162.90
		66%	0.75	4.09	6.12	149.61
		80%	0.835	4.96	6.51	131.35

4. Field implementation

During this study, it was required to investigate the applicability and feasibility of using crumb rubber as a partial or total replacement for the mineral aggregate. The main object of this stage was to ensure the feasibility of constructing rubberize chip seal using the same set of equipment, tools, and procedures that are used today by an average contractor to apply a conventional chip seal.

The rubber-based chip seal was applied to Griessen Road which is located 4.4 miles east of Sedalia, Missouri. The total traffic and its speed at the examined road section are listed in Tables 14 and 15

Table 14: 2857 Griessen Road traffic classification (Pettis 2016)

Motorcycles	Cars	Pickup/ Vans	Buses	Single unit/ 2 Axle	Single unit/ 3 Axle	Single unit/ 4+ Axle	Dual unit/ 3 or 4 Axle	Dual unit/ 5 Axle	Dual unit/ 6+ Axle	Triple unit/ 4 or 5 Axle	Dual unit/ 6 Axle	Dual unit/ 7+ Axle	Total
11	985	556	1	87	3	2	112	1	0	0	0	0	1758

Table 15: 2857 Griessen Road traffic speed (mile/hr.) (Pettis 2016)

<10	11-15	16-20	21-25	26-30	31-35	36-40	41-45	46-50	51-55	56-60	61-65	66-70	70+	Total
15	7	7	8	23	45	119	278	403	442	251	107	39	14	1758

Two chip seal sections with two different crumb rubber replacement ratios namely 50% and 100% were examined. Each section was about 350 feet long. Without any modification, the

traditional chip seal procedure was used to apply the new rubberized chip seal (Fig. 56). An ambient processed crumb rubber was used with a size of 2.3 - 6 mm. This was similar in size to the creek gravel aggregate used in the blend. Emulsion type CRS2P with a temperature of 130 ^{o}F was used while the air temperature was 78 ^{o}F.

Figure 56: Field implementation of new rubberized chip seal with 100% crumb rubber replacement ratio

The emulsion application rate was 0.25 gal/yd^2 and 0.28 gal/yd^2, which equal to 0.175 gal/yd^2 and 0.196 gal/yd^2 of asphalt cement, for chip seal with 100% crumb rubber and 50% crumb rubber respectively.

During the compaction, it was noticed that rubber particles were adherent to the tiers of the rubber tires compactors (Fig. 57). The reason behind this was the flexibility of the rubber particles that allowed the rubber tires to penetrate and squeeze the crumb rubber layer and reach to the emulsion. As a result, the rubber tires compactors were replaced by steel roller compactor which did the compaction appropriately.

Figure 57: Compaction of rubberized chip seal with 100% crumb rubber replacement ratio

4.1 Field tests

4.1.1 Sand patch method

The standard sand patch method was used to determine the MTD of the chip seal coating with the two different crumb rubber replacement ratios. Two volumes of sand namely 125 ml and 60 ml, passing a No. 60 sieve and retained on a No. 80 sieve were prepared in containers. Then, it was spreading uniformly on the surface of each of the investigated spots using an ice hockey puck with its bottom surface be covered with a hard rubber material. A total of 24 spots were tested for the sand patch as shown in Figs. 58 and 59.

Figure 58: On-site sand patch test for chip seal with 100% crumb rubber

Figure 59: On-site sand patch test for chip seal with 50% crumb rubber

The diameter of the spreading sand on each investigated spot was measured at least four times in different orientations (Fig. 60).

Figure 60: On-site sand patch test

The average diameter, D, was determined and implemented in equation 1 to determine the macrotexture depth (MTD) which is an indication of the aggregate embedment depth.

$$MTD = \frac{4\,V}{\pi\,D^2} \tag{1}$$

where V is the sand volume.

The result of the sand patch test is shown in Fig. 61. As shown in the figure the MTD significantly increased with increasing the rubber content.

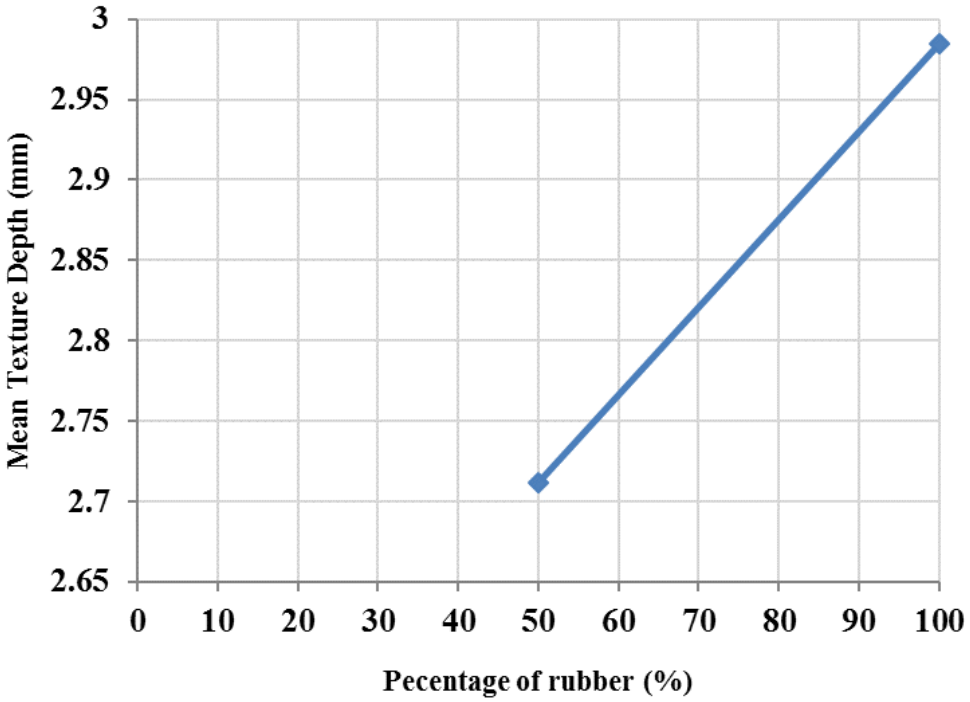

Figure 61: Percentage of crumb rubber versus the macrotexture depth from sand patch test

4.1.2 Skid friction resistance tests

The pendulum of the British Pendulum Tester (BPT) was vertically adjusted in order to achieve a slider contact path on the chip seal surface of 125 ± 1.6 mm (5 ± 1/16 inch). The distance between the center of gravity of the pendulum and the center of oscillation is 411 ± 5 mm (16.2 ± 0.2 inches). Water was sprinkled on the tested surface before running the test per the ASTM E-303. After releasing the pendulum, the British Pendulum Number (BPN) was recorded and used to represent the friction resistance of the surface. The test was repeated four times after one trial test to get the average BPN for each area (Fig. 62). As shown in Fig. 63, the skid resistance was decreasing by increasing the rubber content. This is similar to the measured data in the laboratory; however, as mention earlier, the BPT is not reliable for rough textures such as chip seal.

Figure 62: Skid resistance test

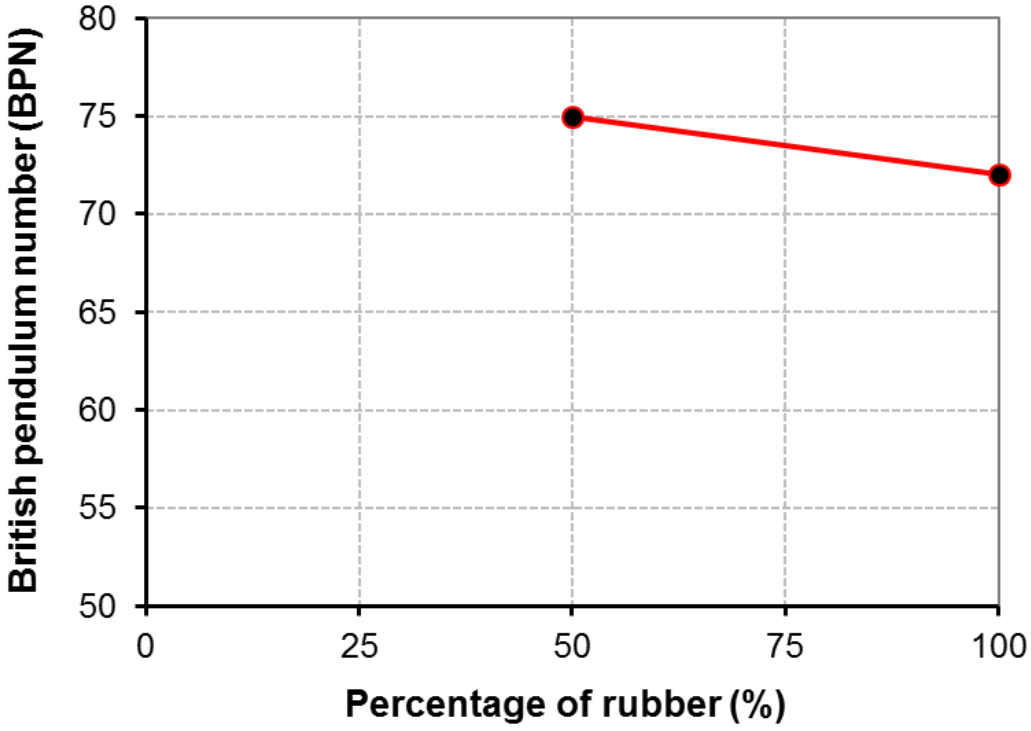

Figure 63: Standard skid test BPN versus percentage of rubber

5. Findings, conclusions, and recommendations

Chip seal is a widespread type of pavement that is used either for maintenance in heavy traffic roads or as the main pavement in rural areas. This study presents a study on chip seal pavement constructed using crumb rubber that was produced from scrap tires as an eco-friendly aggregate. This will help in diverting millions of tons of tires from landfills.

Replacing mineral aggregates in chip seal with crumb rubber aggregate can address several issues linked to using mineral aggregates in chip seal. Mineral aggregate when dislodge represents a serious safety issue to vehicles and human beings. Mineral aggregate chip seal features noisy driving. In addition, it is a common practice in the U.S. to apply a fog seal to finished chip seal to hide its rocky color and display a dark color for better perception by the local community at the chip seal site. The applied fog increases the pavement cost and reduces the pavement friction. Furthermore, crumb rubber has a loose unit weight that is approximately 0.35 of that of mineral aggregate. Hence, for a given aggregate volume, the freight cost of crumb rubber is much cheaper. Crumb rubber aggregate potentially can address all these issues.

A total of 222 specimens of chip seal were prepared using two types of emulsions, two types of asphalt cement, and two types of mineral aggregates and crumb rubber aggregate. Nine different types of tests namely the standard sweep test, modified sweep test, Vialit test, modified Vialit test, Pennsylvania, the microtexture, macrotexture, skid resistance, and skid resistance under high temperature were used to investigate the performance of the different types of aggregates in chip seal. Furthermore, the required binder application rate for a given aggregate embedment depth was experimentally evaluated. A 3D geometrical model was also proposed to simulate the shape of the aggregate which can be used to predict the required binder application rate for a given aggregate embedment depth ratio.

This study revealed that the crumb rubber from recycled tires could be used in the chip seal as aggregates. The crumb rubber showed remarkable performance in aggregate retention because of its low weight and rough surface, which increased the adhesions of the crumb rubber to the asphalt emulsion or asphalt cement. In addition, using crumb rubber improved both macrotexture and microtexture of chip seal. Crumb rubber helped the chip seal to resist high

temperature without significant loss in friction resistance. This study revealed the following particular findings and conclusions:

1- Ambient processed crumb rubber displayed 20% higher surface area compared to that of cryogenically processed crumb rubber. This resulted in significant improvement in the microtexture of crumb rubber aggregates with higher contact area with tires which increase the adhesion component in skid resistance by 20% as well. Hence, it is recommended to use ambient processed rubber as aggregate.
2- All types of aggregates showed a poor performance under the sweep test after one hour of curing. The required curing time is function in the allowable aggregate weight losses, aggregate type, and emulsion type. Assuming an allowable aggregate weight loss of 20%, based on the limited tests carried out during this experimental program, a curing time of 4.5 hours is required before sweeping the chip seal pavement for mineral aggregate and up to 50% rubber replacement. Beyond that rubber replacement, a curing time of 9 hours is required.
3- Chip seal constructed with emulsions and mineral aggregates or 100% crumb rubber aggregate passed the standard Vialit test with no aggregate loss. However, increasing the number of drops to 40 showed that the crumb rubber aggregate outperformed the mineral aggregates with 100% retention versus 65% to 90% for the mineral aggregates. and 40% to 50% for the mineral aggregates in the case of asphalt cement.
4- The retention of crumb rubber aggregate with cement asphalt measured using Vilait test outperformed that of the mineral aggregate. Crumb rubber aggregate showed 100% aggregate retention versus 40% to 50% in the case of mineral aggregate based on the cement asphalt type.
5- The Pennsylvania test showed that the crumb rubber had better retention than the used mineral aggregates for both emulsions. The knock-off weight loss ranged from 1% to 3% for crumb rubber aggregate versus 7% to 12% for mineral aggregates.
6- Sand patch and section image processing showed that replacing mineral aggregates with crumb rubber can improve the macrotexture of chip seal. An increase of 25% and 33% in mean texture depth (MTD) was observed when 100% of the trap rock and creek gravel were replaced with crumb rubber, respectively.

7- While both micro and macrotexture showed significant improvements when crumb rubber was used as aggregate, a reduction ranging from 1.5% to 20% in the British pendulum number (BPN) for specimens with rubber replacement ratios ranging from 25% to 100% were recorded. It should be noted that the BPN is not reliable for rough surface such as chip seal. Hence, more advanced techniques are required to measure the skid resistance of crumb rubber-based chip seal. Furthermore, under high temperatures, crumb rubber-based chip seal outperformed mineral aggregate-based chip seal. Specimens with 100% rubber did not show any loss in BPN under high temperature of 65 ^{o}C while 10% loss was recorded in mineral aggregate-based chip seal.

8- A virtual 3D pyramid shape can be used to simulate aggregate particles to find the required binder application rate that produces chip seal with an embedment depth ranging from 50% to 80% of the average aggregate least dimension.

9- Using crumb rubber as a partial or total replacement for the mineral aggregate was successfully implemented in the field using the traditional procedure and equipment. However, it was required to use steel roller compactor instead of rubber tires compactor to compact the chip seal. Fig. 64 shows the rubberized chip seal after almost five months of cold weather including snow and ice. It also includes several times of snow removals.

Figure 64: Rubberized chip seal after five months from its application

5.1 Future work

While this study showed the feasibility and advantages of using crumb rubber in chip seal, further studies are still required to fine-tune this application niche. Further studies to measure the different components of the surface friction resistance instead of the gross skid resistance (e.g. hysteresis forces and adhesion) as some of the standard tests such as British pendulum tester does not simulate the real case scenario when tires been in contact with chip seal surface. Also, it is recommended to measure the frictional property of chip seal at a varied speed as some component of the friction resistance can be highly affected by speed. Investigating the snow removal, during winter, needs also an in-depth study with different alternatives. The effect of using crumb rubber aggregate on the fuel consumption of travelling vehicles is also another important issue. Maintenance and application of more than one layer of chip seal maybe required during the service life of roads; hence, need to be investigated as well. Examining the applicability of the proposed pyramid shape aggregate model for different aggregate sizes and types is necessary. Extensive field implementation with different traffic conditions and road geometries are also required before a state or national implementation of crumb rubber-based chip seal.

A. Supplementary experimental data

A.1. Aggregate properties

Creek gravel

Trap rock

Crumb rubber

Aggregate sample before washing

Materials passing from sieve No. 200 (Dry sieve)

Washing aggregates without wetting agent

Materials collected on sieve No. 200 (washing)

Figure 65: Sieve analysis to find the dust amount

Steel charges for the test

Testing machine

Figure 66: Tools and equipment used for Micro-Deval

Aggregate soaking before test

Reference Aggregate soaking

Aggregate after testing

Aggregate after testing

Reference aggregate after testing (oven-dried)

Separating the steel charges from aggregate

Figure 67: Micro-Deval test

A.2. Sweep test

Asphalt felt

Sweep test tools

Fig. A.4: Sweep test tools

Emulsion heating to 35^{o}C

Weighing emulsion

Figure 68: Emulsion preparation

Felt is ready to apply chip seal

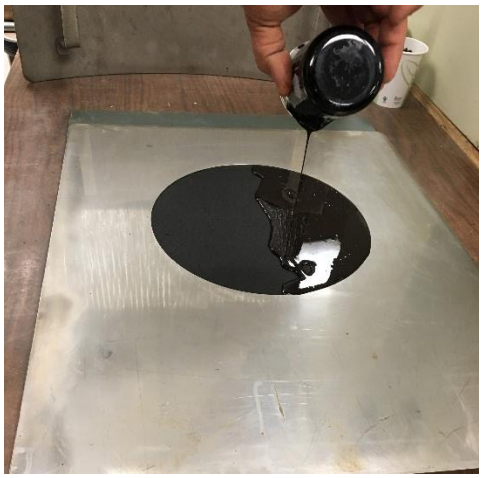

Applying emulsion to asphalt felt

Striking and leveling emulsion

Applying aggregate (50% crumb rubber)

Applying aggregate (creek gravel)

Figure 69: Emulsion and aggregate application for a test specimen

Compacting chip seal from west to east

Compacting chip seal from north to south

Weighing a test specimen before curing

Chip seal curing

Chip seal curing at 35 ^{o}C

Figure 70: Compaction and curing a specimen

Removing the unembedded aggregate

Weighing a specimen before the test

Figure 71: Removing the extra aggregate and weighing a specimen

Mixer

Specimen ready for testing

Sweeping test for creek gravel

Sweeping test for trap rock

Figure 72: Preparation and running the mixer for the sweep test

Removing the loose aggregate

Specimen after testing

Weighing the specimen after testing

Specimen after testing

Figure 73: Specimens after being subjected to sweep test

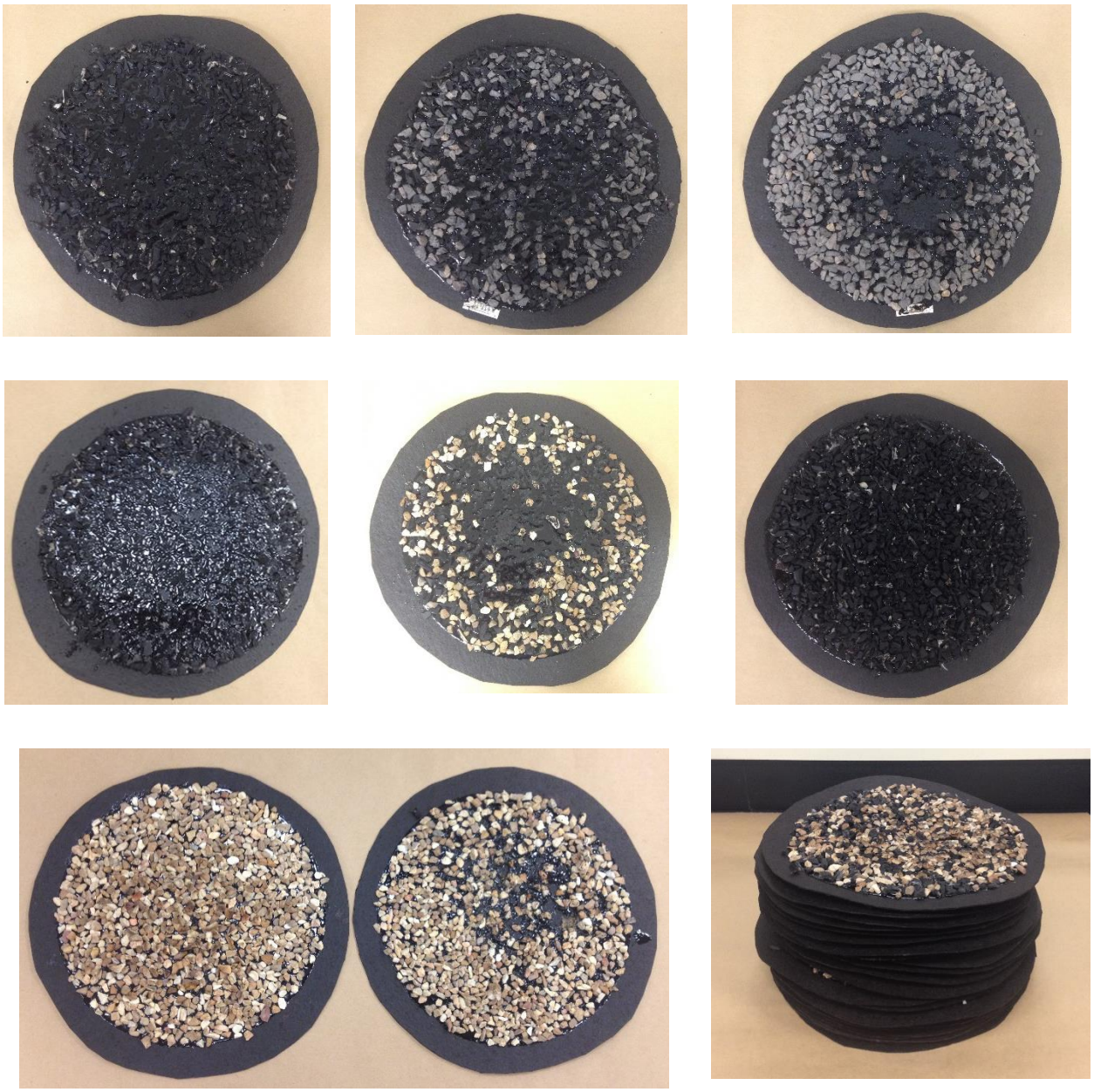

Figure 74: Specimens after being subjected to sweep test

Figure 75: Specimens after being subjected to sweep test

A.3 Vialit test

Vialit drop - test unit

Specimen plates and ball

Fig. A.11: Test apparatus and accessories

Test specimen (creek gravel)

Test specimen (crumb rubber)

Figure 76: Test specimens

Specimens curing for 48 hours at 60 °C

Specimens conditioning for 30 minutes at 25 °C

Specimens freezing for 30 minutes at -22 °C

Specimens under test

Figure 77: Preparation of a specimen for testing

No loose crumb rubber aggregate

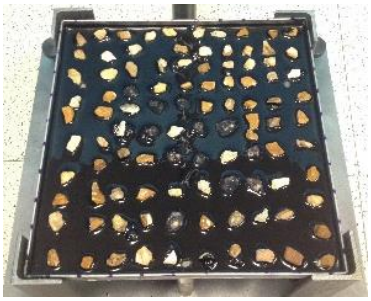

Specimen with dislodged mineral aggregates

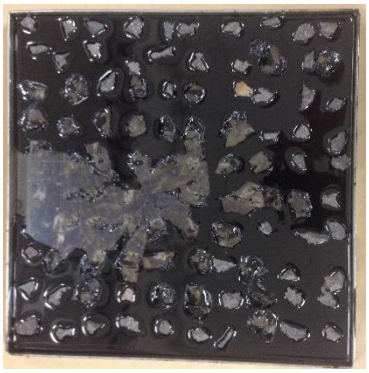

Loose aggregate

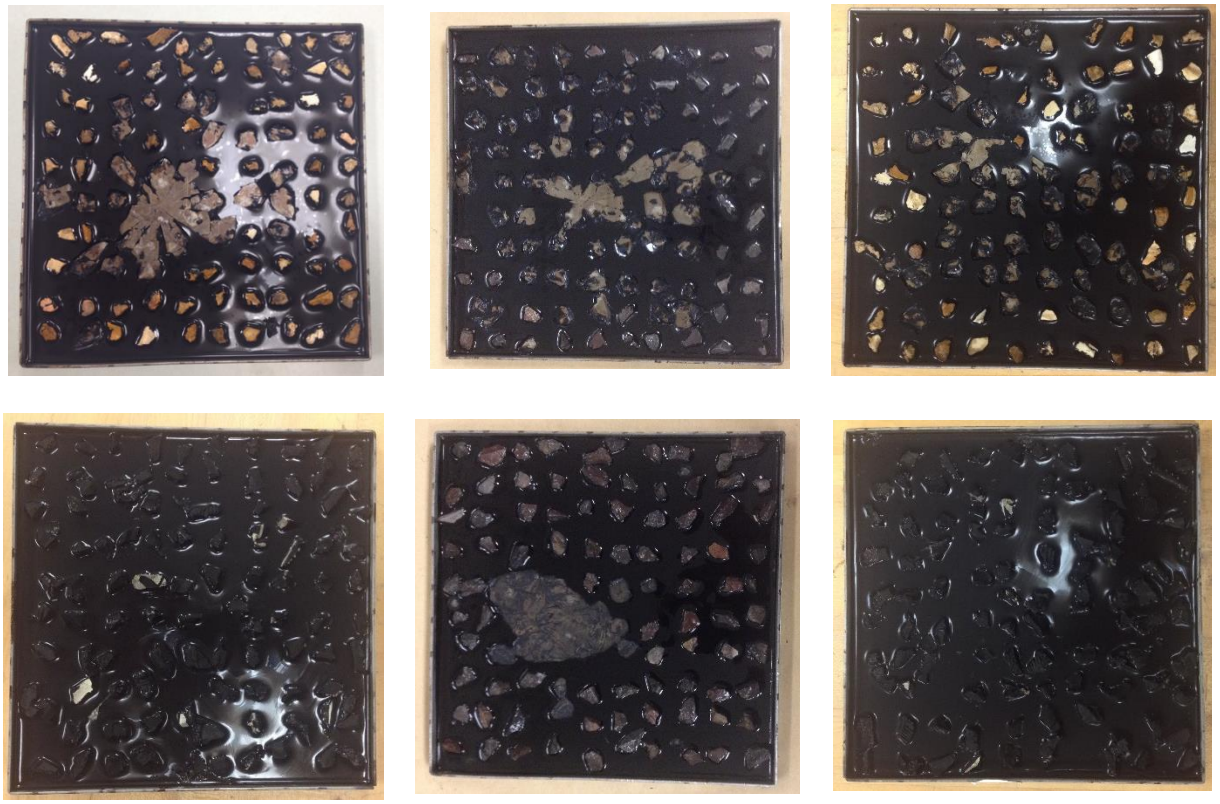

Figure 78: Tested specimens

A.4. Pennsylvania test

Laboratory sieve shaker

Weigh the testing pan

Fig. A.15: Tools required for testing

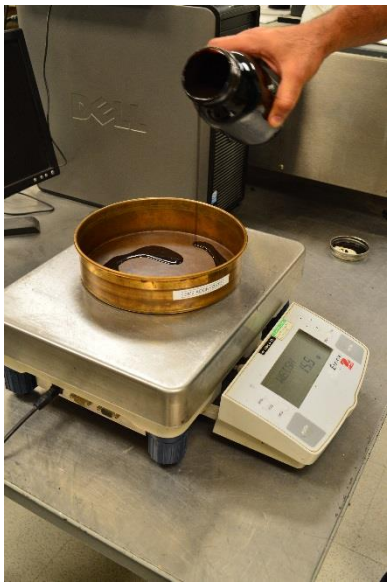

Adding emulsion to testing pan

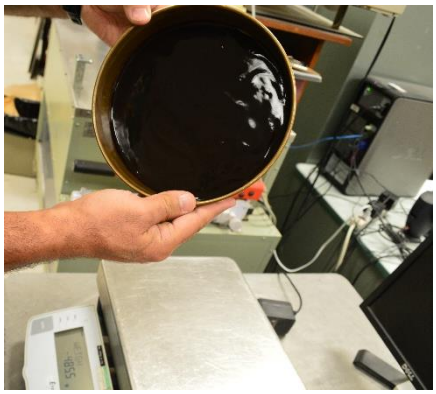

Pan with applied Emulsified Asphalt

Figure 79: Preparing emulsion in pan

Complete assembly for applying aggregate

Complete assembly for applying aggregate

Crumb rubber spread in the pan

Aggregate spread in the pan

Fig. A.17: Passing the aggregate through the different sieves

Chip seal pan with neoprene bearing pad

Sample under compression (compacting)

Figure 80: Compaction of a test specimen

Chip seal pans curing for 24 hours

Initial retention loss

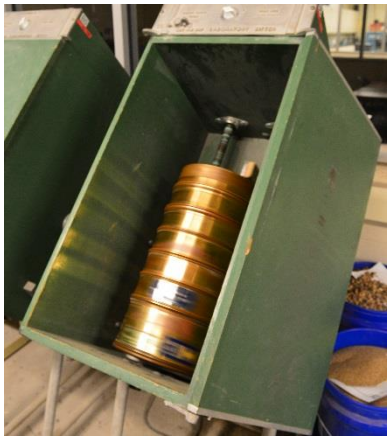

Knock-off test Assembly

Knock-off loss

Specimens after testing

Figure 81: Initial retention and knock-off

A.5. Sand patch test

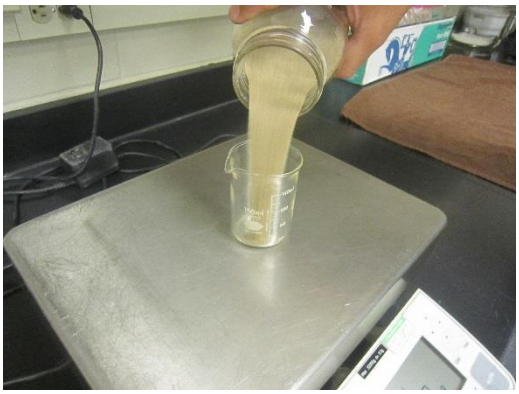

Sand weighing

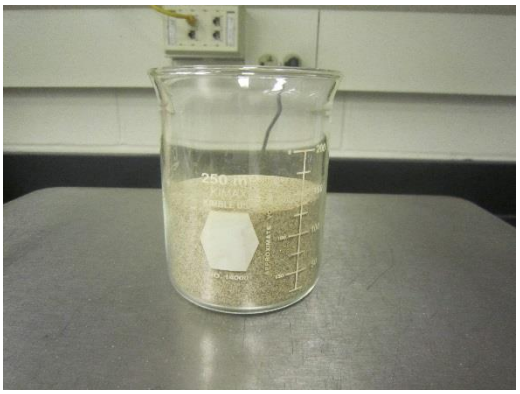

Sand weighing

Figure 82: Sand preparation

Sand spreading on rubberized chip seal specimen

Sand spreading on conventional chip seal specimen

Sand spreading on 50% crumb rubber chip seal specimen

Sand spreading with the disk

Sand spreading with the disk

Sand spreading with the disk

Figure 83: Applying and spreading the sand on different specimens

Chip seal specimens with creek gravel and varied rubber content with sand patch

Chip seal specimens with trap rock and varied rubber content with sand patch

Figure 84: Sand patch applied to different chip seal specimens

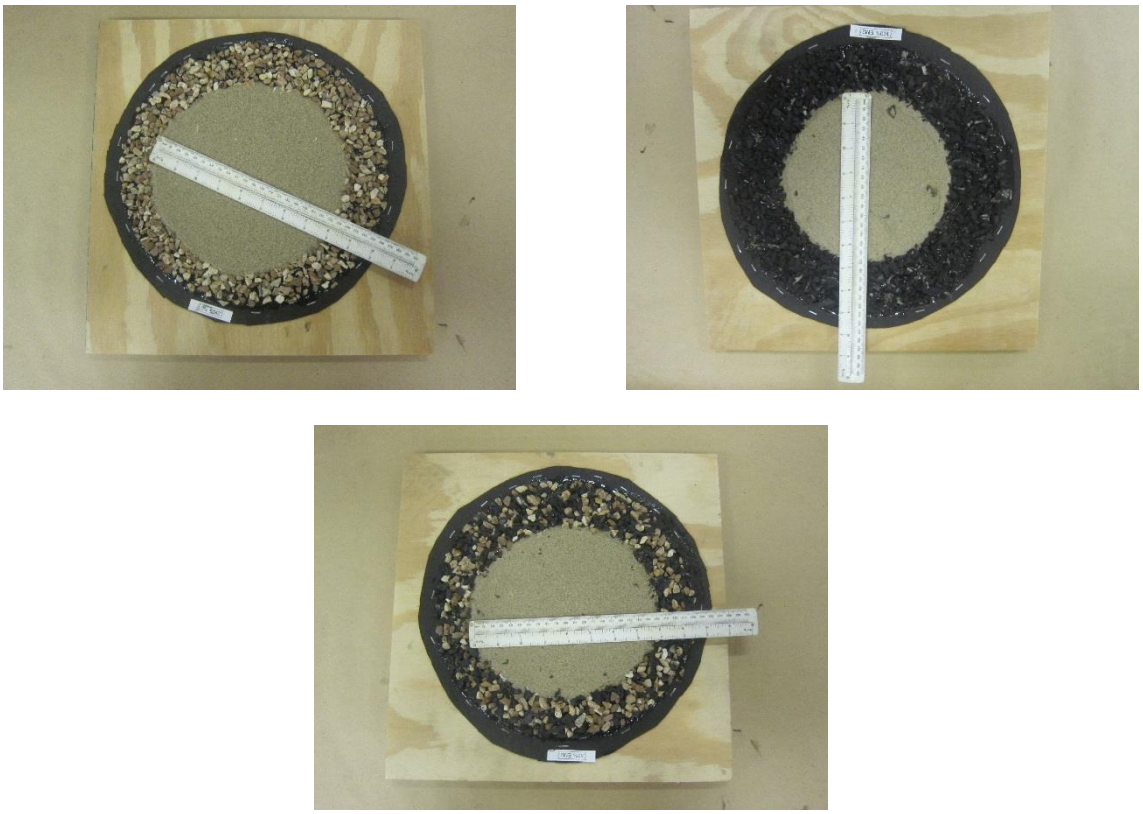

Figure 85: Sand circle diameter measurement

A.6. Standard and modified skid resistance test

Applying emulsion

Applying aggregate

Specimen compaction

Specimen compaction

Figure 86: Specimen preparation

Specimen curing

Specimen is ready for testing

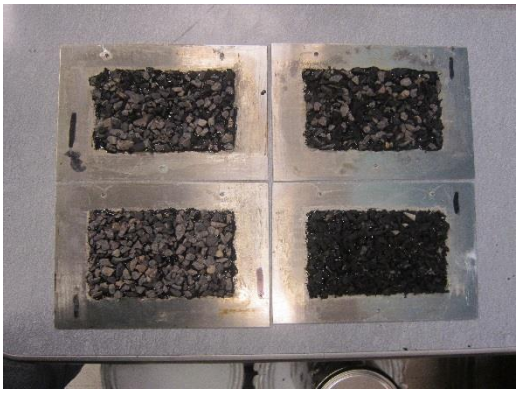

Specimen is ready for testing

Sprinkling water on the specimen before test

Fig. A.24: Specimen curing and moisturizing

Skid resistance apparatus

Chip seal specimen during testing

Figure 87: Specimen during standard testing

Heating pad

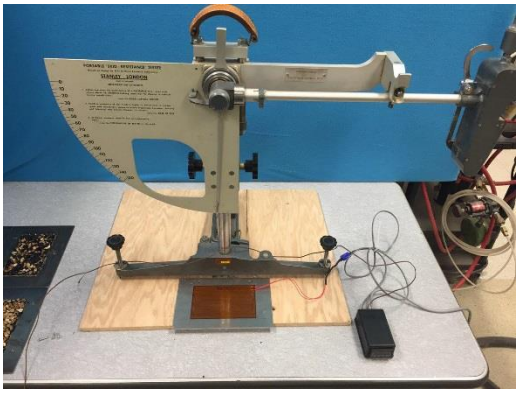

Modified skid resistance apparatus

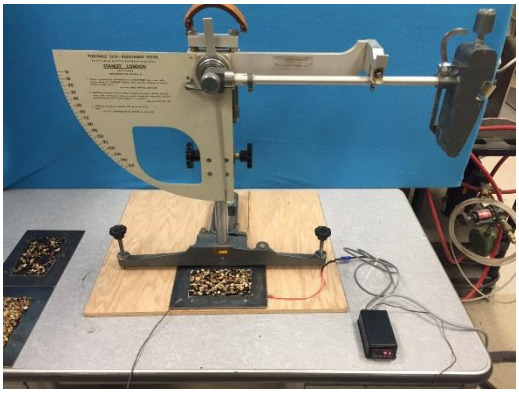

Chip seal specimen during modified test

Specimen having high temperature

Figure 88: Specimen during modified testing

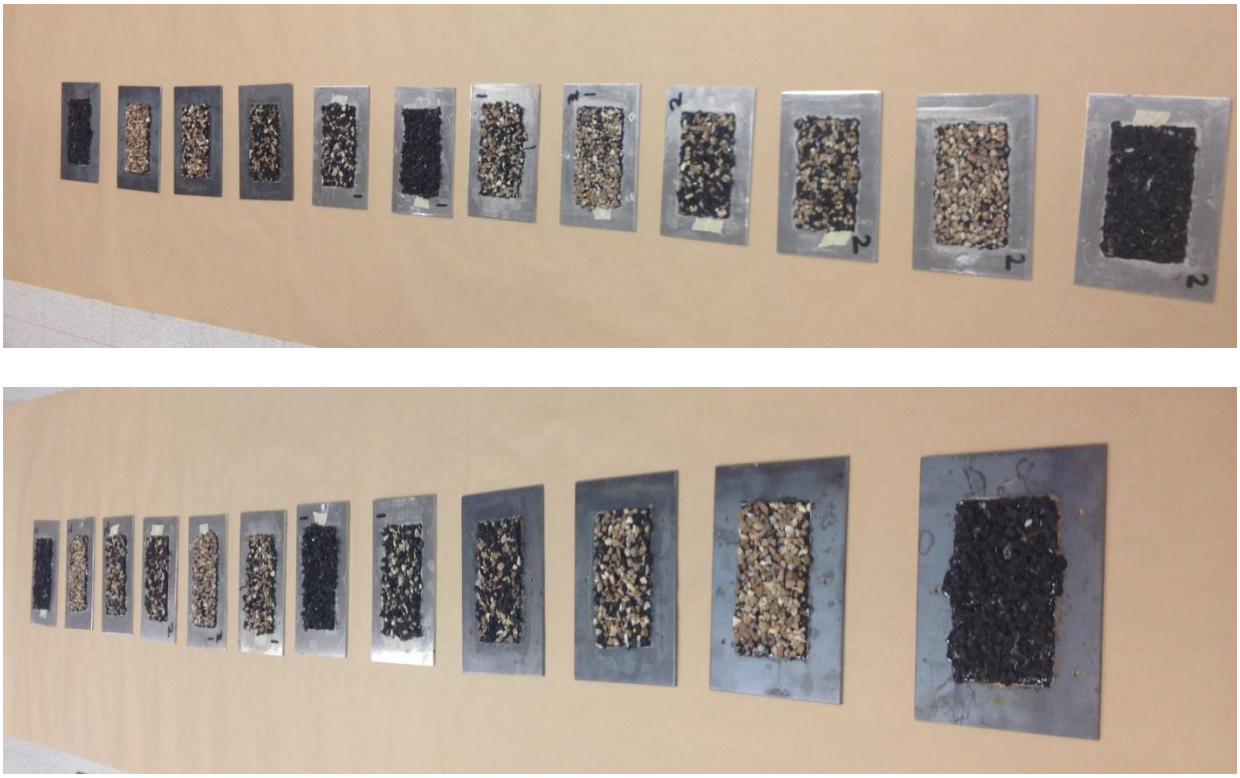

Figure 89: Tested specimens

A.7. Microscope results of the aggregates surface using 3D microscopy

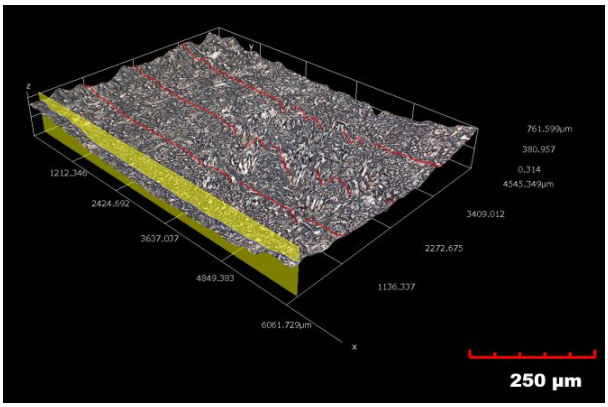

Trap rock

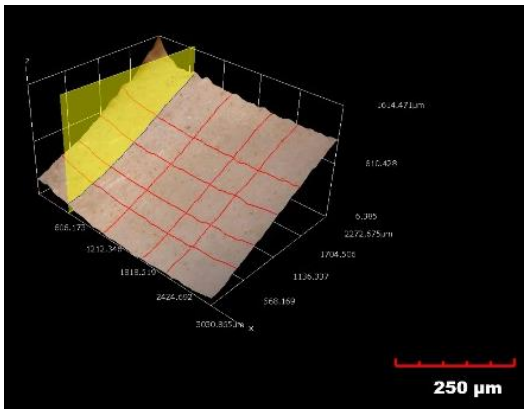

Creek gravel

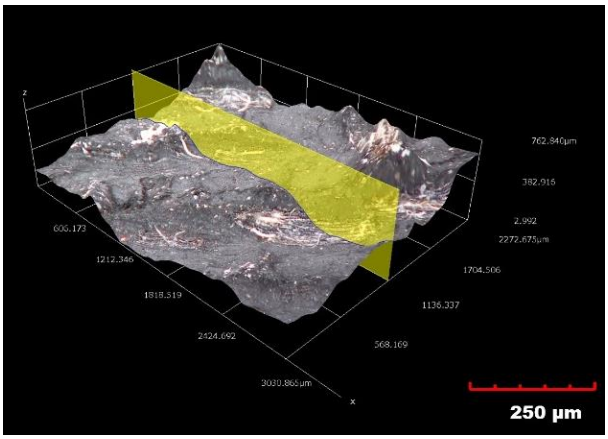

Ambient crumb rubber

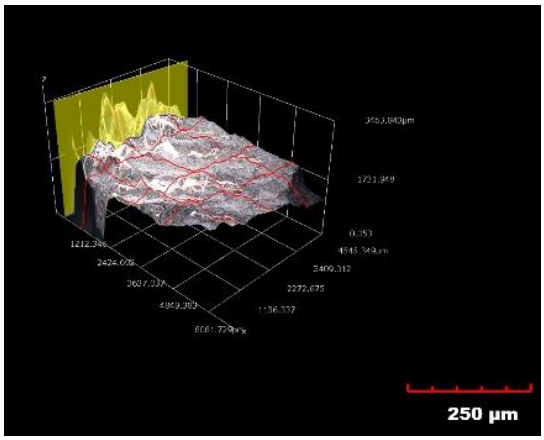

Ambient crumb rubber

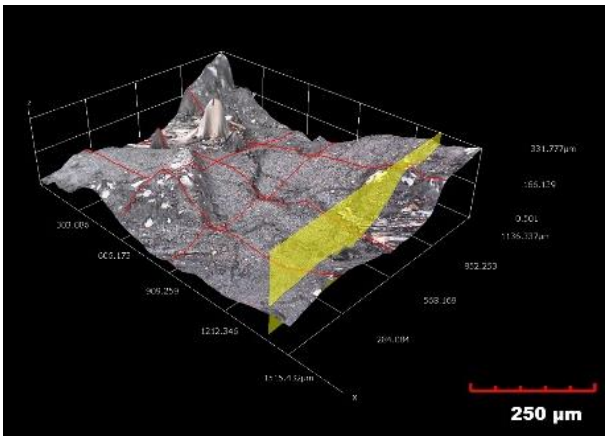

Ambient crumb rubber

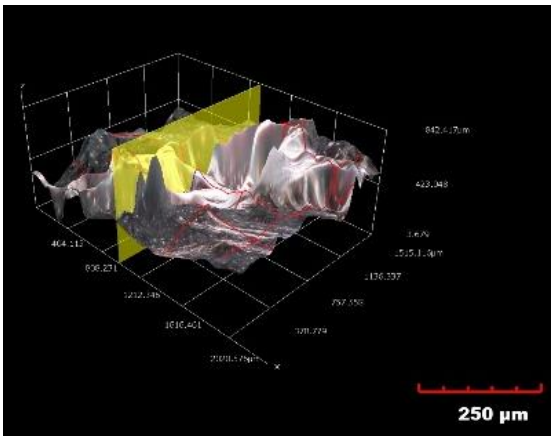

Ambient crumb rubber

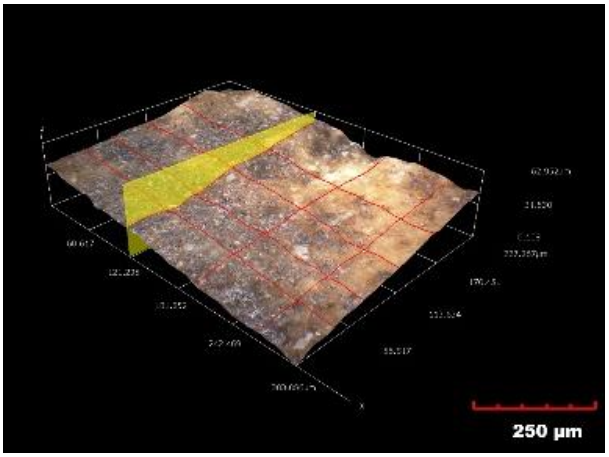

Creek gravel

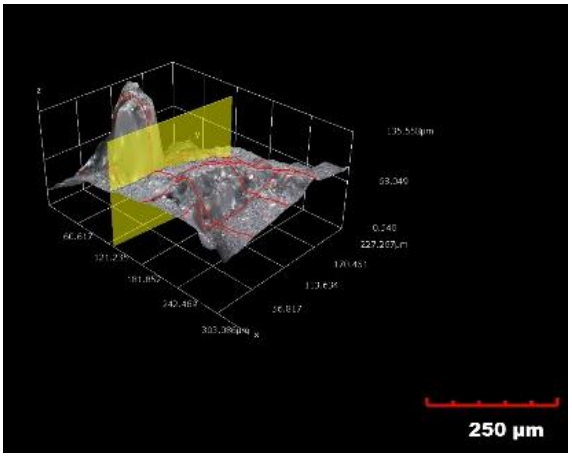

Ambient crumb rubber

Ambient crumb rubber

Trap rock

Creek gravel

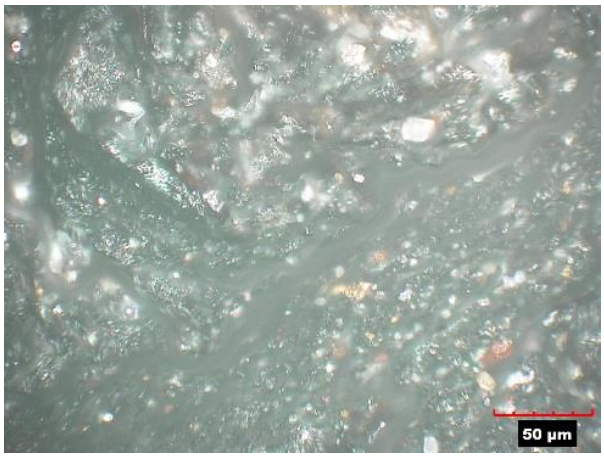

Trap rock

Creek gravel

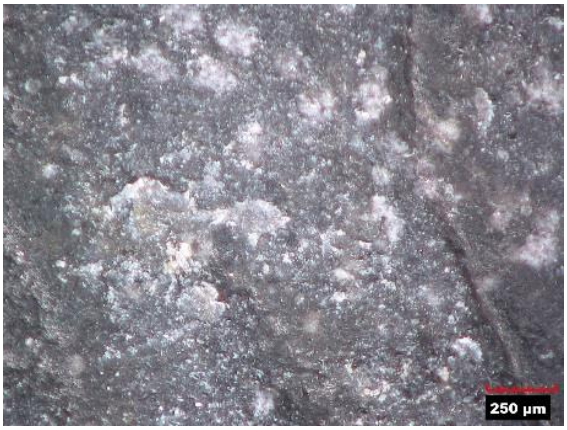

Trap rock

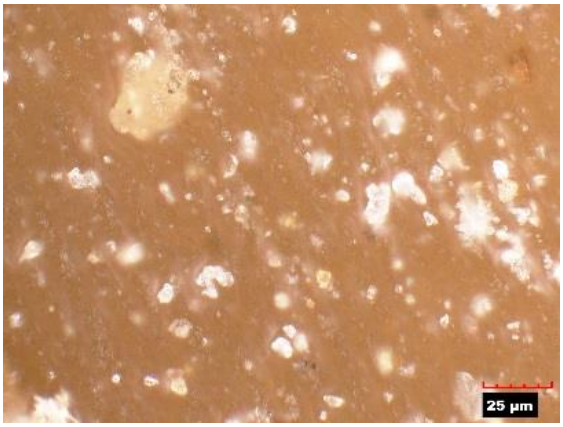

Creek gravel

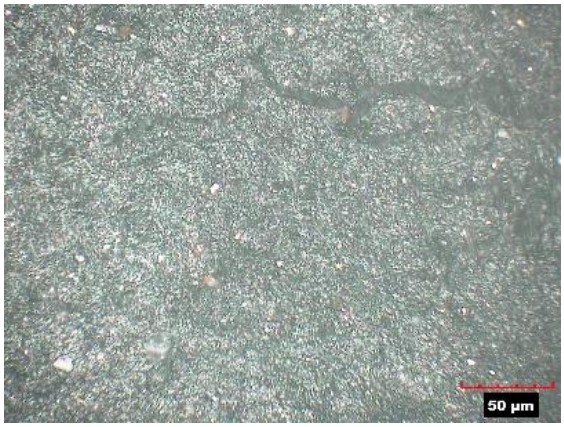

Trap rock

Figure 90: Specimens under 3D microscopy

PART 2

Environmental assessment of using scrap tires as an aggregate in construction

1. Introduction

Scrap tire rubber is a low cost material that can be used in pavement construction. However, leaching of toxic metals could be a concern. There is no research on the leaching of toxic metals from scrap tire when it used with asphalt for pavement construction. We have conducted different tests using scrap tire rubber and asphalt to determine the metal leaching behavior under varies condition, to assess the environmental impact of the beneficial use of scrap tires.

2. Objective

The objective is to assess the potential environmental impact of scrap rubber-integrated chip seals in terms of metal leaching.

3. Experimental Methods

3.1. Overall Task Description:

This study included four tasks.

- **Task 1** was to determine the leaching behavior of heavy metals from bare tire rubber.
- **Task 2** was to determine the acid-extractable metal contents from the tire rubber and asphalt. This was to determine maximum leachable heavy metals from these materials.
- **Task 3** was to determine the metal leaching from the tire rubber and asphalt sample under a simulated acid rain condition in Missouri (west of Mississippi river).
- **Task 4** was to determine the metal leaching behavior of different specimens under the pH range between 4 and 10, or the pH effect on metal leaching.

3.1.1. Task 1 – **Leaching from Bare Tire Rubber**

In this task, two tire samples, frozen (F) and unfrozen (UF) based on cutting method, were studied.

Size distribution

The size distribution of the received sample was measured by using different standard sieves. The procedure is briefly described below:

1. Place standard sized sieves, 3/8'', No.4, No.10, No. 18, and No. 50 from top to bottom.
2. Place 50 g tire rubber sample on the top sieve and seal the top sieve.
3. Shake the sieves for approximately 5 minutes.
4. Weigh the tire rubber sample stayed on each standard sieve

Leaching Experiment

The leaching experiments were conducted under different pH conditions by following EPA method 1313. Based on the sample size distribution data, the majority size (the size that most samples are graded) was used in this experiment. For this experiment, the sample F's majority size was 2 – 4.75 mm; the sample UF's majority size was 4.75-9.52 mm; these two sized samples were used for the leaching experiment, respectively. The solid: liquid ratio of 1:10 was used. The pure water (MQ water) was used as the leaching liquid. The pH of different leaching bottles was adjusted by adding different volumes of stock nitric acid or sodium hydroxide solution at the beginning of the leaching experiment. Different types of control experiments were also performed. The experiment procedure is described below and the experimental matrix is shown in **Table 1**:

1. Add 5 g of the sample into each of the 125-mL pre-acid cleaned plastic leaching bottle (except the blanks).
2. Add 50 mL of MQ water into each of the leaching bottles.
3. Add different volumes of nitric acid or sodium hydroxide solution into different bottles to adjust pH; then seal all bottles tightly.
4. Shake all bottles for 24 hours with at 180 rpm under room temperature.
5. Allow the samples to settle for 1 hour.
6. Filter the solution through 0.22 μm nylon membrane filter.
7. Use partial filtrate to measure pH and TDS.

8. Acidify remaining filtrate with trace metal grade nitric acid to a pH < 2.
9. Analyze thirteen elements in the filtrate using ICP-MS, GFAA or flame AA after appropriate dilution with 1% HNO_3 solution if needed.

3.1.2. **Task 2 – Acid Extraction of Heavy Metals from Tire and Asphalt Samples**

In this task, the tire sample UF and two asphalt samples were digested with acid for heavy metals availability testing.

Sample Pretreatment

There was no pretreatment for the tire sample UF. However, the two asphalt samples were pre-treated using procedures below:

1. Place the melted asphalts on a plexiglass.
2. Transfer the plexiglass (with asphalt) to an oven at a temperature of 60°C for 2 h.
3. Dry the asphalt at 30°C for 24 h within the oven.
4. Use a ceramic knife to cut the asphalt into small pieces (washing procedure for ceramic knife listed in Section 3.6).

Size Selection

The size of the samples was reduced before digestion. The specifically sized samples were selected for the experiment as described below:

1. Place standard sieves, 3/8’’, 1/4’’, and No.4 from top to bottom.
2. Place samples on the top sieve and seal the top sieve.
3. Shake the sieves for approximate 5 minutes.
4. Collect the samples remained on No.4 sieve and use it for digestion experiment (size range 4.75 – 6.30 mm). This size range is consistent with that used in the real pavement.

Digestion Experiment

The digestion experiment was conducted in a microwave digester (ETHOS E, MILESTONE) at Lincoln University, MO, using EPA method 3051A with slight modifications. The mixture of concentrated trace metal grade hydrochloric acid and nitric acid was used as the digestion solution. Different types of control experiments, spike recovery, and blank were also performed. Table 2 shows the sample information. The digestion procedure is described below:

1. Weigh 0.2 g sample into a digestion vessel.
2. Add 3 mL of trace metal grade hydrochloric acid and 9 mL of nitric acid into the digestion vessel. Sample duplicate, sample spike, and blank were also included using different vessels.
3. Seal digestion vessels and load them into the microwave digester.
4. The digestion program includes a 10 min ramp to 180 °C with a 10 min hold, followed by a 10 min cooling time.
5. Remove the digestion vessels from the digester, and wait for about 1 h to cool.
6. Open the digestion vessel and transfer the solution to pre-acid cleaned 50 mL centrifuge tubes; dilute the solution to 50 mL with MQ water.
7. Measure thirteen elements in the digestion solution using ICP-MS or flame AA after appropriate dilutions with 1% HNO_3 (if needed) and filtration through 0.22 µm nylon membrane filter.

3.1.3. Task 3 – Leaching under Simulated Acid Rain Condition

In this task, the leaching behavior of different tire rubber and asphalt samples were tested at a pH 5 by following EPA method 1312. The tests were performed by adding extraction fluid with a pH of 5 (contains sulfuric acid and nitric acid at a ratio of 60:40) to the sample at a solid: liquid ratio of 1:20 followed by mixing at a rate of 180 rpm on a mechanical shaker for 24 h. Several control bottles were also included. The experimental procedure is described below, and the sample information is shown in Table 3:

1. Specimens were prepared by according to the ASTM standard. Specimens contain tire sample UF mixed with each type of asphalt, and aggregate mixed with each type of asphalt. Control group included each of the asphalt, tire, and aggregates.
2. The sample size was reduced by cutting the specimens with a ceramic knife and going through standard size sieve, 3/8'', 1/4'', and No.4. The sample remained on No.4 sieve was used for this experiment (size range 4.75 – 6.30 mm).
3. The pH 5 extraction fluid was prepared by adding 16.5 μL acid mixture (acid mixture prepared by adding 0.15 g H_2SO_4 and 0.10 g HNO_3 in 20 mL MQ water) into 100 mL MQ water at a 125-mL pre-acid cleaned plastic bottle.
4. Five gram of sample was added to each leaching bottles (except the blanks). Bottles were sealed tightly after addition of extraction fluid and sample.
5. The leaching bottles were shaken for 24 hours at 180 rpm of under room temperature.
6. All bottles were settled for 1 hour.
7. The supernatant was filtered through 0.22 μm nylon membrane filter.
8. The pH and TDS were measured using part of the filtrate sample.
9. The rest of the filtrate sample was acidified with trace metal grade nitric acid to a pH < 2.
10. The heavy metal concentrations in the acidified filtrate samples were determined using ICP-MS or flame AA. Appropriate dilution with 1% HNO_3 was needed before ICP-MS measurement.

3.1.4. Task 4 – Effect of pH on Metal Leaching

In this task, the leaching behavior of different specimens was tested in a pH range between 4 and 10 by using EPA method 1313. The S/L ratio of 1:10 was used in this experiment. Several control experiments were also performed. The experiment procedures are similar to the acid rain leaching experiment, except the pH of the leaching bottles are adjusted individually. The detailed experimental information is shown in Table 4:

3.2. Cleaning

To avoid cross contamination, special tools and cleaning procedures were used. The cutting tool used was a ceramic knife instead of a normal metal knife. Before cutting each specimen, the ceramic knife was cleaned with gasoline to dissolve asphalt residual followed by deionized (DI) water rinsing, and then cleaned again with acetone to remove gasoline residual followed by DI water rinsing. This procedure was exactly followed during the experiment for each specimen.

3.3. Quality Assurance/Quality Control

To ensure the high-quality data, most of the recommended QA/QC by the EPA were followed. For analysis using ICP-MS, US EPA method 200.8 QC guidelines were closely followed. ICP-MS was calibrated with standard solutions diluted from a calibration standard mixture containing all the elements purchased from PerkinElmer, Inc. The linear ranges of the calibration were determined and used for the quantitative analysis of the samples. Detailed control samples are listed in Table 1, 2, 3, and 4. Laboratory reagent blank was tested to check any procedural contamination. The blank sample was prepared and measured using the same procedures as for the samples except no solid sample was used. The method detection limits (MDLs) for the leaching test were determined by instrumentation detection limits (IDLs), and MDLs were 10 times of IDLs. The MDLs for the screening test and digestion test were 20 times of IDLs. To make sure the good reproducibility, duplicated samples were performed for some samples. The precision of the duplication was expressed as the relative percentage difference (RPD) and was calculated using the equation below.

RPD (%) = 100 x (C_h-C_l)/C_{av}

where

C_h is detected high concentration of duplicated sample,

C_l is detected low concentration of duplicated sample, and

C_{av} is the average of the C_h and C_l

Sample spike (spike) were tested by adding known concentration standards into the leached sample solution before performing the analysis. The spike recoveries (%) were calculated by the following equation:

Spike recovery (%) = 100 x (detected conc. of spiked sample – control sample)/Spiked concentration

4. Results and Discussion

4.1. Task 1 leaching from bare tire sample

4.1.1. Size distribution

The tire sample information and major size of each type of tire for Task 1 are listed in Table 5. Fig. 1 and 2 show the size distribution of sample F and sample UF, respectively.

4.1.2. Leaching test

The metal leaching concentration from the sample for Task 1 is shown in Table 6. Fig.3 shows the metal concentration in the leaching solution as a function of pHs.

From the leaching test results of Task 1, the major leached out heavy metal from the bare tire is zinc (Zn), followed by Copper (Cu), and Barium (Ba). In the leaching solution, Zn concentration is in parts per million level which are significantly higher than any other metals. The sample F (2 – 4.75 mm) has higher metal leached out than sample UF (4.75 – 9.32 mm). Smaller sized tire tends to leach out more metal because smaller samples have larger specific surface area. The results also show that the acidic condition resulted in more metal leaching than the alkaline condition.

4.2. Task 2 total acid extractable metals

The acid extractable metal content in tire and asphalts were converted from metal concentration in digestion solution, the final volume of digestion solution, and mass of the sample. The metal contents of tire and asphalt are shown in Table 7.

To determine the acid extractable metal content in tire and asphalt samples, the microwave digestion method was applied. The results show the major metal content in the tire is Zn which was about 1.6% of the total tire weight. The major metal content in both types of asphalt is Ni and other metals are very low (below or close to method detection limit). The reproducibility and spike recovery of tire sample are not good through the microwave digestion method, the possible reason is the incomplete digestion of tire sample. After microwave digestion, there were some solid found in the tire digestion vessel which asphalt digestion vessel did not have.

4.3. Task 3 leaching under acid rain condition

The screening test results using simulated acid rain for Task 3 are shown in Table 8. It simulated the condition that material on the field and exposed to the acid rain. From the screening test results, trace amount heavy metal was leached from the sample after 24-hour extraction and all the concentrations are below EPA drinking water standard.

4.4. Task 4 pH effect on leaching from specimen

The metal leaching concentration from the sample for Task 4 (pH effect) is shown in Table 9. Fig. 4 shows the metal concentration in the leaching solution as a function of pHs.

From the results of Task 4, it indicated when tire used with asphalt there is a significant reduction of heavy metal leaching under different pH condition, especially for Zn. Approximate 50% reduction of Zn leaching was found compared with the bare tire. The leaching of Co, Cu, and Ba were also reduced when tire used with asphalt. The leached concentration of Be, Cr, As, Cd, Sb, Tl, and Pb are very low (below or close to method detection limit) in tire, asphalt and tire used with asphalt sample. Besides the effect of using asphalt to cover tire surface, the elevated pH condition also reduced the metal leaching in all types of samples. From the comparison between the control group and tire used with asphalt, the tire contributed most of the metal leaching except Ni which is the major metal element in asphalt.

5. Conclusions

Using scrap tires as an aggregate in construction does not have significant environmental impact. The toxic heavy metals leached from the tire or tire used with asphalt samples were below EPA drinking water standard. The major leached heavy metal from the tire is Zn which is consistent with the tire component (Rhodes, et al., 2012). However, Zn is not regulated in the primary drinking water regulations.

Table E- 1 :Sample matrix for Task 1.

Sample ID	Tire Sample	Acid/Base	Liquid Volume(mL)
F+5	5 g sample F	1.0 mL 6M HNO3	50
F+4	5 g sample F	0.8 mL 6M HNO3	50
F+3	5 g sample F	0.6 mL 6M HNO3	50
F+2	5 g sample F	0.4 mL 6M HNO3	50
F+2D*	5 g sample F	0.4 mL 6M HNO3	50
F+1	5 g sample F	0.2 mL 6M HNO3	50
F	5 g sample F	0	50
F-1	5 g sample F	0.2 mL 10M NaOH	50
F-2	5 g sample F	0.4 mL 10M NaOH	50
F-3	5 g sample F	0.6 mL 10M NaOH	50
F-4	5 g sample F	0.8 mL 10M NaOH	50
F-5	5 g sample F	1.0 mL 10M NaOH	50
MQ	0	0	50
MQ+HNO3	0	1.0 mL 6M HNO3	50
MQ+NaOH	0	1.0 mL 10M NaOH	50
UF+5	5 g sample UF	0.6 mL 1M HNO3	50
UF+4	5 g sample UF	0.4 mL 1M HNO3	50
UF+3	5 g sample UF	0.2 mL 1M HNO3	50
UF+2	5 g sample UF	0.1 mL 1M HNO3	50
UF+1	5 g sample UF	0.2 mL 0.1M HNO3	50
UF	5 g sample UF	0	50
UF-1	5 g sample UF	0.2 mL 0.1M NaOH	50
UF-2	5 g sample UF	0.1 mL 1M NaOH	50
UF-2D*	5 g sample UF	0.1 mL 1M NaOH	50
UF-3	5 g sample UF	0.2 mL 1M NaOH	50
UF-4	5 g sample UF	0.4 mL 1M NaOH	50
UF-5	5 g sample UF	0.6 mL 1M NaOH	50
MQ	0	0	50

Note: * "D" represents sample duplication.

Table E- 2: Detailed information for digestion experiment

Sample ID	Sample Component
T	0.2 g UF tire
T(D)*	0.2 g UF tire
Tspike	0.2 g UF tire with spike
A1	0.2 g Asphalt 1
A2	0.2 g Asphalt 2
A2(D)	0.2 g Asphalt 2
A2spike	0.2 g Asphalt 2 with spike
Blank	N.A.

Note: * "D" represents sample duplication.

Table E- 3:Experimental information for simulated acid rain leaching experiment

Sample ID	Sample	Liquid Volume
T+A1	5 g UF tire asphalt 1 mixture	100 mL extraction fluid
T+A2	5 g UF tire asphalt 2 mixture	100 mL extraction fluid
T+A2(D)*	5 g UF tire asphalt 2 mixture	100 mL extraction fluid
A+A1	5 g aggregate asphalt 1 mixture	100 mL extraction fluid
A+A2	5 g aggregate asphalt 2 mixture	100 mL extraction fluid
A1	5 g asphalt 1	100 mL extraction fluid
A2	5 g asphalt 2	100 mL extraction fluid
T	5 g UF tire	100 mL extraction fluid
A	5 g aggregate	100 mL extraction fluid
Acid	0	100 mL extraction fluid
MQ	0	100 mL MQ water

Note: * "(D)" represents sample duplication.

Table E- 4:Experimental information for leaching test of Task 4.

Sample ID	Sample Component (in 50 mL MQ)	Acid/Base
TA1-1	5 g UF tire with asphalt 1	0.20 mL 0.1 M HNO3
TA1-2	5 g UF tire with asphalt 1	0.14 mL 0.1 M HNO3
TA1-2(D)*	5 g UF tire with asphalt 1	0.14 mL 0.1 M HNO3
TA1-3	5 g UF tire with asphalt 1	0.07 mL 0.1 M HNO3
TA1-4	5 g UF tire with asphalt 1	0
TA1-5	5 g UF tire with asphalt 1	0.05 mL 0.1 M NaOH
TA1-6	5 g UF tire with asphalt 1	0.14 mL 0.1 M NaOH
TA1-7	5 g UF tire with asphalt 1	0.20 mL 0.1 M NaOH
TA2-1	5 g UF tire with asphalt 2	0.20 mL 0.1 M HNO3
TA2-1(D)	5 g UF tire with asphalt 2	0.20 mL 0.1 M HNO3
TA2-2	5 g UF tire with asphalt 2	0.14 mL 0.1 M HNO3
TA2-3	5 g UF tire with asphalt 2	0.08 mL 0.1 M HNO3
TA2-4	5 g UF tire with asphalt 2	0
TA2-5	5 g UF tire with asphalt 2	0.06 mL 0.1 M NaOH
TA2-6	5 g UF tire with asphalt 2	0.14 mL 0.1 M NaOH
TA2-7	5 g UF tire with asphalt 2	0.20 mL 0.1 M NaOH
T1	5 g UF tire	0.40 mL 0.1 M HNO3
T2	5 g UF tire	0.30 mL 0.1 M HNO3
T3	5 g UF tire	0.20 mL 0.1 M HNO3
T3(D)	5 g UF tire	0.20 mL 0.1 M HNO3
T4	5 g UF tire	0.08 mL 0.1 M HNO3
T5	5 g UF tire	0.06 mL 0.1 M NaOH
T6	5 g UF tire	0.14 mL 0.1 M NaOH
T7	5 g UF tire	0.20 mL 0.1 M NaOH
A1-1	5 g Asphalt 1	0.05 mL 0.1 M HNO3
A1-1(D)	5 g Asphalt 1	0.05 mL 0.1 M HNO3
A1-2	5 g Asphalt 1	0
A1-3	5 g Asphalt 1	0.03 mL 0.1 M NaOH
A1-4	5 g Asphalt 1	0.06 mL 0.1 M NaOH
A1-5	5 g Asphalt 1	0.09 mL 0.1 M NaOH
A1-6	5 g Asphalt 1	0.12 mL 0.1 M NaOH
A1-7	5 g Asphalt 1	0.30 mL 0.1 M NaOH
A2-1	5 g Asphalt 2	0.08 mL 0.1 M HNO3
A2-2	5 g Asphalt 2	0.05 mL 0.1 M HNO3
A2-3	5 g Asphalt 2	0.02 mL 0.1 M HNO3
A2-4	5 g Asphalt 2	0.03 mL 0.1 M NaOH
A2-5	5 g Asphalt 2	0.06 mL 0.1 M NaOH
A2-5(D)	5 g Asphalt 2	0.06 mL 0.1 M NaOH

Table E-4 (Cont'd): Experimental information for leaching test of Task 4.

A2-6	5 g Asphalt 2	0.15 mL 0.1 M NaOH
A2-7	5 g Asphalt 2	0.30 mL 0.1 M NaOH
Acid	N.A.	0.4 mL HNO3
Base	N.A.	0.3 mL NaOH
MQ	Blank	N.A.

Note: * "D" represents sample duplication.

Table E- 5:Tire sample information and size distribution

Sample ID	**Major sample size (mm)**	**Mass (%)**
F	2	79.68
UF	4.75	89.38

Table E- 6: Leaching data for Task 1.

Sample ID	pH	TDS	Be**	Cr	Co	Ni	Cu	As	Se	Cd	Sb	Ba	Pb	Tl**	Zn***
		(mg/L)	(µg/L)	(µg/L)	(µg/L)	(µg/L)	(µg/L)	(µg/L)	(µg/L)	(µg/L)	(µg/L)	(µg/L)	(µg/L)	(µg/L)	(mg/L)
MQ	N.A.	N.A.	<MDL	<MDL	<MDL	<MDL	<MDL	<MDL	<MDL	<MDL	<MDL	<MDL	<MDL	<MDL	<MDL
MQ+HNO3	N.A.	N.A.	<MDL	<MDL	<MDL	<MDL	<MDL	<MDL	<MDL	<MDL	<MDL	<MDL	<MDL	<MDL	<MDL
MQ+NaOH	N.A.	N.A.	<MDL	<MDL	<MDL	<MDL	<MDL	<MDL	<MDL	<MDL	<MDL	<MDL	<MDL	<MDL	<MDL
F+5	1.56	17100	<MDL	22.93	66.17	48.01	506.05	2.63	4.09	0.55	6	96.73	91.41	<MDL	21.75
F+4	1.62	16800	<MDL	15.79	61.72	17.95	510.72	2.02	3.41	0.43	5.67	98.17	103.73	<MDL	20.94
F+3	1.7	16700	<MDL	12.65	56.41	13.84	455.96	1.67	3.37	0.36	6.54	68.57	54.1	<MDL	19.17
F+2	1.82	17600	<MDL	13.26	43.54	9.74	425.5	1.31	3.94	0.4	6.37	86.6	58.51	<MDL	18.86
F+2D****	1.8	17000	<MDL	13.34	57.8	10.12	418.73	1.24	3.05	0.44	4.56	123.39	57.19	<MDL	20.15
F+1	2.02	16900	<MDL	12.59	48.49	17.29	584.23	1.51	3.06	0.56	5.43	66.56	63.45	<MDL	19.5
F	6.96	16300	<MDL	2.49	32.19	<MDL	44.24	<MDL	1.95	<MDL	1.65	37.73	1.94	<MDL	10.62
F-1	12.77	16900	<MDL	3.82	9.47	<MDL	173.98	1.54	5.87	<MDL	11.9	7.06	10.96	<MDL	11.33
F-2	13.07	15600	<MDL	5.48	13.84	39.81	154.09	3.54	15.2	<MDL	14.6	10.21	21.46	<MDL	13.49
F-3	13.21	15500	<MDL	7.9	18.14	<MDL	162.49	2.09	3.91	<MDL	22.09	12.79	17.68	<MDL	14.84
F-4	13.31	15400	<MDL	10.91	25.14	<MDL	177.04	1.76	3.14	<MDL	18.79	6.26	29.86	<MDL	14.66
F-5	13.41	14200	<MDL	10.06	25.46	<MDL	142.81	2.3	6.35	<MDL	19.9	10.72	17.86	<MDL	15.3
MQ	N.A.	N.A.	<MDL	<MDL	<MDL	<MDL	<MDL	<MDL	<MDL	<MDL	<MDL	<MDL	<MDL	<MDL	<MDL
UF+5	2.27	1650	<MDL	9.49	29.8	8.78	1215.21	1.05	1.11	0.41	7.47	188.62	105.24	<MDL	9.57
UF+4	2.44	1410	<MDL	10.75	23.82	10.83	1379.29	1.46	2.14	0.47	25.1	135.82	90.16	<MDL	7.89
UF+3	2.67	870	<MDL	8.58	21.42	8.49	1091.94	1.47	2.14	0.26	6.99	98.95	71.09	<MDL	6.41
UF+2	2.99	420	<MDL	7.56	25.55	13.11	873.71	0.51	<MDL	0.27	13.84	156.8	79.99	<MDL	5.91
UF+1	3.85	80	<MDL	<MDL	19.08	<MDL	17.67	<MDL	1.05	<MDL	11.28	61	1.15	<MDL	5.02
UF	7.92	170	<MDL	0.54	2.52	<MDL	<MDL	0.42	1.16	<MDL	3.48	53.17	<MDL	<MDL	0.13
UF-1	9.62	30	<MDL	0.62	0.98	<MDL	<MDL	0.68	1.82	<MDL	16.21	13.15	1.39	<MDL	<MDL
UF-2	11.35	170	<MDL	1.06	1.64	<MDL	12.79	0.51	2.85	<MDL	10.68	7.04	2.71	<MDL	0.12
UF-2D***	11.4	220	<MDL	0.9	1.03	<MDL	9.63	0.38	1.3	<MDL	14.3	10.32	2.54	<MDL	0.16
UF-3	11.77	400	<MDL	1.06	1.32	<MDL	14.22	1.19	4.33	<MDL	54.35	10.87	2.32	<MDL	0.33
UF-4	12.11	990	<MDL	2.04	1.64	<MDL	27.49	1.43	3.74	<MDL	73.17	5.37	3.17	<MDL	0.65
UF-5	12.31	990	<MDL	2.33	2.33	<MDL	83.42	1.82	7.41	<MDL	32.48	7.48	11.5	<MDL	0.92
MDL			10	0.5	0.25	5	5	0.25	1	0.25	0.25	0.25	1	10	1/0.01
EPA drinking	6.50-8.50	0.5	4	100	N.A.	N.A.	1300	10	50	5	6	2000	15	2	5000
water standard															
F Spike recovery(%)			N.A.	109.4	101.62	148.43	-51.76	113.13	101.92	112.75	112.18	99.52	104.86	N.A.	N.A.
UF+1 Spike recovery(%)			N.A.	95.05	87.63	235.81	112.26	100.93	97.47	100.49	99.86	78.71	105.35	N.A.	N.A.
UF-1 Spike recovery(%)			N.A.	92.3	92.46	103	24.99	95.41	87.48	92.79	88.35	83.86	94.07	N.A.	N.A.
F+2 RPD(%) *****	1.1	3.47	N.A.	0.66	28.16	3.79	1.6	5.67	25.47	8.7	33.1	35.04	2.29	N.A.	6.64
UF-2 RPD(%)*****	0.44	25.64	N.A.	16.82	45.7	0	28.2	29.1	74.45	0	28.96	37.87	6.41	N.A.	29.66

Note:
* Real sample concentration converted from ICP-MS or Flame AA data. The dilution factor, acid used to acidify sample, and acid or base used to adjust pH were corrected in the conversion.
** Be and Tl were measured by GFAA.
*** Zinc concentration was very high, so samples were analyzed using Flame AA except control group, UF, UF-1, UF-2, UF-2D, UF-3, UF-4, and UF-5. MDL of Flame AA and ICP-MS was is 1 and 0.01 mg/L, respectively.
**** "D" represents sample duplication.
***** Some high RPD (%) is caused by the sample concentration is very close to method detection limit.

Table E- 7:Metal contains in tire and asphalts

Sample ID	Be	Cr	Co	Ni	Cu	As	Se	Cd	Sb	Ba	Tl	Pb	Zn*
	(ug/g)	(ug/g)	(ug/g)	(ug/g)	(ug/g)	(ug/g)	(ug/g)	(ug/g)	(ug/g)	(ug/g)	(ug/g)	(ug/g)	(mg/g)
T	<MDL	4.97	286.04	3.28	244.85	24.78	2.68	0.73	2.22	4.42	<MDL	1.73	17.06
T(D)**	<MDL	5.52	227.66	3.16	59.63	26.65	6.58	0.96	2.44	4.97	<MDL	2.95	15.94
Tspike***	2.54	6.13	30.41	31.48	78.29	24.05	7.11	2.81	3.73	5.88	1.74	20.47	21.5
Spiked Conc****	2.5	2.5	10	25	50	2.5	5	2.5	2.5	2.5	2.5	10	5
T recovery(%)	101.75	35.11	-209.65	113.03	-147.91	-66.79	49.55	78.33	55.95	47.49	69.54	181.22	100
A1	<MDL	4.4	<MDL	65	4.73	21.72	0.87	<MDL	0.98	1.58	<MDL	0.57	0.09
A2	<MDL	5.91	<MDL	72.96	<MDL	26.57	0.96	<MDL	1.2	1.28	<MDL	<MDL	0.12
A2(D)	<MDL	5.21	<MDL	67.05	<MDL	23.62	0.7	<MDL	0.78	1.28	<MDL	<MDL	0.11
A2spike	2.62	8.19	1.94	124.99	30.65	29.6	4.93	2.64	3.41	3.88	1.7	5.85	7.05
Spiked Conc*****	2.5	2.5	2.5	50	25	2.5	5	2.5	2.5	2.5	2.5	5	10
A2 recovery(%)	104.74	105.06	77.62	109.97	122.6	180.23	82.01	105.41	96.92	103.86	68.00	116.94	70.5
Blank	<MDL	2.61	<MDL	<MDL	<MDL	19.57	1.05	<MDL	0.8	0.44	<MDL	<MDL	<MDL
MDL	0.125	0.25	0.625	2.5	2.5	0.125	0.5	0.125	0.125	0.125	0.125	0.5	0.005/0.5
T RPD(%)	N.A.	10.49	22.73	3.88	121.67	7.28	84.22	27.09	9.33	11.82	N.A.	52.12	6.73
A2 RPD(%)	N.A.	12.67	N.A.	8.44	N.A.	11.77	31.67	N.A.	42.12	0.34	N.A.	N.A.	6.56

Note:
* Zinc concentration was measured by flame AA except A1, A2, and A2(D). The MDL of ICP-MS and Flame AA are 0.005 and 0.5 mg/g, respectively.
** "(D)" represents duplicate.
***"T spike" means tire sample spiked with certain metal concentration at the beginning of microwave digestion.
**** "Spike conc" means the spiked metal concentration for each element.

Table E- 8:Experimental results using simulated acid rain (Task 3*).

Sample ID	pH	TDS (mg/L)	Be (µg/L)	Cr (µg/L)	Co (µg/L)	Ni (µg/L)	Cu (µg/L)	As (µg/L)	Se (µg/L)	Cd (µg/L)	Sb (µg/L)	Ba (µg/L)	Pb (µg/L)	Tl (µg/L)	Zn** (mg/L)
T+A1	7.10	21.20	<MDL	<MDL	3.25	<MDL	37.52	<MDL	<MDL	<MDL	<MDL	11.94	<MDL	<MDL	0.46
T+A2	6.51	16.10	<MDL	<MDL	4.22	<MDL	<MDL	<MDL	9.72	<MDL	<MDL	11.89	<MDL	<MDL	0.51
T+A2(D)***	7.35	17.90	<MDL	<MDL	3.54	<MDL	<MDL	<MDL	<MDL	<MDL	0.61	12.41	<MDL	<MDL	0.29
A+A1	7.59	17.40	<MDL	<MDL	0.64	<MDL	28.16	<MDL	<MDL	<MDL	<MDL	5.83	<MDL	<MDL	<MDL
A+A2	6.95	16.90	<MDL	<MDL	0.72	<MDL	17.29	<MDL	<MDL	<MDL	<MDL	5.17	<MDL	<MDL	<MDL
A1	4.40	24.00	<MDL	<MDL	0.97	10.73	49.75	<MDL	<MDL	<MDL	<MDL	<MDL	<MDL	<MDL	0.24
A2	4.28	26.20	<MDL	<MDL	1.00	<MDL	<MDL	<MDL	8.34	<MDL	<MDL	<MDL	<MDL	<MDL	0.18
T	7.10	12.60	<MDL	<MDL	9.50	<MDL	16.08	<MDL	<MDL	<MDL	3.13	30.68	2.11	<MDL	0.40
A	7.26	5.48	<MDL	<MDL	<MDL	<MDL	<MDL	<MDL	<MDL	<MDL	<MDL	0.74	<MDL	<MDL	<MDL
Acid	4.60	N.A.	<MDL	<MDL	<MDL	<MDL	<MDL	<MDL	<MDL	<MDL	<MDL	<MDL	<MDL	<MDL	<MDL
MQ	N.A.	N.A.	<MDL	<MDL	<MDL	<MDL	<MDL	<MDL	<MDL	<MDL	<MDL	<MDL	<MDL	<MDL	<MDL
MDL			0.50	1.00	0.50	10.00	10.00	0.50	2.00	0.50	0.50	0.50	2.00	0.50	0.10
EPA drinking water standard	6.50-8.50	500	4	100	N.A.	N.A.	1300	10	50	5	6	2000	15	2	5
T+A1 Spike recovery(%)			104.00	94.79	99.34	85.25	8.94	103.88	104.79	99.60	104.64	102.08	95.95	104.41	N.A.
T+A2 RPD(%)	12.12	10.59	N.A.	N.A.	17.63	N.A.	N.A.	N.A.	N.A.	N.A.	N.A.	4.27	N.A.	N.A.	54.95

Note:
* Real sample concentration was converted from ICP-MS or FAA data. The dilution factor and volume of acid used to acidify sample were applied in the conversion of ICP-MS/FAA data to real concentration
** Zinc concentration was measured by flame AA.
*** "(D)" represents duplicate.

Table E- 9:The effect of pH on leaching (Task 4).

Sample ID	pH	TDS	Be	Cr	Co	Ni	Cu	As	Se	Cd	Sb	Ba	Tl	Pb	Zn*
		(mg/L)	(μg/L)	(μg/L)	(μg/L)	(μg/L)	(μg/L)	(μg/L)	(μg/L)	(μg/L)	(μg/L)	(μg/L)	(μg/L)	(μg/L)	(mg/L)
TA1-1	4.11	65.6	<MDL	1.39	8.10	19.39	116.54	<MDL	4.71	<MDL	2.43	27.73	<MDL	4.59	2.74
TA1-2	4.73	122.3	<MDL	<MDL	7.15	14.83	59.62	<MDL	3.80	<MDL	2.17	25.38	<MDL	1.10	2.52
TA1-2(D)**	4.76	55.3	<MDL	<MDL	6.99	9.53	92.41	<MDL	3.84	<MDL	1.21	40.66	<MDL	3.04	2.52
TA1-3	6.49	43.4	<MDL	<MDL	11.28	7.52	<MDL	<MDL	7.00	<MDL	3.32	31.86	<MDL	<MDL	1.63
TA1-4	7.03	42.9	<MDL	<MDL	6.75	10.12	<MDL	<MDL	10.11	<MDL	2.40	20.93	<MDL	<MDL	0.30
TA1-5	7.64	41.9	<MDL	0.89	3.62	14.73	11.35	<MDL	5.67	<MDL	1.57	18.29	<MDL	<MDL	0.16
TA1-6	8.7	35	<MDL	0.61	2.36	7.12	22.75	<MDL	5.12	<MDL	1.95	9.77	<MDL	1.27	0.10
TA1-7	9.56	51.8	<MDL	0.63	2.09	6.06	19.12	<MDL	18.69	<MDL	1.46	10.68	<MDL	<MDL	0.12
Acid	N.A.	N.A.	<MDL	<MDL	<MDL	<MDL	<MDL	<MDL	<MDL	<MDL	<MDL	<MDL	<MDL	<MDL	<MDL
Base	N.A.	N.A.	<MDL	<MDL	<MDL	<MDL	<MDL	<MDL	<MDL	<MDL	<MDL	<MDL	<MDL	<MDL	<MDL
MQ	N.A.	N.A.	<MDL	<MDL	<MDL	<MDL	<MDL	<MDL	<MDL	<MDL	<MDL	<MDL	<MDL	<MDL	<MDL
TA1-2 spike recovery(%)			106.35	112.21	105.18	108.18	113.29	109.52	113.84	111.25	106.18	114.19	107.32	107.44	N.A.
TA1-2 RPD(%)	0.63	75.45	N.A.	N.A.	2.33	43.48	43.14	N.A.	1.04	N.A.	56.95	46.26	N.A.	93.59	0.00
TA2-1	3.99	66.3	<MDL	0.58	6.71	12.03	86.94	<MDL	1.71	<MDL	2.17	20.51	<MDL	5.35	2.08
TA2-1(D)	4.16	60.7	<MDL	0.52	9.21	12.34	77.95	<MDL	6.99	1.78	2.81	21.37	<MDL	4.37	2.30
TA2-2	5.49	51.9	<MDL	<MDL	10.32	8.06	14.67	<MDL	4.98	<MDL	3.98	31.78	<MDL	<MDL	2.08
TA2-3	6.07	38.9	<MDL	<MDL	4.78	<MDL	<MDL	<MDL	9.93	<MDL	1.20	19.87	<MDL	<MDL	1.63
TA2-4	6.66	37	<MDL	<MDL	7.09	<MDL	<MDL	<MDL	5.14	<MDL	0.84	12.70	<MDL	<MDL	0.52
TA2-5	7.52	33.3	<MDL	<MDL	2.78	<MDL	<MDL	<MDL	17.79	<MDL	0.63	11.10	<MDL	<MDL	0.10
TA2-6	8.84	41.2	<MDL	0.68	2.24	5.33	12.54	<MDL	4.03	<MDL	1.49	8.06	<MDL	<MDL	0.05
TA2-7	9.73	52.5	<MDL	0.59	2.32	<MDL	10.21	<MDL	7.23	<MDL	1.07	7.36	<MDL	<MDL	0.09

Note:
* Zinc concentration was measured by flame AA and some low concentration was measured by ICP-MS. The MDLs of flame AA and ICP-MS are 0.1 and 0.01 ppm, respectively.
** "(D)" represents duplicate.

Table E- 10:The effect of pH on leaching (Task 4).

Sample ID	pH	TDS	Be	Cr	Co	Ni	Cu	As	Se	Cd	Sb	Ba	Tl	Pb	Zn*
		(mg/L)	(μg/L)	(μg/L)	(μg/L)	(μg/L)	(μg/L)	(μg/L)	(μg/L)	(μg/L)	(μg/L)	(μg/L)	(μg/L)	(μg/L)	(mg/L)
TA2-7 spike recovery(%)			102.56	106.14	104.17	101.96	98.84	110.67	109.21	107.93	101.98	108.80	101.00	101.58	N.A.
TA2-1 RPD(%)	4.17	8.82	N.A.	11.39	31.48	2.55	10.91	N.A.	121.20	N.A.	25.74	4.11	N.A.	20.18	10.15
T1	4.55	69.3	<MDL	0.98	27.64	9.02	379.84	<MDL	2.32	0.41	8.43	95.08	<MDL	2.51	6.38
T2	5.44	56.8	<MDL	<MDL	31.41	8.32	26.10	<MDL	4.11	0.40	7.24	79.64	<MDL	<MDL	5.93
T3	5.86	46.5	<MDL	<MDL	25.78	5.52	<MDL	<MDL	3.40	0.32	5.56	61.52	<MDL	<MDL	4.52
T3(D)	6.09	45.1	<MDL	<MDL	19.13	<MDL	<MDL	<MDL	1.91	0.31	6.81	76.59	<MDL	<MDL	4.08
T4	6.6	29.7	<MDL	0.72	19.90	<MDL	6.30	<MDL	1.72	0.30	3.51	46.17	<MDL	<MDL	2.74
T5	7.96	22.4	<MDL	<MDL	<MDL	<MDL	<MDL	<MDL	2.38	0.21	5.14	24.12	<MDL	<MDL	0.07
T6	8.93	27.1	<MDL	0.62	<MDL	<MDL	5.17	<MDL	1.61	0.21	3.90	15.99	<MDL	<MDL	0.04
T7	9.6	35.2	<MDL	0.66	<MDL	<MDL	<MDL	<MDL	3.43	0.15	3.22	11.08	<MDL	<MDL	0.05
T4 spike recovery(%)			104.26	94.24	99.40	97.26	92.64	100.31	106.71	95.46	102.93	99.47	103.11	100.81	N.A.
T3 RPD(%)	3.85	3.06	N.A.	N.A.	29.60	N.A.	N.A.	N.A.	56.30	2.73	20.27	21.83	N.A.	N.A.	10.34
A1-1	3.99	29.00	<MDL	<MDL	<MDL	17.61	73.52	<MDL	<MDL	0.49	<MDL	4.01	<MDL	4.64	0.44
A1-1(D)	3.80	41.50	<MDL	<MDL	<MDL	24.17	35.40	<MDL	1.82	<MDL	<MDL	4.00	<MDL	8.73	0.44
A1-2	5.86	12.70	<MDL	1.21	<MDL	16.74	7.94	<MDL	<MDL	<MDL	<MDL	4.52	<MDL	<MDL	0.34
A1-3	6.09	20.20	<MDL	0.67	<MDL	15.52	<MDL	<MDL	2.21	0.25	<MDL	3.89	<MDL	<MDL	0.30
A1-4	6.60	23.50	<MDL	<MDL	<MDL	<MDL	<MDL	<MDL	<MDL	<MDL	<MDL	2.63	<MDL	<MDL	0.06
A1-5	7.96	24.00	<MDL	0.65	<MDL	<MDL	<MDL	<MDL	<MDL	<MDL	<MDL	2.09	<MDL	<MDL	<MDL
A1-6	8.93	29.80	<MDL	0.83	<MDL	<MDL	<MDL	<MDL	1.67	<MDL	<MDL	2.16	<MDL	<MDL	<MDL
A1-7	9.82	68.40	<MDL	<MDL	<MDL	<MDL	<MDL	<MDL	2.24	<MDL	<MDL	2.37	<MDL	<MDL	0.01
A1-1 spike recovery(%)			99.10	97.90	90.10	93.91	95.55	97.65	103.73	92.87	100.85	94.74	103.73	96.73	N.A.
A1-1 RPD(%)	4.88	35.46	N.A.	N.A.	N.A.	31.41	70.00	N.A.	N.A.	N.A.	N.A.	0.24	N.A.	61.13	0.52
A2-1	4.09	45.60	<MDL	<MDL	<MDL	23.78	35.00	<MDL	1.76	<MDL	<MDL	5.06	<MDL	2.87	0.19
A2-2	4.79	23.80	<MDL	<MDL	<MDL	13.53	29.58	<MDL	1.56	<MDL	<MDL	2.82	<MDL	1.22	0.26
A2-3	5.96	15.50	<MDL	<MDL	<MDL	<MDL	<MDL	<MDL	1.52	0.27	<MDL	3.44	<MDL	<MDL	0.16
A2-4	6.64	26.70	<MDL	0.72	<MDL	8.21	<MDL	<MDL	<MDL	0.25	<MDL	2.87	<MDL	<MDL	0.08
A2-5	7.63	20.50	<MDL	<MDL	<MDL	<MDL	<MDL	<MDL	1.94	<MDL	<MDL	2.35	<MDL	<MDL	<MDL
A2-5(D)	7.64	46.00	<MDL	<MDL	<MDL	<MDL	<MDL	<MDL	1.33	<MDL	<MDL	3.83	<MDL	<MDL	0.01
A2-6	8.64	42.80	<MDL	<MDL	<MDL	<MDL	<MDL	<MDL	1.19	<MDL	<MDL	3.39	<MDL	<MDL	<MDL
A2-7	10.08	71.30	<MDL	<MDL	<MDL	<MDL	<MDL	<MDL	0.72	<MDL	<MDL	2.95	<MDL	<MDL	<MDL
A2-1 spike recovery(%)			103.18	104.13	106.22	100.31	111.73	101.20	97.65	98.54	105.59	101.36	106.34	96.98	N.A.
A2-5 RPD(%)	0.13	76.69	N.A.	N.A.	N.A.	N.A.	N.A.	N.A.	37.39	N.A.	N.A.	48.07	N.A.	N.A.	N.A.
EPA drinking	6.50-8.50	500	4	100	N.A.	N.A.	1300	10	50	5	6	2000	2	15	5
water standard															
MDL			0.25	0.5	0.25	5	5	0.25	1	0.25	0.25	0.25	0.25	1	0.01/0.1

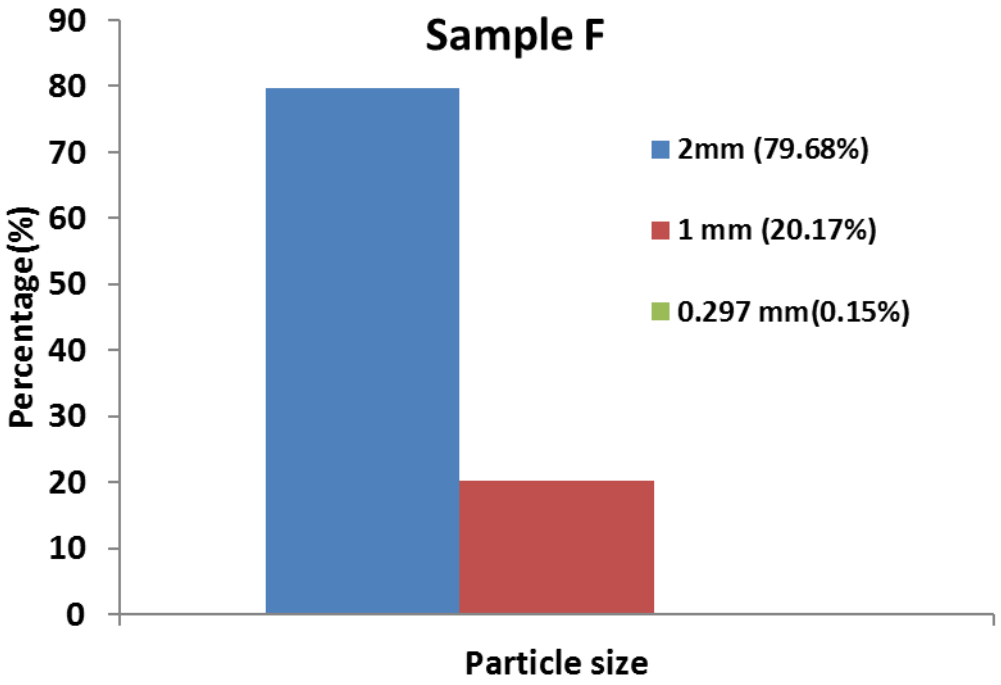

Figure E- 1: Size distribution of sample F.

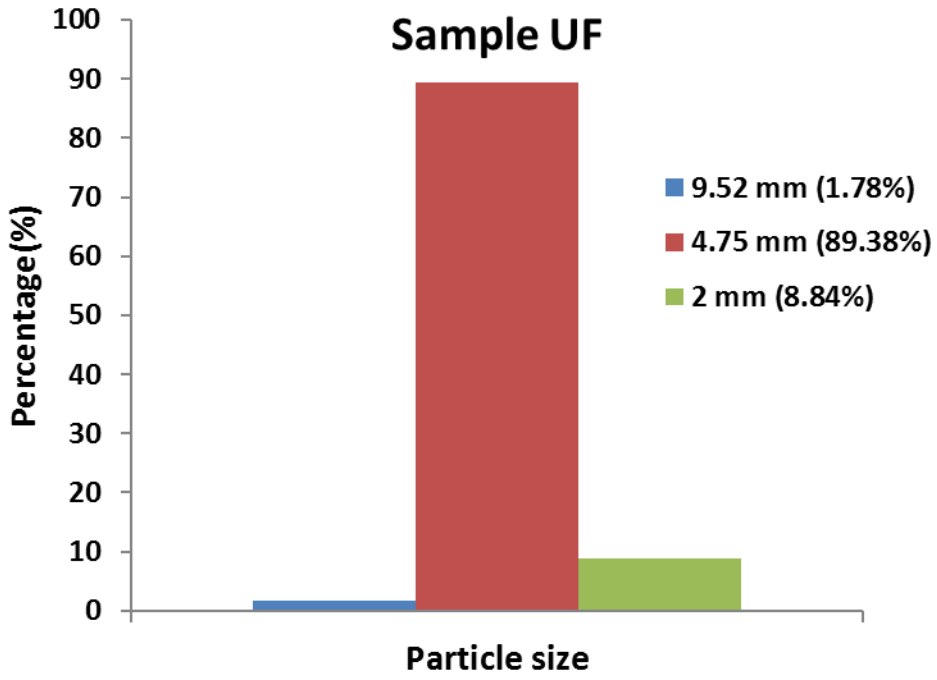

Figure E- 2: Size distribution of sample UF.

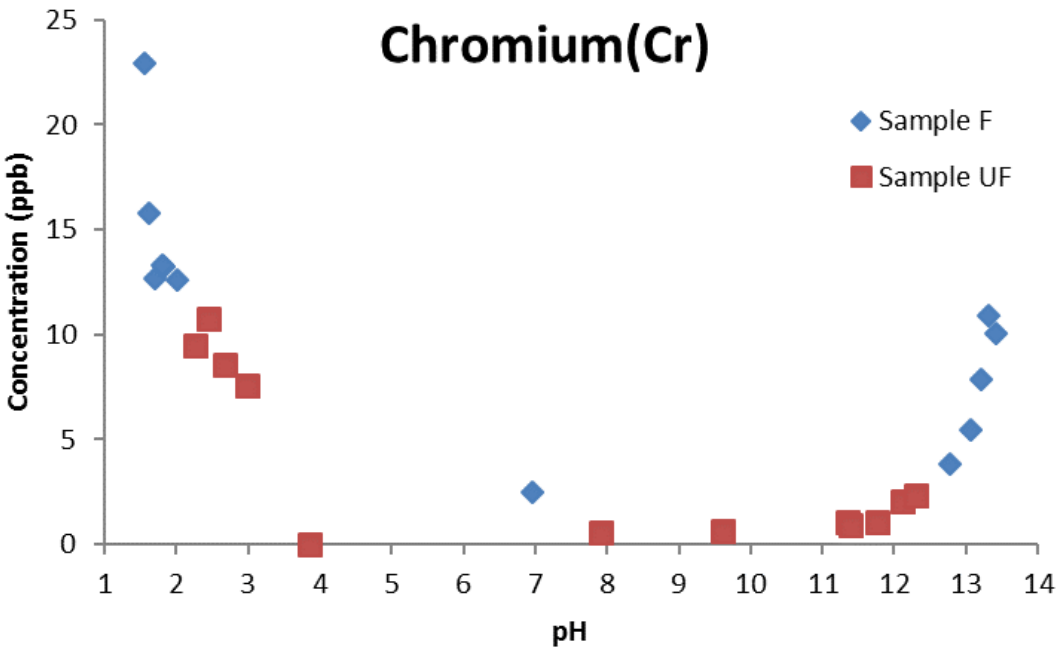

Figure E- 3:Metal concentration in leaching solution as function of pHs (Task 1)

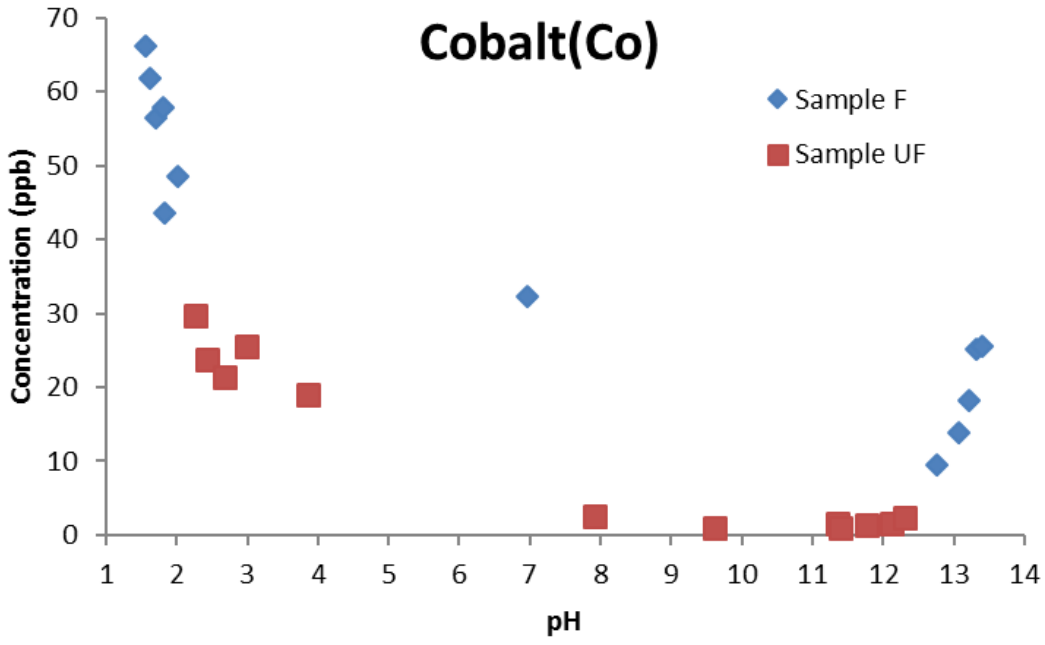

Figure E- 4:Metal concentration in leaching solution as function of pHs (Task 1)

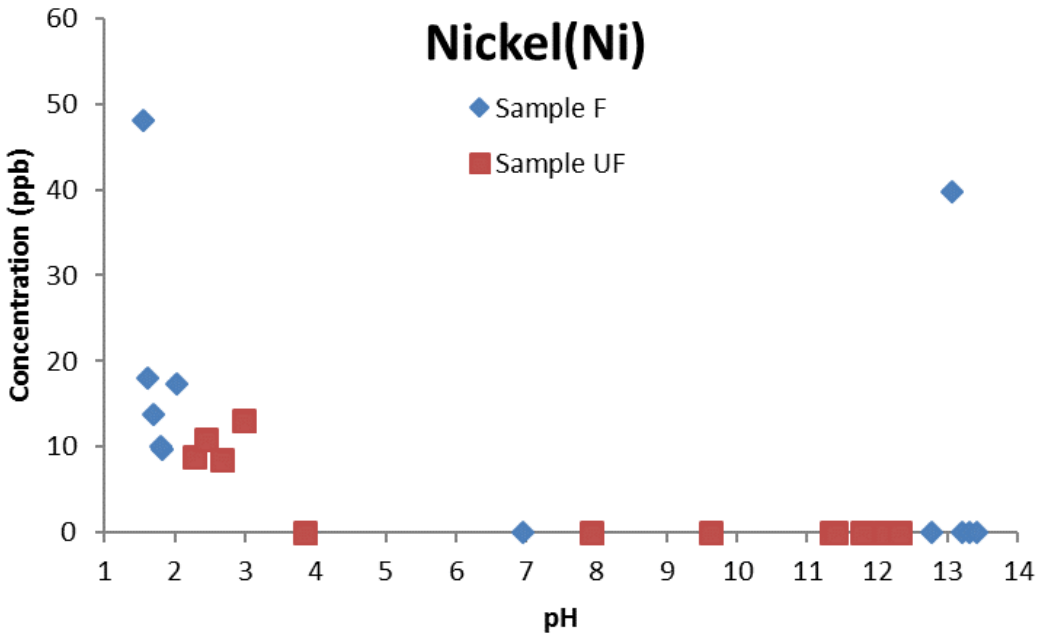

Figure E- 5:Metal concentration in leaching solution as function of pHs (Task 1)

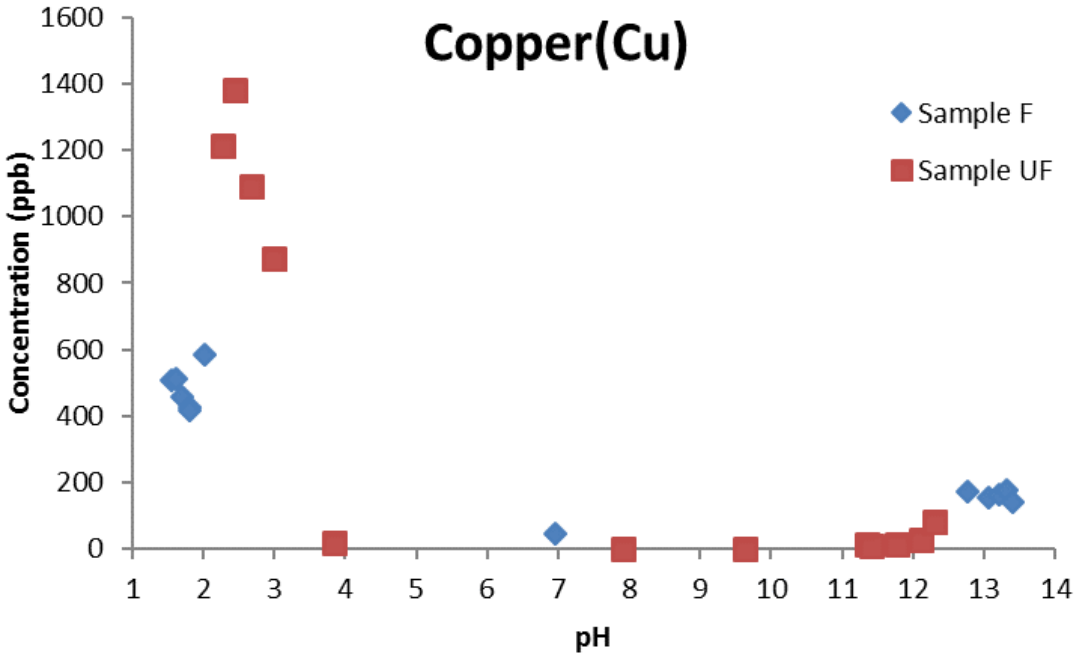

Figure E- 6:Metal concentration in leaching solution as function of pHs (Task 1)

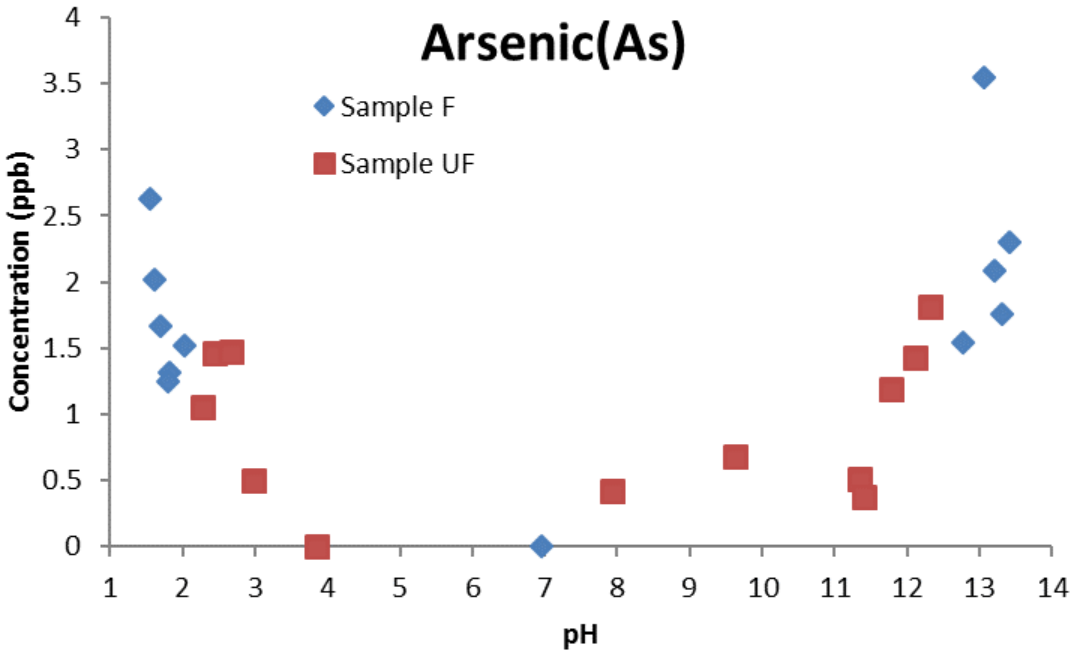

Figure E- 7:Metal concentration in leaching solution as function of pHs (Task 1)

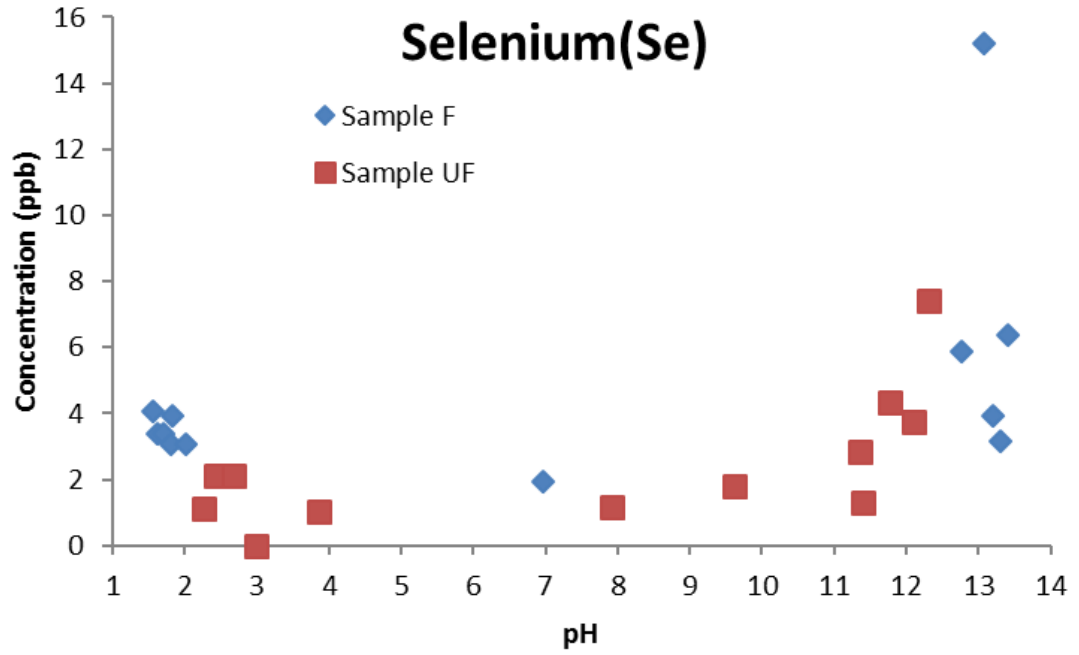

Figure E- 8:Metal concentration in leaching solution as function of pHs (Task 1)

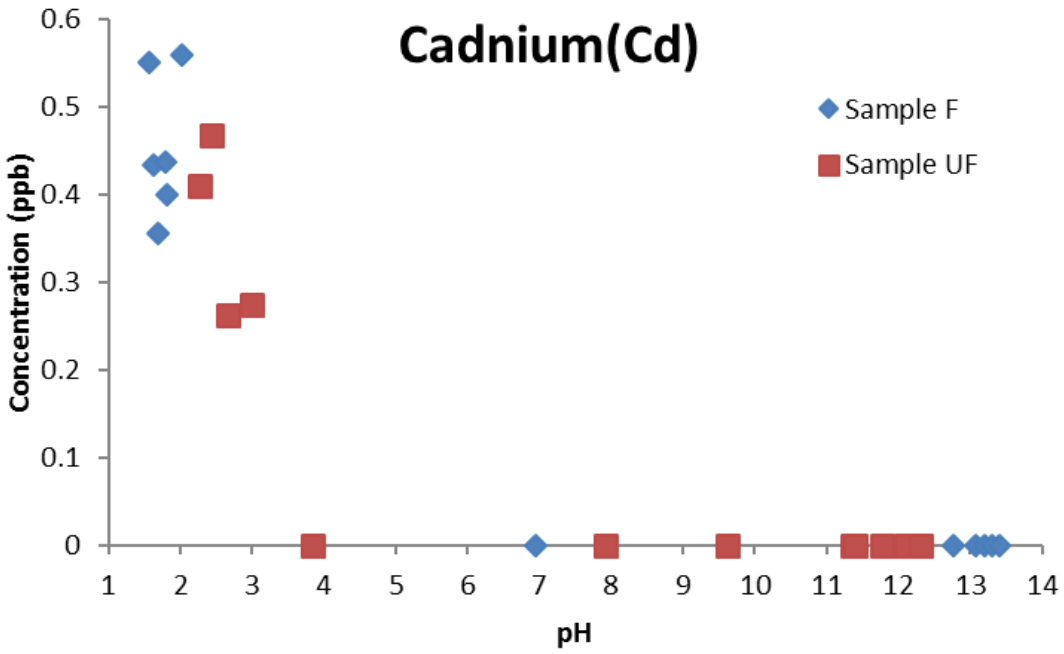

Figure E- 9:Metal concentration in leaching solution as function of pHs (Task 1)

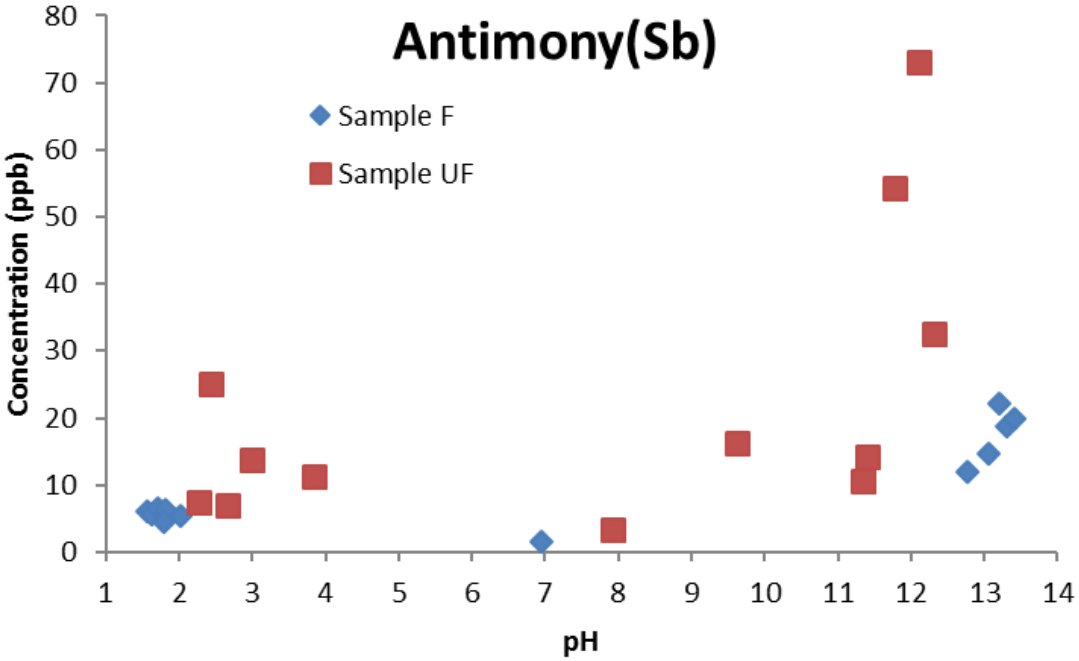

Figure E- 10:Metal concentration in leaching solution as function of pHs (Task 1)

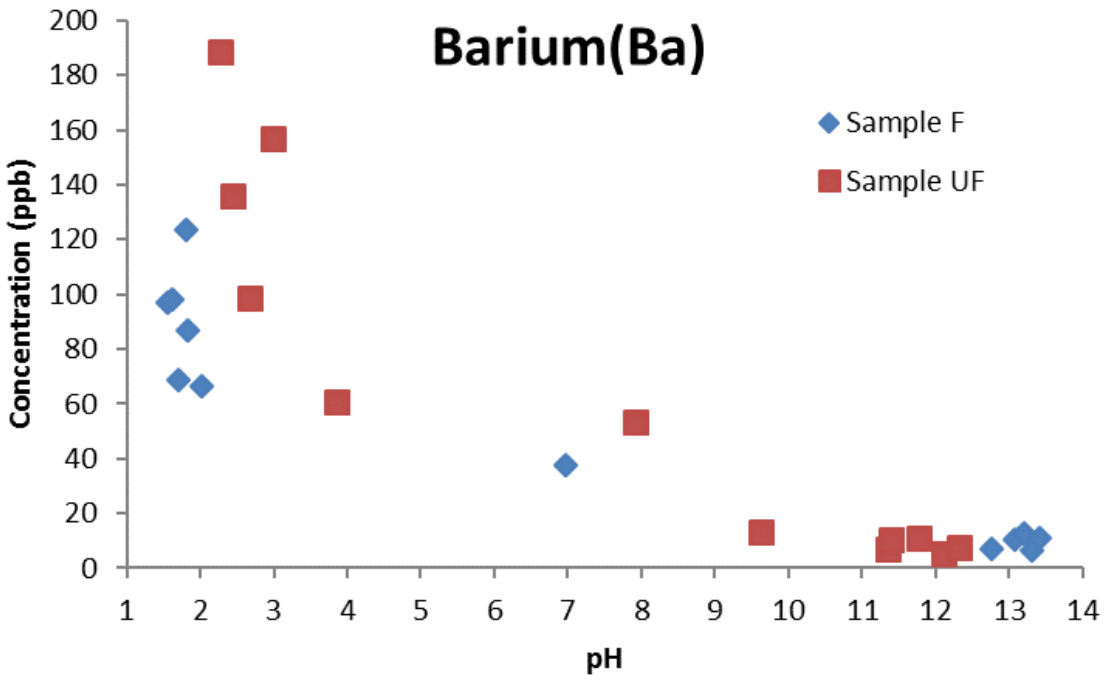

Figure E- 11:Metal concentration in leaching solution as function of pHs (Task 1)

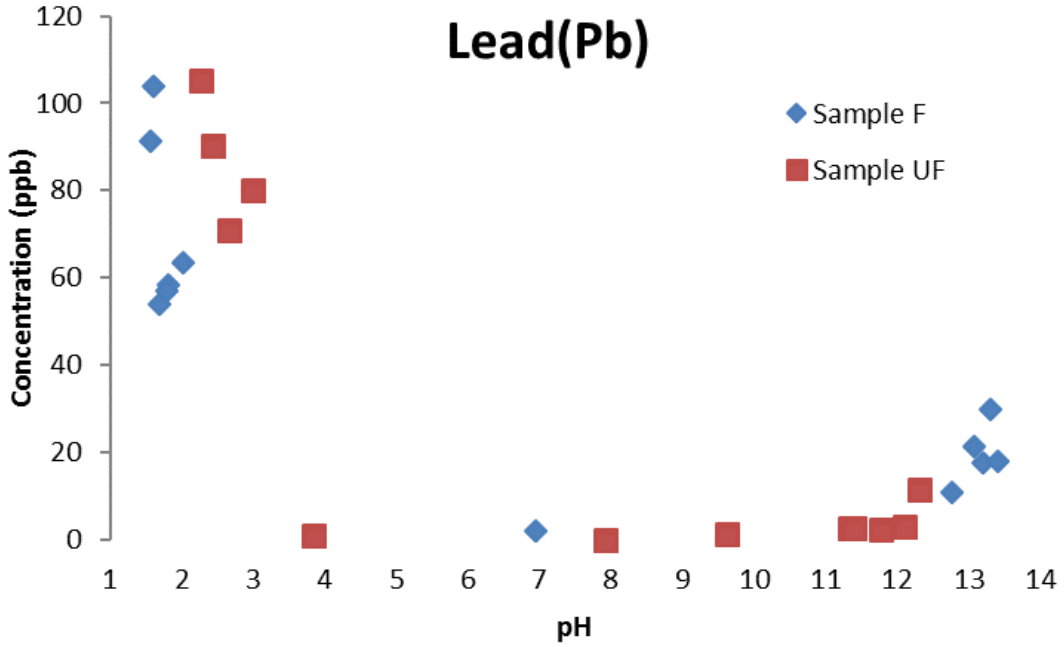

Figure E- 12:Metal concentration in leaching solution as function of pHs (Task 1)

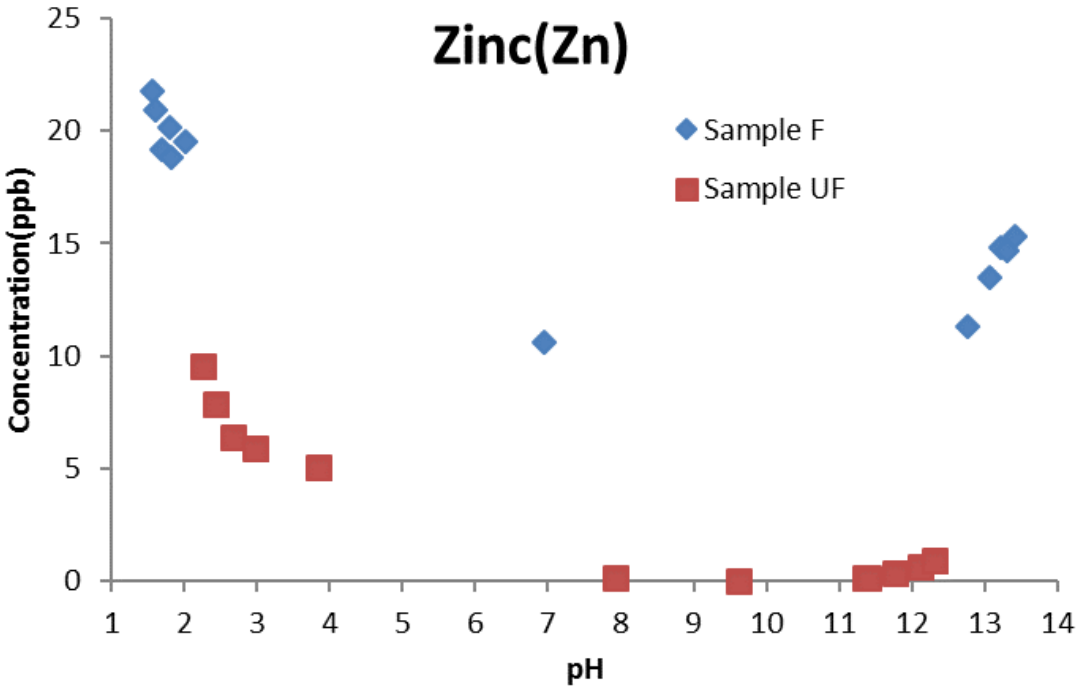

Figure E- 13:Metal concentration in leaching solution as function of pHs (Task 1)

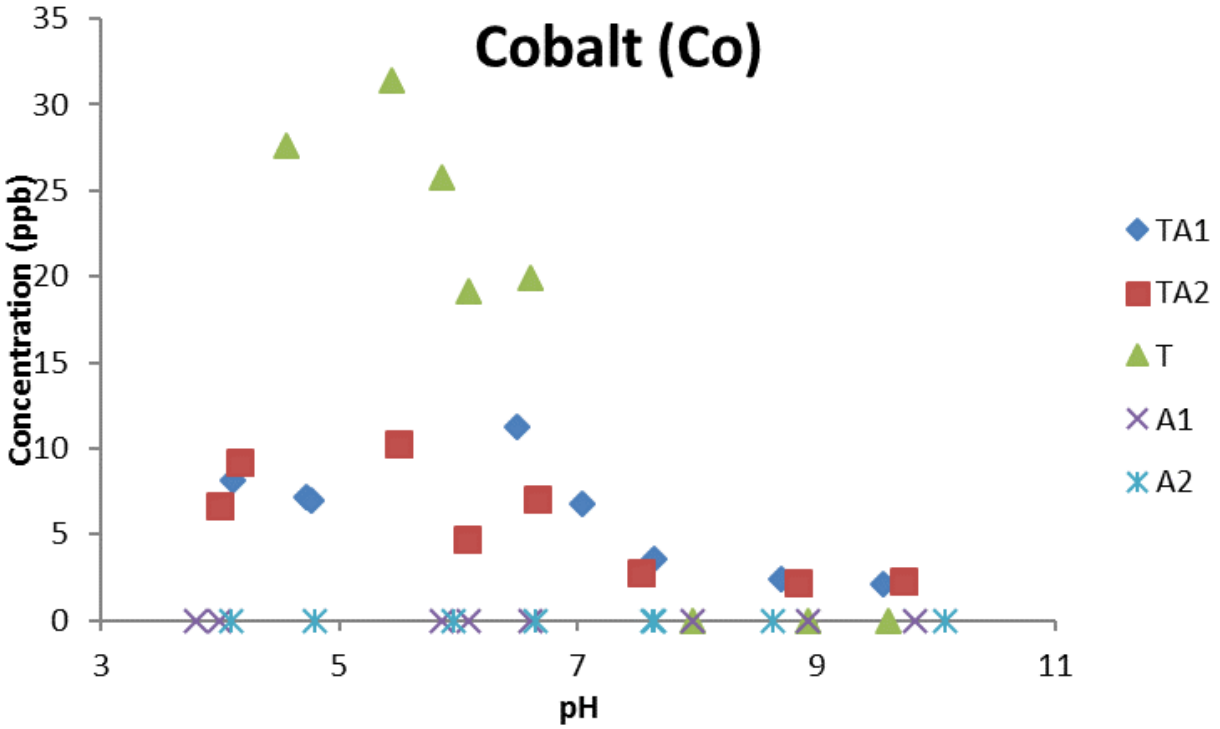

Figure E- 14:Metal concentration in leaching solution as function of pHs (Task 4)

Note: * Other elements are close or below MDLs.

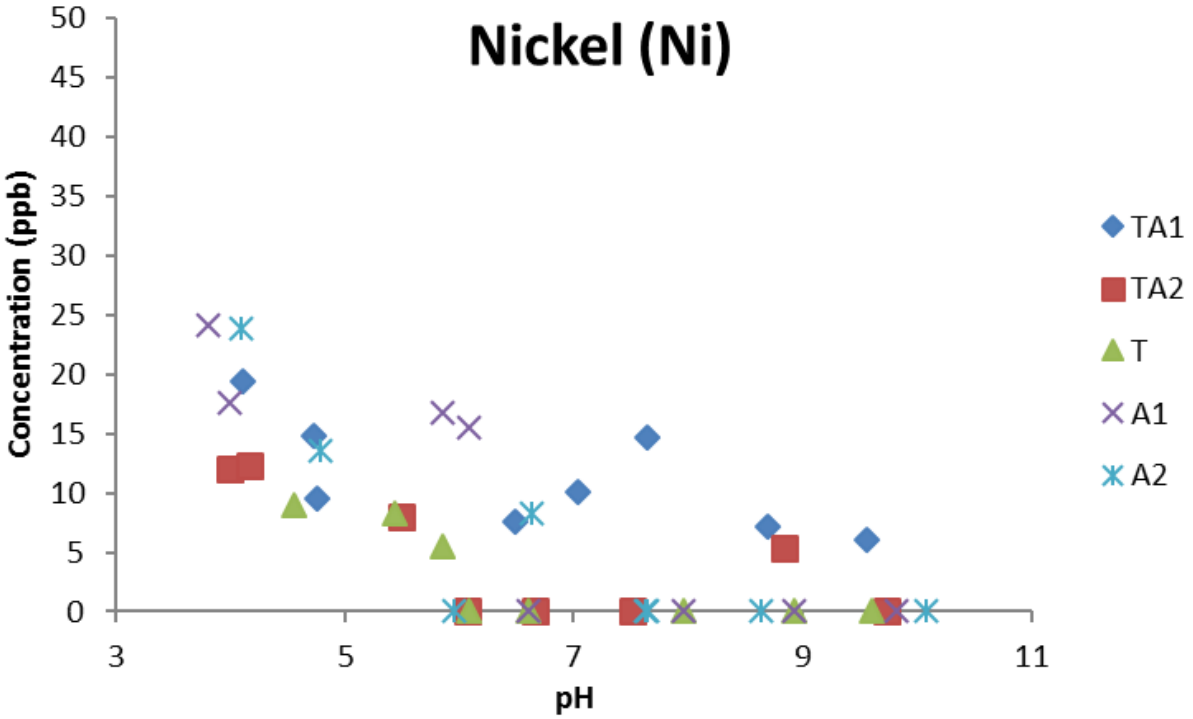

Figure E- 15:Metal concentration in leaching solution as a function of pHs *(Task 4).

Note: * Other elements are close or below MDLs.

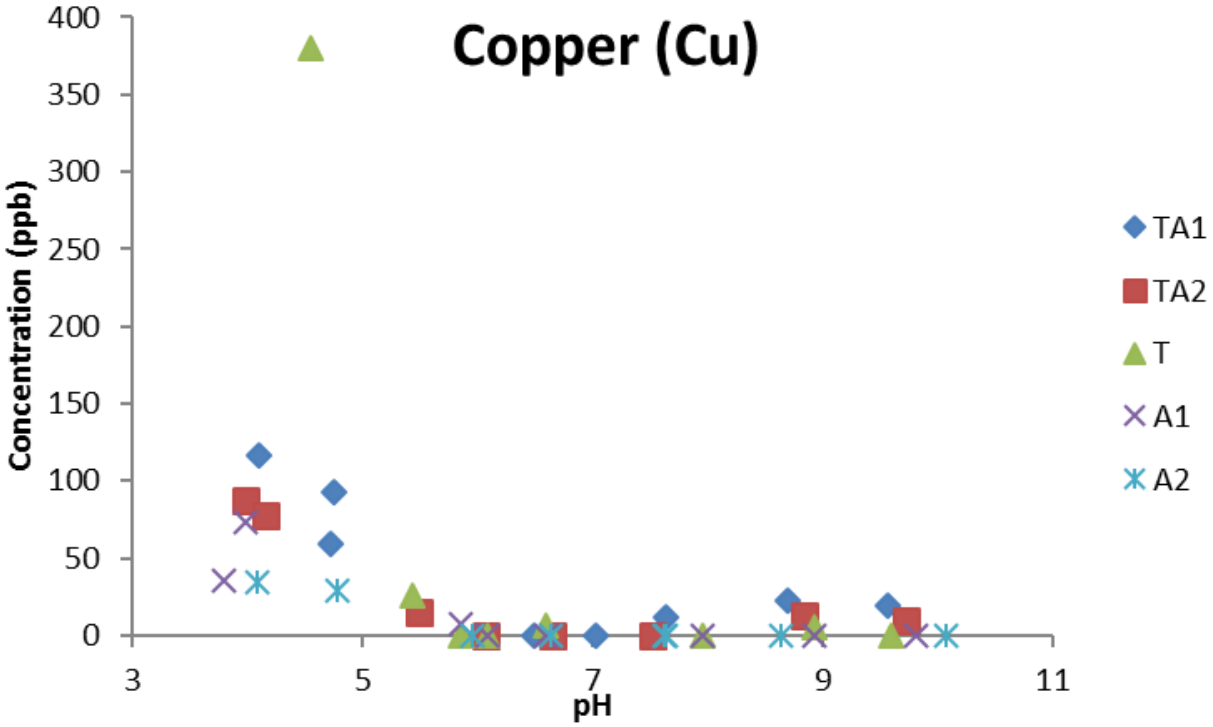

Figure E- 16:Metal concentration in leaching solution as a function of pHs *(Task 4).

Note: * Other elements are close or below MDLs.

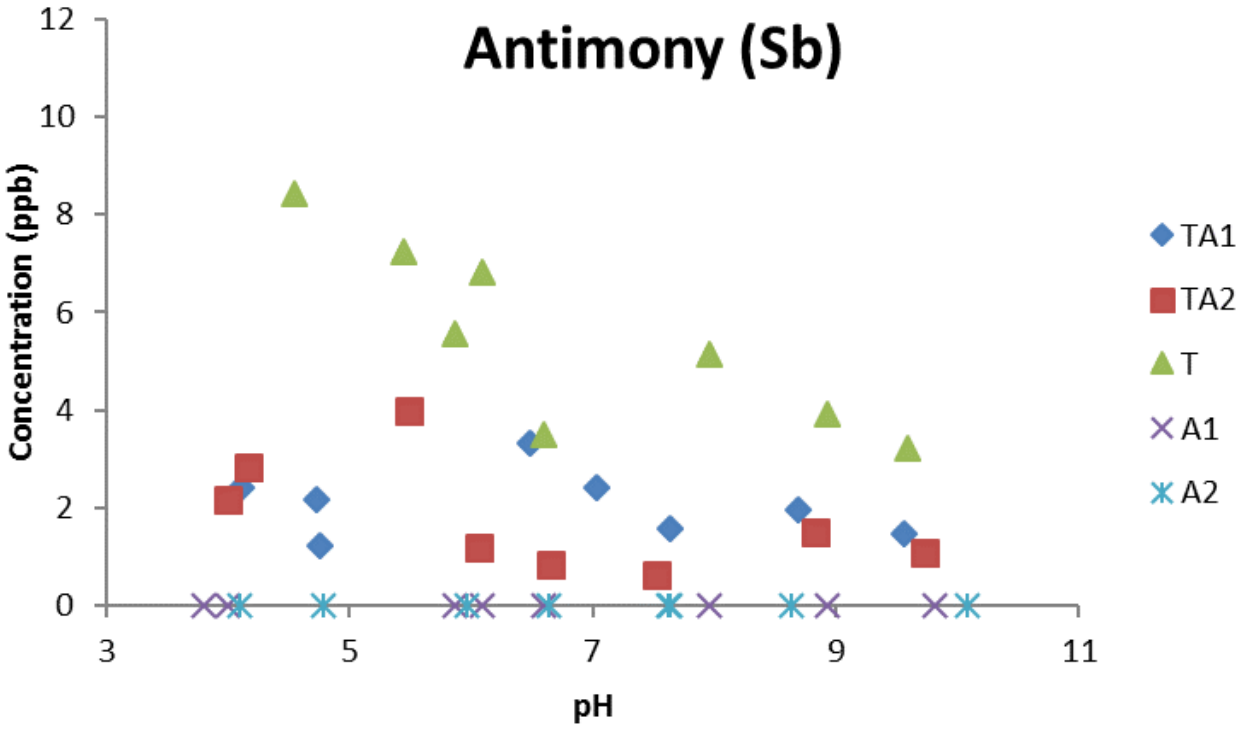

Figure E- 17:Metal concentration in leaching solution as a function of pHs *(Task 4).

Note: * Other elements are close or below MDLs.

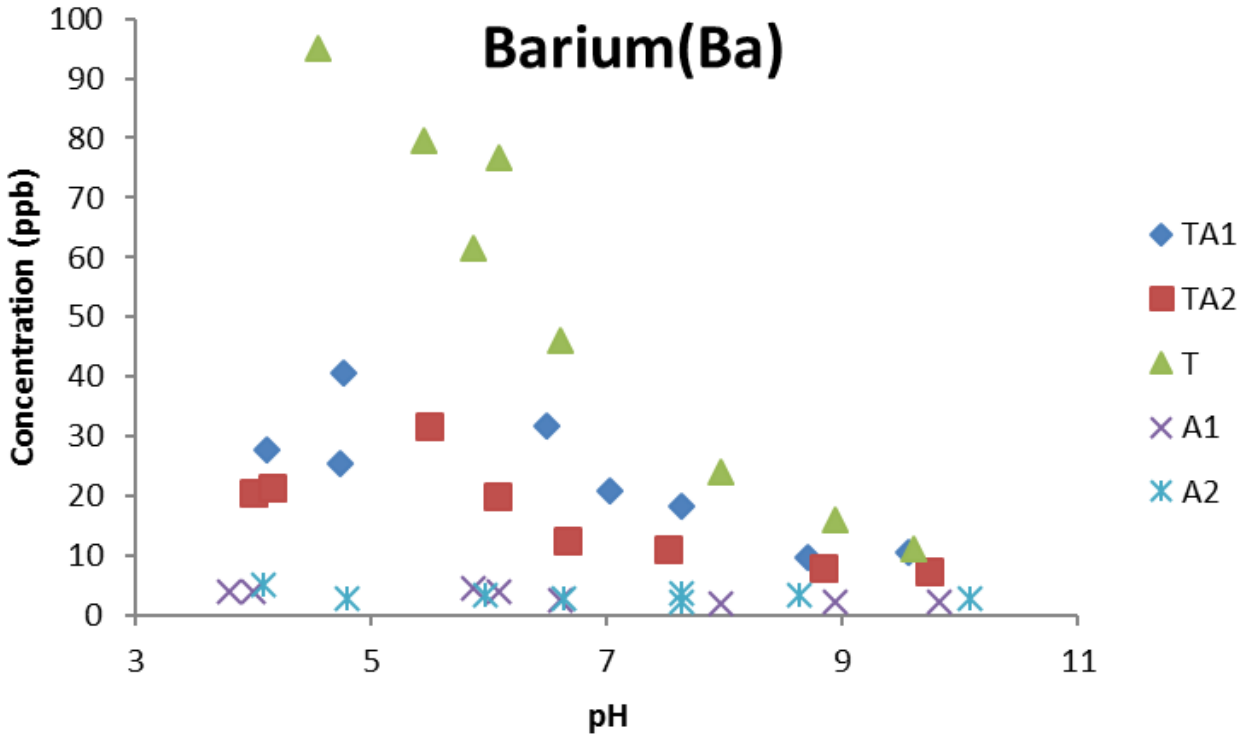

Figure E- 18:Metal concentration in leaching solution as a function of pHs *(Task 4).

Note: * Other elements are close or below MDLs.

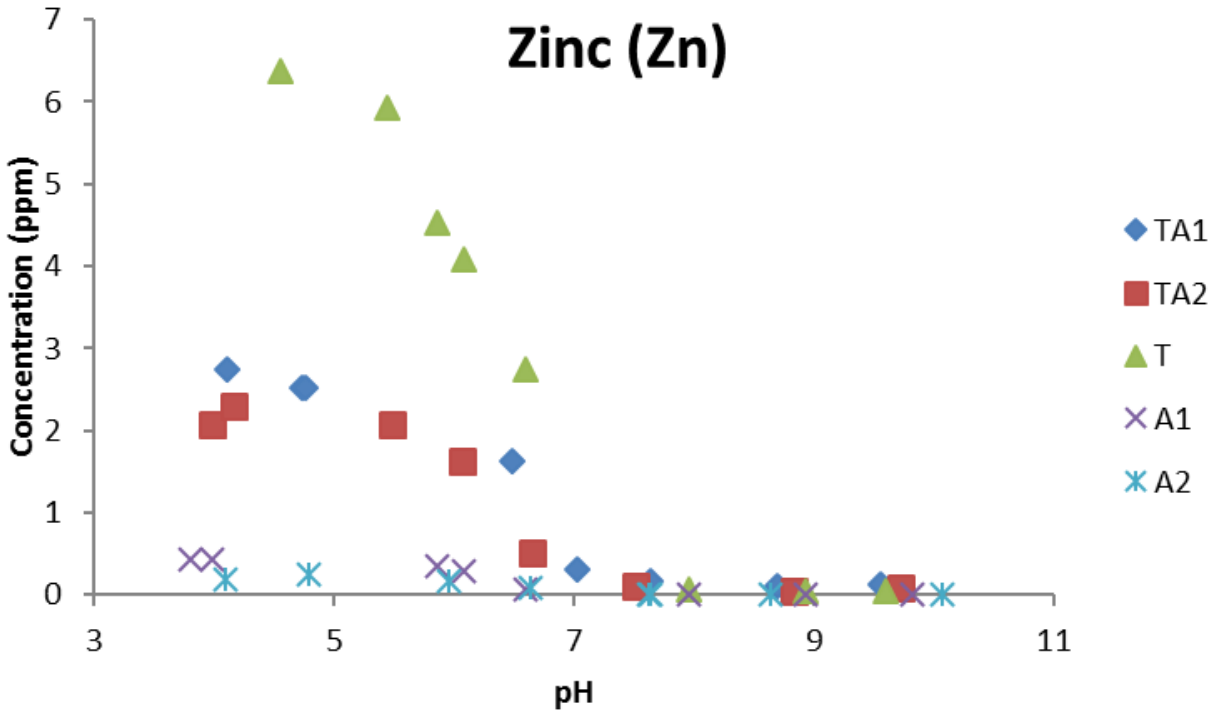

Figure E- 19:Metal concentration in leaching solution as a function of pHs *(Task 4).

Note: * Other elements are close or below MDLs.

6. References

Abe, H., A. Tamai, J. Henry and J. Wambold (2001). "Measurement of pavement macrotexture with circular texture meter." Transportation Research Record: Journal of the Transportation Research Board(1764): 201-209.

Alvarado, A. and I. L. Howard (2014). Investigation into Compatibility of Chip Seal Aggregates and Emulsions. Transportation Research Board 93rd Annual Meeting.

Amirkhanian, S. N. (2001). "Utilization of crumb rubber in asphaltic concrete mixtures–South Carolina's Experience." See ref **3**: 163-174.

Ang, G. and V. Marchal (2013). "Mobilising private investment in sustainable transport: The case of land-based passenger transport infrastructure." OECD Environment Working Papers(56): 0_1.

Asi, I. M. (2007). "Evaluating skid resistance of different asphalt concrete mixes." Building and Environment **42**(1): 325-329.

ASTM (2011). ASTM D7000 Standard Test Method for Sweep Test

of Bituminous Emulsion Surface Treatment Samples,. ASTM International, West Conshohocken, PA

Banerjee, A., A. de Fortier Smit and J. A. Prozzi (2012). "Modeling the effect of environmental factors on evaporative water loss in asphalt emulsions for chip seal applications." Construction and Building Materials **27**(1): 158-164.

Brown, E. R. (1988). "Preventative Maintenance of Asphalt Concrete Pavements." National Center for Asphalt Technology, Auburn, AL.

Choubane, B., C. Holzschuher and S. Gokhale (2004). "Precision of locked-wheel testers for measurement of roadway surface friction characteristics." Transportation Research Record: Journal of the Transportation Research Board(1869): 145-151.

Do, M.-T., H. Zahouani and R. Vargiolu (2000). "Angular parameter for characterizing road surface microtexture." Transportation Research Record: Journal of the Transportation Research Board(1723): 66-72.

EN, B. (2003). "12272-3. Surface dressing." Test methods-determination of binder aggregate adhesivity by the vialit plate shock test method.

Flintsch, G., E. de León, K. McGhee and I. AI-Qadi (2003). "Pavement surface macrotexture measurement and applications." Transportation Research Record: Journal of the Transportation Research Board(1860): 168-177.

Forster, S. W. (1981). Aggregate microtexture: Profile measurement and related frictional levels.

Gransberg, D. (2006). "Correlating chip seal performance and construction methods." Transportation Research Record: Journal of the Transportation Research Board(1958): 54-58.

Gransberg, D. and D. James (2005). "NCHRP Synthesis of Highway Practice 342: Chip Seal." Transportation Research Board, National Research Council, Washington, DC.

Gransberg, D., S. Senadheera and I. Karaca (1998). "Analysis of statewide seal coat constructability review." Texas Department of Transportation Research Report TX-98/0-1787-1R.

Gransberg, D. D. and D. M. James (2005). Chip seal best practices, Transportation Research Board.

Gransberg, D. D., I. Karaca and S. Senadheera (2004). "Calculating roller requirements for chip seal projects." Journal of construction engineering and management **130**(3): 378-384.
Hanson, D., J. Epps and R. Hicks (1996). "Construction Guidelines for Crumb Rubber Modified Hot Mix Asphalt." Federal Highway Administration Report DTFH61-94-C-00035.
Hanson, D. I. and B. D. Prowell (2004). Evaluation of circular texture meter for measuring surface texture of pavements, the Center.
Hemdorff, S., L. Leden, K. Sakshaug, M. Salusjärvi and R. Schandersson (1989). Trafiksäkerhet och vägytans egenskaper (TOVE): slutrapport, Valtion teknillinen tutkimuskeskus. Tie-ja liikennelaboratorio.
Henry, J. J. (2000). Evaluation of pavement friction characteristics, Transportation Research Board.
Howard, I. L. and G. Baumgardner (2009). US Highway 84 Chip Seal Field Trials and Laboratory Test Results, Mississippi Department of Transportation.
Islam, M. S. (2010). Evaluation of lightweight aggregates in chip seal, Kansas State University.
Islam, S. and M. Hossain (2011). "Chip seal with lightweight aggregates for low-volume roads." Transportation Research Record: Journal of the Transportation Research Board **2205**(1): 58-66.
Islam, S. and M. Hossain (2011). "Chip seal with lightweight aggregates for low-volume roads." Transportation Research Record: Journal of the Transportation Research Board(2205): 58-66.
Janisch, D. W. and F. S. Gaillard (1998). "Minnesota seal coat handbook." Physical Research Section, Office of Minnesota Road Research, Minnesota Department of Transportation, Maplewood, MN.(http://www. mrr. dot. state. mn. us/research/mnroad_project/restools/sealcoat. asp).
Jordan III, W. S. and I. L. Howard (2011). "Applicability of Modified Vialit Adhesion Test for Seal Treatment Specifications." Journal of Civil Engineering and Architecture **5**(3).
Kandhal, P. S. and J. B. Motter (1991). Criteria for accepting precoated aggregates for seal coats and surface treatments.
Karasahin, M., B. Aktas, A. Gungor, F. Orhan and C. Gurer (2014). "Laboratory and In Situ Investigation of Chip Seal Surface Condition Improvement." Journal of Performance of Constructed Facilities **29**(2): 04014047.
Kearby, J. (1953). Tests and theories on penetration surfaces. Highway Research Board Proceedings.
Kim, Y. R. and J. Adams (2011). "Development of a new chip seal mix design method." Final Report for HWY-2008-04. FHWA, North Carolina Department of Transportation.
Kotek, P. and M. Kováč (2015). "Comparison of Valuation of Skid Resistance of Pavements by two Device with Standard Methods." Procedia Engineering **111**: 436-443.
Lee, S.-J., C. K. Akisetty and S. N. Amirkhanian (2008). "The effect of crumb rubber modifier (CRM) on the performance properties of rubberized binders in HMA pavements." Construction and Building Materials **22**(7): 1368-1376.
Liu, L., M. Hossain and R. Miller (2010). Life of Chip Seal on Kansas Highways. Compendium of Papers from First International Conference on Pavement Preservation.
Masad, E. (2007). Test methods for characterizing aggregate shape, texture, and angularity, Transportation Research Board.
Mataei, B., H. Zakeri, M. Zahedi and F. M. Nejad (2016). "Pavement Friction and Skid Resistance Measurement Methods: A Literature Review." Open Journal of Civil Engineering **6**(04): 537.

McLeod, N. W., C. Chaffin, A. Holberg, C. Parker, V. Obrcian, J. Edwards, W. Campen and W. Kari (1969). A general method of design for seal coats and surface treatments. Association of Asphalt Paving Technologists Proc.
Mohseni, A. (1998). LTPP seasonal asphalt concrete (AC) pavement temperature models.
Moore, D. F. (1972). The friction and lubrication of elastomers, Pergamon.
Moustafa, A. and M. A. ElGawady (2015). "Mechanical properties of high strength concrete with scrap tire rubber." Construction and Building Materials **93**: 249-256.
O'Brien, L. G. (1989). Evolution and benefits of preventive maintenance strategies.
Papagiannakis, A. and T. Lougheed (1995). A REVIEW OF CRUMB-RUBBER MODIFIED ASPHALT CONCRETE TECHNOLOGY. RESEARCH REPORT.
Persson, B. (2013). Sliding friction: physical principles and applications, Springer Science & Business Media.
Presti, D. L. (2013). "Recycled tyre rubber modified bitumens for road asphalt mixtures: a literature review." Construction and Building Materials **49**: 863-881.
Rahman, F., M. Islam, H. Musty and M. Hossain (2012). "Aggregate retention in chip seal." Transportation Research Record: Journal of the Transportation Research Board(2267): 56-64.
Rangaraju, P. and S. Gadkar (2012). "Durability evaluation of crumb rubber addition rate on Portland cement concrete." Department of Civil Engineering, Clemson University, Clemson: 1-126.
RMA, R. M. A. (2016). "Scrap tire markets in the United States."
Ruud, H. (1981). "Kjørefart på saltede och usaltede veger: målinger i Akershus og Vestfold 1980 og 1981." Transportøkonomisk Institutt. Oslo.
Shuler, S. (1998). "DESIGN AND CONSTRUCTION OF CHIP SEALS FOR HIGH TRAFFIC." Flexible Pavement Rehabilitation and Maintenance **1348**: 96.
Shuler, S. (2011). NCHRP Report 680: Manual for Emulsion-Based Chip Seals for Pavement Preservation.
Shuler, S. (2011). Use of Waste Tires, Crumb Rubber, on Colorado Highways, Colorado Department of Transportation, DTD Applied Research and Innovation Branch.
Stockton, W. R. and J. A. Epps (1975). ENGINEERING ECONOMY AND ENERGY CONSIDERATIONS. SEAL COAT ECONOMICS AND DESIGN.
Temple, W., S. Shah, H. Paul and C. Abadie (2002). "Performance of Louisiana's chip seal and microsurfacing program, 2002." Transportation Research Record: Journal of the Transportation Research Board(1795): 3-16.
Wallman, C.-G. and H. Åström (2001). "Friction measurement methods and the correlation between road friction and traffic safety: A literature review."
Wilson, D. J. and R. Dunn (2005). Analysing Road Pavement Skid Resistance. ITE 2005 Annual Meeting and Exhibit Compendium of Technical Papers.
Wood, T. J., D. W. Janisch and F. S. Gaillard (2006). Minnesota seal coat handbook 2006.
Wood, T. J. and R. C. Olson (2007). "Rebirth of chip sealing in Minnesota." Transportation Research Record: Journal of the Transportation Research Board **1989**(1): 260-264.
Yandell, W. (1971). "A new theory of hysteretic sliding friction." Wear **17**(4): 229-244.
Yandell, W. and S. Sawyer (1994). "Prediction of tire-road friction from texture measurements." Transportation Research Record(1435).
Youssf, O., M. A. ElGawady and J. E. Mills (2016). "Static cyclic behaviour of FRP-confined crumb rubber concrete columns." Engineering Structures **113**: 371-387.

EPA method 1313 Liquid-solid partitioning (LSP) as a function of eluate pH using a parallel batch extraction procedure.

EPA method 3051A Microwave Assisted Acid Digestion of Sediments, Sludges, Soils, and Oils.
EPA method 1312 - Synthetic Precipitation Leaching Procedure (SPLP).
Rhodes, E.P., Ren, Z., and Mays, D.C. “Zinc Leaching from Tire Crumb Rubber.” Environ. Sci. Technol. 2012 (46), 12856−12863.